Politecnico di Torino

Master's Degree Course in Aerospace Engineering

Master's Degree Thesis

Development and application of Link Budget calculator for a Spacecraft mission: GSN design and Link Budget analysis for SROC support

Supervisors:
Prof. Stesina Fabrizio
Prof. Corpino Sabrina

Company Supervisors:
Buttari Giuseppe
Montaldi Serafino

Candidate:
Di Francesco Dario
279016

Academic Year 2021/2022

A mia madre e mio padre,
ai loro sforzi e sacrifici per
supportare le mie aspirazioni

Acknowledgements

Abstract

This thesis stems from the work done during the internship at Telespazio and its main topic is the study of Link Budget calculation for telemetry, telecommand and ranging signals in satellite communications to analyse the Earth-to-space interface.

The main goal was to develop a tool that would autonomously perform all the calculations necessary for margin assessment to determine whether the link is closed or not. This software, implemented with MATLAB, was conceived as an advancement of the tools used by Telespazio, aiming for greater completeness, additional configurations, more complex features, and increased user friendliness, trying to adapt it to any kind of scenario.

The software has been tested and exploited to study the link budget of some missions managed by Telespazio, proving that it is fully functional and the results it produces are reliable, but its most important application has been the study of the link budget of SROC (Space Rider Observation Cubesat) mission, conceived by Politecnico di Torino.

Considering that Telespazio will provide additional ground stations to the mission, the goal has been the design of a feasible and efficient ground station network, with the right antennas and a reliable ground-to-satellite interface to ensure effective communication at all times. Given the practical, econimic and logistic limitations of this type of task, the use of link budget software was critical for the choice of equipment and all features. In addition, to complete the work, visibility analysis was also carried out to study the coverage provided by the GSN, particularly in a critical phase such as docking.

Contents

List of Figures

List of Tables

Nomenclature

ACU   Antenna control unit

AOS   Acquisition of signal

AR   Axial ratio

AT   Adverse tolerance

AWGN Additive white Gaussian noise

BB   Baseband

BER   Bit error rate

BPSK Binary phase-shift keying

BW   Bandwidth

D/C   Down converter

DW   Downlink

EIRP Effective Isotropic Radiated Power

FEC   Forward error correction

FM   Frequency modulation

FSK   Frequency-shift keying

FT   Favourable tolerance

G/S   Ground station

G/T   Antenna gain-to-noise-temperature

GEO   Geostationary Earth Orbit

GMSK Quadrature phase-shift keying

GSN   Ground station network

HK   Housekeeping

HPA   High power amplifier

LEO   Low Earth orbit

LEOP Launch and Early orbit phase

LHCP Left-handed circular polarization

LNA   Low noise amplifier

LOS   Loss of signal

m/i   Modulation index

MCC   Mission control centre

MEO   Medium Earth orbit

MPCD Multi-Purpose CubeSat Dispenser

NCC   Network control centre

NRZ-L Non-return to zero - level

OQPSK Offset Quadrature phase-shift keying

PCM   Pulse code modulation

PCM   Pulse-Code modulation

PFD   Power flux density

PL   Payload

PLL   Phase-locked loop

PM   Phase modulation

PSK   Phase-shift keying

QPSK Quadrature phase-shift keying

R-S   Reed-Solomon

RF   Radio frequency

RG   Ranging

RHCP Right-handed circular polarization

RSS   Residual sum of squares

Rx   Reception

S/C   Spacecraft

s/c   Subcarriers

S/N   Signal-to-noise ratio

SNR   Signal-to-noise ratio

SP-L Split phase - level

SR   Space Rider

SROC Space Rider Observer CubeSat

TC   Telecommand

TLE   Two-line element

TM   Telemetry

TT&C   Telemetry, Tracking and Control

Tx   Transmission

U/C   Up converter

UHF   Ultra high frequency

UP   Uplink

VHF   Very high frequency

VT   Viterbi

XPD   Crosspolar discrimination

Chapter 1

Introduction

Satellite communications have two main components: the ground segment, consisting of one or more fixed or mobile stations, and the space segment, in particular its communications system.

The Telemetry, Tracking and Command (TT&C) or communications system provides the interface between the spacecraft (S/C) and the ground station (G/S). Payload mission data and Spacecraft housekeeping data pass from the spacecraft to the operation centres (Uplink), whereas commands pass from ground to the spacecraft (Downlink). Important TT&C functions can be summarized as:

- Telecommand (TC) reception and detection, that is receive the Uplink signal and process it;

- Telemetry (TM) modulation and transmission, that is process data and transmit them as a Downlink signal;

- Ranging (RG), which means receive, process and transmit Ranging signal to determine the spacecraft's position;
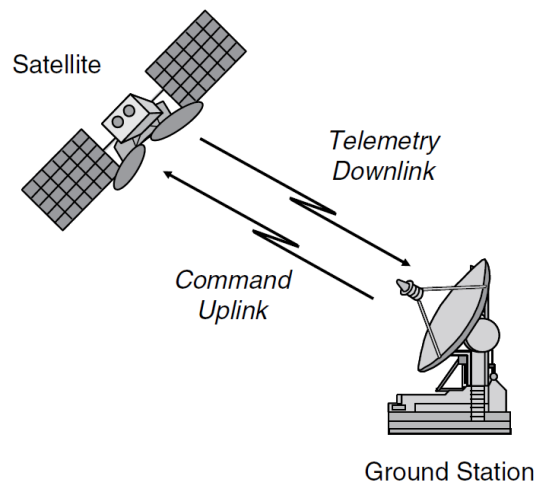
Figure 1.1: *Example of TT&C link*

1

1.1   RF Communication System

The main functional components of a RF Communication System can be schematized as follows:

- Baseband signal: contains the data bit stream (data rate, data volume);

- Encoder/Decoder: coding is a technique used in data transmission for reducing the bit error rate (BER);

- Modulator/Demodulator: modulation is the process of varying one or more properties of the Carrier signal, typically a high-frequency periodic waveform, with a separate modulating signal, which is the baseband signal;

- Transmitter: amplifies the modulated signal without distortions and provides the transmitting antenna with an high RF Power; its main comoponent is the High power amplifier (HPA);

- Receiver: its main function is to increase the signal-to-noise ratio (S/N), amplifying the very weak signal from the receiving antenna while rejecting interferences and noise; the main component is the Low noise amplifier (LNA);

- Antenna: transducer designed to transmit and receive radio waves; it is an array of conductors that converts electromagnetic waves into an electric alternating current.
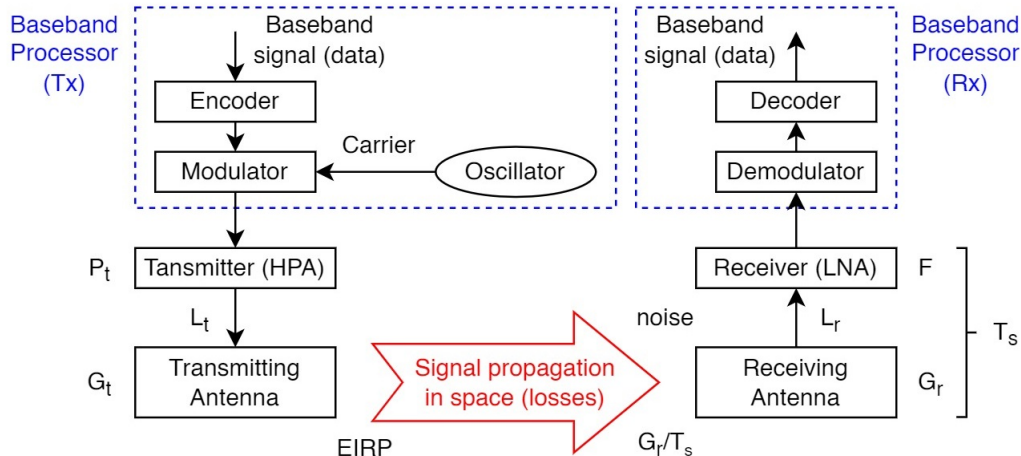
Figure 1.2: *Generic RF Communication System functional block diagram*

1.2 Link Budget

A link budget consists in the calculation of the received power from the transmitter power, after the attenuation of the transmitted signal due to propagation, as well as the antenna gains, feedline and other losses, and amplification of the signal in the receiver.

It is a fundamental design factor of a satellite link to define the capability of the communication system to guarantee an effective communication (i.e. the information is received intelligibly) between space segment and ground segment. The final purpose of a link budget is to calculate the technical design parameters needed for the signal (data rate, type of modulation, error correction encoding, etc.), for the earth station and, possibly, for the space station. Link budget computation shall be performed for each communication link, for downlink and uplink, if necessary.

A simple link budget equation looks like this:

Received power [dBW] = *Transmitted power* [dBW] + *Gains* [dB] − *Losses* [dB]

Power levels are expressed in dBW (Decibel watts, which is a unit for the measurement of the strength of a signal expressed in decibels relative to one watt), Power gains and losses are expressed in dB (decibels), which is a logarithmic measurement, so adding decibels is equivalent to multiplying the actual power ratios. The conversion from watt (for example) to dBW is given by the formula:

$$P_{\text{dBW}} = 10 \log_{10}(P_{\text{W}}) \qquad (1.1)$$

Chapter 2

Link Budget Calculator

To easily and quickly calculate the link budget, a calculator has been developed whose main component is a MATLAB script that takes input data from an Excel interface, processes it, calculates output results, and transcribes them to the same interface.

2.1 Concept and characteristics

The process of manually calculating the link budget can be time-consuming and complex, depending on the level of detail involved in the analysis to be done. The main theme of this thesis is the development of a Link Budget calculation method that aims to have the following characteristics:

- Automatic and fast: The link budget is a tool for the preliminary design phase, so it often happens so it is often required to change the parameters involved and repeat the analysis, which can even be done several times, to analyze various types of configurations. For this reason, the goal is for a system that gives the ability to input data, change them at will, and get all the results automatically and immediately.

- Simple and intuitive: A huge amount of data and mission characteristics are involved in the calculation, so that it is easy to get confused. Input and output should be easily accessible and recognizable, to avoid confusion or getting lost within the analysis.

- Schematic and compact: The interface should have a professional and tabular appearance, reporting the parameters with a logical sequence, divided and identified in categories and subcategories, avoiding superfluous elements that lead to confusion and time loss .

- Generalized and flexible: The purpose of the program is to provide a calculation base as general as possible in order to deal with all the possible scenario that can occur concerning the Link Budget for TT&C functions

(Telemetry, Telecommand and Ranging) in the various types of space missions (GEO, LEO/MEO, LEOP) with various communication architectures. Therefore it must include a large archive of possible configurations that the user can select to direct the code on the right path to perform the calculation. It should also be able to derive unavailable parameters and bypass unnecessary calculations.

- Exhaustive and robust: The method takes in account all the theories and standards necessary to ensure a complete and reliable analysis. It is important in the design phase to use a worst-case approach, that is to consider more demanding operating conditions and underperforming parameter values in order to assume a worst-case scenario. This results in an underestimation of the margins leading to an oversizing of the components, to obtain the most safe and robust communication architecture in all phases of the mission, which can deal also with degradations and failures. Possible parameter fluctuations come into play by considering three values for each parameter (nominal, adverse and favourable) but always sticking to a worst-case philosophy.

2.2 Development and overview

The main steps that led to the development of the calculator are listed below, with an overview of the tasks that each section performs.

2.2.1 Material review and User interface

In-depth study of the spreadsheet used by Telespazio to calculate the Link Budget, which is entirely implemented in Excel and, even if powerful and well done, it turned out to be huge, complex and somewhat confusing, so it is preferable to do the calculation part in MATLAB and leave the user to have access only through the excel interface to choosing configurations, input data and reading the output. However, great importance was given to the level of detail and depth applied by the developer to the old spreadsheet, giving absolute priority to the need to mantain all the implemented features, but rather trying to identify where it seemed fragile or showed gaps.

To prevent a major gap from the previous instrument, the user interface is made in Excel and consists of one spreadsheet for the input table and two others for the Uplink and Downlink output tables; the first section of the input table implements a series of drop-down menus to select, among various options, mission configuration characteristics. More details on configuration selection and input data can be found in Section 2.3.

2.2.2 Input acquisition and Preprocessing

The first part of the MATLAB code involves acquiring the input data table through the function 'importfile' generated specifically to read the data table (using the MATLAB function 'readtable') from a specific range of cells in the 'input sheet' of the Excel document (whose 'filename' indicates its directory) and return to the main code a matrix of numeric data:

Listing 2.1: *"importfile" function calling*

```
1  filename = 'C:\Users\hp\Desktop\LINK_BUDGET_v5\Link_Budget_v5.xlsx';
2  sheet_input = 'Input';
3  IN = importfile(filename,sheet_input);
```

Listing 2.2: *"importfile" function script*

```
1  function IN = importfile(workbookFile,sheetName,dataLines)
2  % Specify sheet and range
3  opts.Sheet = sheetName;
4  dataLines = [3, 134];
5  opts.DataRange = A + dataLines(1, 1) + :K + dataLines(1, 2);
6  % Import the data
7  IN = readtable(workbookFile, opts, UseExcel, false);
8  for idx = 2:size(dataLines, 1)
9      opts.DataRange = A + dataLines(idx, 1) + :K + dataLines(idx, 2);
10     tb = readtable(workbookFile, opts, UseExcel, false);
11     IN = [IN; tb];
12 end
13 % Convert to output type
14 IN = table2array(IN);
15 end
```

This matrix is then divided into submatrices and vectors which divide the inputs by function or category, specifically:

- Matrix 1 has a flag indicating the orbit configuration and the position and altitude data of G/S and S/C;

- Matrix 2 has a series of vectors containing flags indicating modulation and encoding configurations;

- Matrices 4, 5, 6, and 7 consist of three vectors each, containing the nominal, adverse, and favorable values of the parameters that characterize (respectively) the G/S, S/C, Hearth-to-Space path, communication, and modulation;

- For each of these four matrices there is a vector of flags indicating whether that associated parameter was entered by the user or not.

2.2.3 Script core and Data processing

The core script is divided into many subsections according to the origin of the data it processes or the destination of the results that are obtained; it starts from the calculation of the high-level parameters that are not available, all the way to the main goal which is the calculation of margins, which is discussed in chapter 3. In order to do this, it was necessary to consider and carry out an in-depth study of many theories, formulas, and regulations.

The key feature of this calculator is that the user can freely choose whether to directly enter a high-level parameter (such as the EIRP or G/T) or the lower-level parameters required to derive it. Through the flags associated with the data matrices in fact, the script is able to figure out whether a certain parameter has been entered or not and, through 'if' loops it is able to ignore parameters and calculations that are not needed; if the high-level parameter is present, its value is taken directly and the low-level ones are set as 'NaN' (so as not to appear in the results), otherwise the low-level parameters are read and the high-level one is calculated from them (all of them will appear in the results).

Listing 2.3: *G/S EIRP calculation script*

```
1  % GS EIRP [dBW]
2  if F3(5)==1
3      eirpG = IN3(5,:);
4      Pt_G = NaN(1,3);
5  elseif F3(5)==0
6      Pt_G = IN3(6,:);              % GS Tx output Power [W]
7      eirpG = 10*log10(Pt_G) − LT_G + Gt_G;
8  end
```

The most time-consuming and onerous calculations are delegated to auxiliary subfunctions, the most complex of which being those dealing with the calculation of Atmospheric and Modulation losses, which are proper sub-codes based on long and complex theories; Slant range and TM acquisition treshold calculations are also tricky topics. All these themes are discussed in chapter 4.

2.2.4 Postprocessing and Output transcription

The outputs are merged into various matrices according to the code section from which they were calculated. For each of these matrices, statistical analysis is performed, which consists of calculating (when it is required) adverse and favourable tolerance (AT=*nom−adv*, FT=*fav−nom*), mean, variance σ^2 and AT^2. The calculation of the Mean and Root mean square σ varies according to the assumptions about the distribution of the value under consideration (Uniform, Triangular or Gaussian). This information is contained in a vector of flags that is acquired from the output sheets for Uplink and Downlink through a function similar to the one dealing with input.

	Uniform	**Triangular**	**Gaussian**
Mean	$\frac{adv+fav}{2}$	$\frac{nom+adv+fav}{3}$	$\frac{adv+fav}{2}$
σ^2	$\frac{(fav-adv)^2}{12}$	$\frac{(mean)^2}{2} - \frac{nom\cdot adv+nom\cdot fav+adv\cdot fav}{6}$	$\frac{(fav-adv)^2}{12}$

Table 2.1: *Statistical parameters*

From the values of σ^2 and AT^2 related to the various parameters, it is possible to calculate, by summing all the contributions of the parameters involved (related to basic and acquisition sections), the values of 3σ and RSS (Residual sum of squares) respectively, which are needed for the calculation of Margins from statistical analysis for each acquisition section:

$$3\sigma = \left(\sum_i \sigma_i^2 \right)_{\text{basic}} + \left(\sum_j \sigma_j^2 \right)_{\text{acq}} \tag{2.1}$$

$$\text{RSS} = \left(\sum_i \text{AT}_i^2 \right)_{\text{basic}} + \left(\sum_j \text{AT}_j^2 \right)_{\text{acq}} \tag{2.2}$$

What is obtained is then grouped in two large matrices, one for Uplink and one for Downlink, which are transcribed into the related 'output sheet' through the MATLAB function 'writecell'. By clicking the 'run' button, the code compiles and the automatically opens (with 'winopen') the Excel document with the output tables filled with the results.

Listing 2.4: *Output transcription script*

```
1  sheet_outup = 'Output Up';
2  sheet_outdw = 'Output Dw';
3  writecell(OUT_UP,filename,'Sheet',sheet_outup,'Range','E4',...
4      'AutoFitWidth',0)
5  writecell(OUT_DW,filename,'Sheet',sheet_outdw,'Range','E4',...
6      'AutoFitWidth',0)
7  winopen C:\Users\hp\Desktop\LINK_BUDGET_v5\Link_Budget_v5.xlsx
```

2.3   User manual

The Excel user interface consists of one sheet for the input table (configuration selection and data input) and two for the output tables (in Uplink and Downlink). After compiling the input table, the document must be closed to allow the code (after starting the run) to transcribe the results and reopen the document filled with the results.

2.3.1   Configuration selection

The choice of configuration is made using convenient drop-down menus that show the user the options provided in an extensive database; possible choices are listed below:

- Orbit configuration: LEO, MEO, GEO, LEOP. The user must always enter the latitude, longitude and altitude of the G/S reference, and the same should be done with the S/C for GEO and LEOP cases, while for a LEO/MEO satellite it is only required to enter the altitude. For LEO/MEO and LEOP the user must also enter the elevation angle ε (5° is assumed for a worst case approach), which is instead calculated by the script in the GEO case. The choice affects, among other things, the routine that the code performs to calculate the Slant range.

- Uplink/Downlink Modulation configuration: PM with s/c (subcarriers), PM direct, BPSK, QPSK, OQPSK, GMSK, 8PSK, 16APSK, 32APSK, FSK, FM with s/c. FM with s/c is available only in Uplink.

- Uplink Carrier can be modulated by:

  1. TC only, which is always set as active if Uplink is present;

  2. RG only, if the TC and RG signals are separated;

  3. TC + RG, if the TC and RG signals are simultaneous; Ranging is possible only in case of analog modulation (PM or FM).

- Downlink Carrier can be modulated by:

  1. TM only, if there is no RG signal in Uplink;

  2. TM + RG, TM and RG signals in Downlink are simoultaneous if there is RG signal in Uplink;

  3. TC echo, if there is disturbance due to TC echo in Downlink.

  It is also possible to inhibit the output of the entire Uplink budget in cases where only Downlink is applicable.

- Ranging type: Code RG, Tone RG. The presence or absence of RG is defined by the configuration of the Uplink carrier, so this selection is not taken into account when there is no RG. it is also possible to include the budget related to RG Measurement Accuracy.

- TC/TM PCM Code type: NRZ-L (Non-return to zero - level), SP-L (Split phase - level). These are the two types of digital signal waveforms with which the analog signals of CT and TM can be represented using Pulse-Code modulation (PCM):

- TM encoding varies depending on the communication protocol adopted:

  1. CCSDS (Consultative committee for space data systems) is the most common, and implies that TM should be encoded with a combination

of Viterbi convolutional code (rates 1/2, 2/3, 3/4, 5/6 or 7/8 and Reed-Solomon code (255,223 or 255,239) codes;

2. DVB-S2 (Digital video broadcasting - satellite - second generation) involves various combinations (MODCOD) of modulation (QPSK, 8PSK, 16APSK or 32APSK) and FEC (Forward error correction) channel coding with various rates (which depend on the modulation)

3. AX.25 does not provide any encoding for TM

For TC there has hardly been so far any encoding in transmission other than the intrinsic Hamming one, so no choice is made.

- TC/TM BER requirement: from 1.00E-2 to 1.00E-8. Typical values are 1.00E-5 for TC and 1.00E-6 for TM.

Tag	MODULATION CONFIGURATION						
MOD1	Uplink Modulation type	BPSK	▼	TC only	RG only	TC+RG	
MODU	↳ Up Carrier modulated by			Yes	No	No	
MOD2	Downlink Modulation type	BPSK	▼	TM only	TM+RG	TC echo	Dw only
MODD	↳ Dw Carrier modulated by			Yes	No	No	No
MOD3	Ranging type	Code RG	▼				DWO
MOD4	↳ Ranging Measurement Accuracy	No	▼				
	PCM Code type						
MOD5	↳ TC	NRZ-L	▼			COD	DVB
MOD6	↳ TM	NRZ-L	▼	Protocol	Viterbi	R-S	MODCOD
PRT	TM Coding			CCSDS	VT(1/2)	No	No
	BER Requirement						
MOD7	↳ TC	1.00E-05	▼				
MOD8	↳ TM	1.00E-06	▼				

Figure 2.1: *Configuration selection interface*

the 'level' columns indicate the level of the associated parameter (1 to 4): any parameter that has an arrow next to the level may not be entered and is calculated by next-level parameters, which are listed in the 'notes' column (often these are simply the ones below).

2.3.2 Data input

For the available parameters, the user must enter the nominal, adverse and favorable values (in the appropriate column) taking into account the typical value and any maximum, minimum, degradation or margin of error conditions. These parameters are divided into the following categories:

1. G/S Tx channel parameters, for the calculation of G/S EIRP; to be filled only if Uplink is active;

2. G/S Rx channel parameters, for the calculation of G/S G/T;

3. S/C Tx channel parameters, for the calculation of S/C EIRP; to be filled only if Uplink is active;

4. S/C Rx channel parameters, for the calculation of S/C G/T;

5. Earth-to-Space path parameters, for the calculation of Slant range and all the Space losses;

6. Communication parameters, which includes Uplink and Downlink frequencies and data rates, plus all the parameters that characterize the acquisition of Uplink and Downlink carrier and TC, TM and RG signals. The areas to be populated depend on the choice made about the modulating signals in Uplink and Downlink, which will be discussed in Subsections 2.3.3 and 2.3.3;

7. Modulation parameters, for the calculation of Modulation loss. The areas to be populated depend on the choice made about the Uplink and Downlink modulations.

Level			GROUND STATION PARAMETERS	Symbol	m/u	NOM	ADV	FAV
			G/S TRANSMITTING CHANNEL					
1			G/S Antenna Diameter	D	m	10.0	10.0	10.0
1			G/S Antenna Tx Efficiency	η_T	---	0.6	0.6	0.6
1	↘		G/S Axial Ratio	X_G	dB	1.0	1.0	1.0
	2		G/S Crosspolar Discrimination	XPD_G	dB			
1	↘		G/S EIRP	$EIRP_G$	dBW	68.0	68.0	68.0
	2		G/S Transmitted Power	$(P_t)_G$	W			
1	↘		G/S Transmission Loss	$(L_T)_G$	dB			
	2		G/S Tx Chain Loss	$(L_t)_G$	dB			
	2		G/S Tx Antenna Loss	$(L_A)_G$	dB			
1	↘		G/S Antenna Tx Gain	$(G_t)_G$	dBi			
1	→		G/S Half Power Beamwidth (up)	$HPBW_{up}$	deg			

Figure 2.2: *Data input interface (G/S Tx channel section)*

2.3.3 Output tables

Uplink output

The Uplink output table is populated by the program only if the Uplink is active, otherwise it is left empty; it is divided into the following categories:

1. Uplink basic: from G/S Tx channel (S/C EIRP), through Earth-to-Space path and S/C Rx channel, up to the calculation of Uplink $S/N0$ (received at S/C);

2. Uplink Carrier recovery: calculation of Uplink C/N and the Margin for Downlink Carrier acquisition; this section is not active when selecting a modulation with green carrier, which are digital ones, while it is active in case of PM modulation (with s/c or direct);

3. TC recovery: calculation of Uplink Eb/N0 and the Margin for TC acquisition; this section is always active if Uplink is present;

4. RG Carrier recovery: calculation of Uplink RG C/N and the Margin for Downlink RG Carrier acquisition; this section is active only if the Carrier is modulated by TC and RG signal separately;

5. Uplink RG (Major) Tone recovery: calculation of Uplink RG (Mj) Tone SNR

in RG video-BW; this section is active only if there is RG signal. We talk about RG Major Tone if we have Tone RG with a Major and a Minor Tone, otherwise the term 'Major' is omitted.

Downlink output

The Downlink output table is divided into the following categories:

1. Downlink basic: from S/C Tx channel (S/C EIRP), through Earth-to-Space path and G/S Rx channel, up to the calculation of Downlink S/N0 (received at G/S);

2. Downlink Carrier recovery: calculation of Downlink C/N and the Margin for Downlink Carrier acquisition; As for Uplink, this section is also active only in case of PM modulation;

3. TM recovery: calculation of Downlink Eb/N0 and the Margin for TM acquisition; this section is always active;

4. Downlink RG (Major) Tone recovery: calculation of Downlink RG (Mj) Tone SNR in RG video-BW and Margin for RG (Mj) Tone Acquisition; this section is active only if there is RG signal;

5. Downlink RG Minor Tone recovery: calculation of Downlink RG Mn Tone SNR in RG video-BW and Margin for RG Mn Tone Acquisition; this section is active only in case of Tone RG;

6. RG measurement accuracy: calculation of Margin for RG measurement accuracy, depending on the accuracy requirement that has been set; this section is active only if the RG measurement accuracy is active.

Chapter 3

Link Margin evaluation

This chapter discusses all the equations that form the basis for the calculations that constitute the main part of the script, which lead to the evaluation of Link Margin as result.

3.1   Radio frequencies for Space communications

Satellite communications are accomplished by Radio frequencies, which are a part of the Electromagnetic spectrum. With the variety of satellite frequency bands that can be used, designations have been developed so that they can be referred to easily. The higher frequency bands typically give access to wider bandwidths and larger throughput, but are also more susceptible to signal degradation due to rain fade.

Band	Frequency range
VHF	from 30 to 300 MHz
UHF	from 300 MHz to 1 GHz
L-band	from 1 to 2 GHz
S-band	from 2 to 4 GHz
C-band	from 4 to 8 GHz
X-band	from 8 to 12 GHz
Ku-band	from 12 to 18 GHz
K-band	from 18 to 26 GHz
Ka-band	from 26 to 40 GHz

Table 3.1: *Satellite frequency bands*

A parameter directly related to communication frequency is wavelength, the calculation of which, if we consider frequency in MHz, is given by the following formula:

$$\lambda \,[\text{m}] = \frac{c}{f} = \frac{300}{f \,[\text{MHz}]} \tag{3.1}$$

3.2 Uplink and Downlink basic

3.2.1 G/S Transmitting channel (Uplink)

Usually as available data we have:

- G/S Transmitted power $(P_t)_G$ (in W), to be converted in dB;

- G/S Antenna diameter;

- G/S Transmission loss, which is given by the sum of Tx Line and Antenna losses (expressed in dB):

$$(L_T)_G \,[\text{dB}] = (L_t)_G + (L_a)_G \tag{3.2}$$

Antenna Gain

To calculate the EIRP, it is first necessary to know the Antenna Gain, which determines the antenna directional property; it is capability of the antenna to focus the energy into a beam on transmission and to effectively gather the reflected energy during reception.
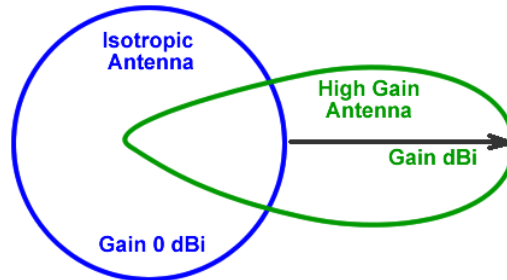
Figure 3.1: *Antenna radiation pattern*

G/S Antenna Gain is sometimes already known from G/S characteristics, but for a Parabolic dish type antenna it can be calculated through a reliable formula given by Antenna theory:

$$(G_t)_G \,[\text{dB}] = 10 \log_{10} \left(\eta_t \frac{\pi D f_{up}}{300} \right)^2 \tag{3.3}$$

where η_t is the G/S Antenna Tx efficiency, usually assumed to be a value between 0.5 and 0.65.

This was the case of Tx Gain, but obviously, the same applies to Rx Gain $(G_r)_G$ considering Antenna Rx efficiency η_r (usually equal to that in Tx) and Downlink frequency f_{dw}

Effective isotropic radiated power

The effective isotropic radiated power (EIRP) is the hypothetical power that would have to be radiated by an isotropic antenna to give the same ("equivalent") signal strength as the actual source antenna in the direction of the antenna's strongest beam. Let us consider to antenna with the same EIRP:

- Low power + High antenna gain = Limited coverage antenna

- High power + Low antenna gain = Higher coverage antenna
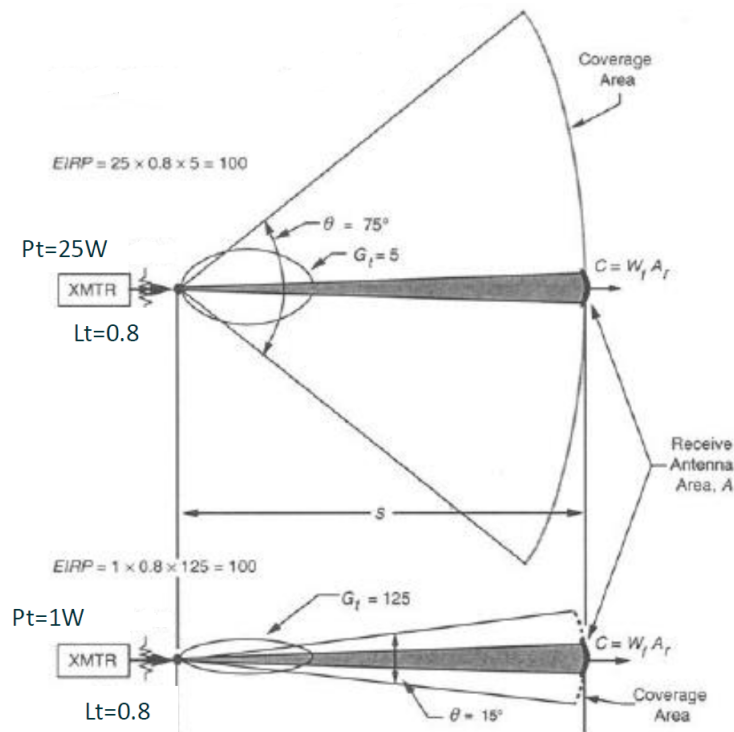
Figure 3.2: *Antenna coverage area*

G/S EIRP is usually one of the main parameters defined by G/S characteristics, but can be calculated as the sum of Tx power and Antenna Gain minus Tx loss (expressed in dB):

$$EIRP\,[dB] = P_t - L_T + G_t \tag{3.4}$$

This equation is valid for both G/S and S/C Tx channels.

Axial ratio and Crosspolar discrimination

The Axial Ratio (AR) of an antenna is defined as the ratio between the major and minor axis of a circularly polarized antenna pattern. If an antenna has perfect circular polarization then this ratio would be 1 (0 dB). However, if the antenna has

an elliptical polarization then this ratio would be greater than 1 ($>$ 0 dB). This ratio tells us the deviation of an antenna from the ideal case of circular polarization over a specified angular range.

Crosspolar discrimination (XPD) is the proportion of signal that is transmitted in the orthogonal polarization to that which is required. In receive mode, it is the antenna's ability to maintain the incident signal's polarization purity. For example, if a perfectly vertically polarized signal (containing no horizontal component) were incident upon a single polarized receive antenna, electrical and mechanical imperfections will introduce a small amount of ellipticity to the polarization of the signal. The signal can be thought of as having both vertical and horizontal components; the ratio of the horizontal to vertical components is the XPD.

These two parameters are related to each other and are necessary for the calculation of Polarization loss. Only one of the parameters is given in the antenna characteristics, so it is important to establish a relationship to calculate one from the other and vice versa (a direct and an inverse formula):

1. XPD calculation from AR:

$$\text{XPD [dB]} = 20 \log_{10}\left(\frac{r+1}{r-1}\right) \tag{3.5}$$

where r is the AR expressed as a number (and not in dB):

$$r = 10^{\frac{\text{AR}}{20}} \tag{3.6}$$

2. AR calculation from XPD:

$$\text{AR [dB]} = 20 \log_{10}(r) \tag{3.7}$$

where r is obtained from XPD by inverting the previous formula

$$r = \frac{10^{\frac{\text{XPD}}{20}} + 1}{10^{\frac{\text{XPD}}{20}} - 1} \tag{3.8}$$

These equations are valid for both G/S and S/C Tx channels.

Half-power beamwidth

Half-power beamwidth (HPBW) is the angular separation in which the magnitude of the radiation pattern decrease by 50% (or -3 dB) from the peak of the main beam. It is an index of signal degradation due to G/S Antenna off-pointing, in fact it is important to extimate Pointing loss.

Uplink and Downlink HPBW for a Parabolic dish Antenna, are calculated from Antenna diameter D and Wavelength λ (both expressed in m):

$$\text{HPBW}_G \text{ [deg]} = 72.8\frac{\lambda}{D} \tag{3.9}$$

For other antenna types, the value must be entered manually by the user.
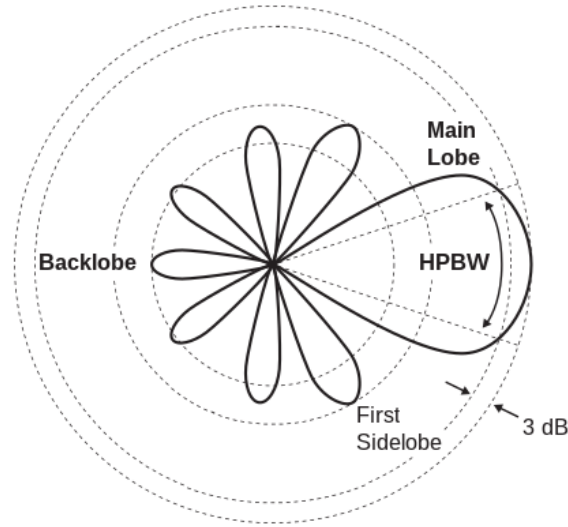
Figure 3.3: *Antenna Half-power beamwidth*

3.2.2 S/C Transmitting channel (Downlink)

S/C EIRP is often given as a known parameter by spacecraft manufacturer, otherwise it can be calculated in a completely analogous way as described for G/S Tx channel.

The only major difference is the calculation of S/C Transmission loss, which are given by the sum of Tx Insertion and Tx Reflection losses (expressed in dB):

$$(L_T)_S \, [\text{dB}] = (L_{\text{ins}T})_S + (L_{\text{ref}T})_S \tag{3.10}$$

Where Tx Reflection loss can be calculated from W_R, which is the product of the individual VSWRs (Voltage standing wave ratio)) of each involved unit (adimensional parameter):

$$(L_{\text{ref}T})_S \, [\text{dB}] = 10 \log_{10} \left[\frac{(1 + W_T)^2}{4 W_T} \right] \tag{3.11}$$

The same is applicable for Rx Reflection loss $(L_{\text{ref}R})_S$, considering instead W_R in the formula.

Another important difference is that the S/C antenna is different from the G/S antenna and definitely not a parabolic dish type (it is probably a patch or dipole type) so the Gain value cannot be calculated through the formula previously discussed, but must be provided from S/C manufacturer.

Moreover, unlike G/S whose axial ratio has a single value, S/C axial ratio can be different in reception and transmission since, for example, the receiving and the transmitting antenna might be different; so it is necessary to separate the values of $(X_R)_S$ and $(X_T)_S$

3.2.3 Earth-to-Space path

The calculation of Total Propagation loss is obtained from the same procedure in both Uplink and Downlink and it is given from the sum of various contributions that are discussed below.

Free Space loss

In Space loss, the governing effect is the quadratic distance effect: signal power distributed over an area decreases with the square of the distance. From the Slant range, whose calculation is discussed in Section 4.1, we calculate Path loss, which depend only on the path traveled by the signal:

$$L_P \ [\text{dB}] = 10 \log_{10}(4\pi 10^6 S^2) \tag{3.12}$$

Then we calculate Free Space loss, which also depend on the communication frequency:

$$L_f \ [\text{dB}] = L_P - 10 \log_{10}\left(\frac{22500}{\pi f}\right) \tag{3.13}$$

Antenna Pointing accuracy loss

Antenna pointing loss is caused by a pointing error between the beam of the two antennas;it strictly depends on the ADCS (Antenna direction control system) accuracy performance and it can be caused, for example, by the effect of wind. It can be calculated from the G/S Antenna Pointing error (or accuracy) θ_u, usually known from G/S characteristics (That you must first convert from deg to rad):

$$u = \frac{\pi D f \sin(\theta_u)}{300} \tag{3.14}$$

$$L_u \ [\text{dB}] = -20 \log_{10}\left(\frac{2 J_1(u)}{u}\right) \tag{3.15}$$

where J_1 is the Bessel function of order 1 of u.

Antenna Pointing offset loss

Antenna Pointing offset loss are caused by a mismatch between the S/C and the target towards which the G/S antenna is pointing; this situation occurs when, for example, the antenna is pointing to a main body, but at the same time it is also necessary to communicate with another object (for example, a small satellite orbiting the mother ship). The distance between the two objects is the Offset distance d_o, and once it is turned into an angular measurement (Pointing offset θ_o), it allows us to calculate Pointing Offset loss:

$$\theta_o = \arcsin\left(\frac{d_o}{S}\right) \tag{3.16}$$

$$L_o \ [\text{dB}] = 12 \left(\frac{\theta_o}{\text{HPBW}}\right)^2 \tag{3.17}$$

Polarization mismatch loss

Polarization mismatch loss occurs when a receiver is not matched to the polarization of an incident electromagnetic field; it is calculated from G/S and S/C Axial ratios and the formula is different in case of nominal, worst or best value:

$$(L_H)_{\text{nom}} \, [\text{dB}] = 10 \log_{10} \left[\frac{4(1 + \text{AR}_S^2)(1 + \text{AR}_G^2)}{(1 + \text{AR}_S)^2(1 + \text{AR}_G)^2} \right] \tag{3.18}$$

$$(L_H)_{\text{worst}} \, [\text{dB}] = 10 \log_{10} \left[\frac{(1 + \text{AR}_S^2)(1 + \text{AR}_G^2)}{(\text{AR}_S + \text{AR}_G)^2} \right] \tag{3.19}$$

$$(L_H)_{\text{best}} \, [\text{dB}] = 10 \log_{10} \left[\frac{(1 + \text{AR}_S^2)(1 + \text{AR}_G^2)}{(\text{AR}_S \text{AR}_G + 1)^2} \right] \tag{3.20}$$

Atmospheric, Ionospheric and Radome losses

Atmospheric loss L_{atm} is due to troposphere layers composition and its value rises as the communication frequency increases; its calculation is very complex and it is fully discussed in Section 4.2.

Ionospheric loss L_{ion} is due to scintillation caused by electrons in the ionosphere, which is neglectable for frequencies above 1 GHz, while for UHF we usually assume a value between 0.2 and 0.4 dB; for lower frequencies (VHF), losses due to ionospheric scintillation can become very high and are predominant over Atmospheric losses.

Radome losses L_{rad} are possibly present when the use of a radome is required, which is a structural, weatherproof enclosure that protects a radar antenna, often used in cold areas to prevent ice and freezing rain from accumulating on antennas. The radome is constructed of material transparent to radio waves, but still causes some loss, whose value is known from G/S characteristic (usually around 0.4 dB).

Total propagation losses and Power flux density

Total propagation loss is given by the sum of Free space, Polarization mismatch, Atmospheric, Ionospheric and Radome contributions (expressed in dB):

$$L_T \, [\text{dB}] = L_f + L_H + L_{\text{atm}} + L_{\text{ion}} + L_{\text{rad}} \tag{3.21}$$

The Power flux density (PFD) is the measure of the strength of the radiation in the far field; Its measuring unit is W/m^2 (Watt per square metre). It characterises the energy flowing per time unit through an area vertical to the distribution direction of the radiation; if the radiation is emitted by an antenna, the greater the distance from the antenna the less the power flux density.

We define the Power Flux density in Free Space at S/C (Uplink) or G/S (Downlink) as:

$$\Phi_f \, [\text{dB}] = \text{EIRP} - L_P \tag{3.22}$$

If we also include all other losses (expressed in dB), we get the power flux density at S/C (Uplink) or G/S (Downlink):

$$\Phi\,[\text{dB}] = \Phi_f - L_H - L_{\text{atm}} - L_{\text{ion}} - L_{\text{rad}} - L_u - L_o \tag{3.23}$$

3.2.4 S/C and G/S Receiving channels

The receiving equipment is characterized by a level of Noise which is due to the fact that metal contains free electrons that speed up as the temperature rises; as they move, they make random currents and hence electromagnetic fields, disturbing the signal on reception. This is why noise can be measured in terms of temperature (K).

System noise temperature

Receiver Noise temperature is the equivalent noise temperature of the receiving system and it is calculated from Rx Line loss L_r and Receiver Noise figure F (both expressed in dB) assuming $T_0 = 290K$, through the equation:

$$T_R\,[\text{K}] = T_0(10^{\frac{L_R}{10}} \cdot 10^{\frac{F}{10}} - 1) \tag{3.24}$$

From this, adding Antenna Noise temperature T_A (expressed in K) we can obtain System Noise temperature:

$$T_s\,[\text{dBK}] = 10\log_{10}(T_A + T_R) \tag{3.25}$$

In this way, a hypothetical theoretical estimate of T_s (and consequently of G/T) can be made by taking the values of the various parameters (which differ for S/C ang G/S Rx channels) from the following table :

	Downlink			Uplink	
Frequency (GHz)	< 2	$2-12$	> 12	< 20	> 20
Rx Line loss (dB)	0.5	0.5	0.5	0.5	0.5
Receiver Noise figure (dB)	0.5	1.0	3.0	3.0	4.0
Receiver Noise temperature (dB)	36	75	289	289	438
Antenna Noise temperature (K)	150	25	100	290	290
System Noise temperature (dB)	23.4	21.3	26.3	27.9	28.8

Table 3.2: *Typical Noise temperatures in clear weather*

Antenna Gain-to-Noise-temperature

Antenna Gain-to-Noise-temperature (G/T) is a figure of merit in the characterization of the Receiving channel performance, which compares the Antenna Rx gain G_r (in dB) and the System Noise temperature T_s (in dBK). It is usually known from S/C manufacturer or G/S characteristics, however, it can also be calculated

by knowing G_r and making an estimate of T_s through through the method that was just discussed (applicable for both S/C and G/S):

For G/S Receiving channel, G/T is simply the difference between G_r and T_s (both expressed in dB):

$$\left(\frac{G}{T}\right)_G \text{[dB/K]} = G_r - T_s \tag{3.26}$$

While for S/C Receiving channel, one must also subtract the contribution related to S/C Rx Reflection loss:

$$\left(\frac{G}{T}\right)_S \text{[dB/K]} = G_r - T_s - (L_{\text{ref}R})_S \tag{3.27}$$

Basic Signal-to-Noise-density ratio

Signal-to-Noise-density ratio (S/N$_0$) is a measure of the strength of the desired signal, received at S/C (Uplink) or G/S (Downlink), compared to background noise (undesired signal); it is calculated as:

$$\frac{S}{N_0} \text{[dB/K]} = \text{EIRP} - L_T - L_o - L_u + \frac{G}{T} - k_b \tag{3.28}$$

Where $k_b = 1.38 \cdot 10^{-23} \frac{\text{W}}{\text{Hz K}} = -228.6 \frac{\text{dBW}}{\text{Hz K}}$ is the Boltzmann costant.

3.3 Uplink and Downlink signal acquisition

3.3.1 Carrier acquisition

A Carrier recovery (also called Coherent demodulation) system is a circuit used to estimate and compensate for frequency and phase differences between a received signal's carrier wave and the receiver's local oscillator for the purpose of coherent demodulation.

In the transmitter of a communications carrier system, a carrier wave is modulated by a baseband signal. At the receiver, the baseband information is extracted from the incoming modulated waveform. In an ideal communications system, the carrier signal oscillators of the transmitter and receiver would be perfectly matched in frequency and phase, thereby permitting perfect coherent demodulation of the modulated baseband signal. However, transmitters and receivers rarely share the same carrier oscillator. Communications receiver systems are usually independent of transmitting systems and contain their oscillators with frequency and phase offsets and instabilities. All these frequencies and phase variations must be estimated using the information in the received signal to reproduce or recover the carrier signal at the receiver and permit coherent demodulation.

Carrier-to-Noise-density ratio

Carrier-to-Noise-density ratio (C/N_0) is the ratio of the Carrier power C to the Noise power density N_0, whcih is defined as the amount of (white) noise energy per bandwidth unit (normalized noise level relative to 1 Hz). It is similar as C/N but C/No does not factor the actual noise bandwidth in.

C/N_0 determines whether a receiver can lock on to the carrier and if the information encoded in the signal can be retrieved, given the amount of noise present in the received signal. The Carrier-to-Noise-density ratio is usually expressed in dBHz.

It is calculated subtracting from basic S/N_0, received at S/C or G/S, the following contributions:

- Carrier modulation (or suppression) loss, whose calculation is discussed in Section 4.3:

    1. Uplink Carrier Modulation loss X_{upC}, for Uplink Carrier acquisition by S/C receiver;

    2. Uplink RG Carrier Modulation loss $(X_{upC})_R$, for Uplink Carrier acquisition by S/C receiver, in case TC and RG are separated;

    3. Downlink Carrier Modulation loss X_{dwC}, for Downlink Carrier acquisition by G/S receiver;

- Carrier acquisition Technical loss, which are the Receiver implementation losses, whose estimation are derived from the Baseband processor analysis and usually we can assume:

    1. S/C Carrier acquisition Technical loss $(L_{th})_{upC}$ = 2 dB (Uplink)

    2. G/S Carrier acquisition Technical loss $(L_{th})_{dwC}$ = 0 dB (Downlink)

$$\frac{C}{N_0} \text{ [dBHz]} = \frac{S}{N_0} - X_C - (L_{th})_C \qquad (3.29)$$

Phase-locked loop

Carrier recovery can be accomplished by a Phase-locked loop (PLL, which is a control system that generates an output signal whose phase is related to the phase of an input signal. The simplest type is an electronic circuit consisting of a variable frequency oscillator and a phase detector in a feedback loop. The oscillator's frequency and phase are controlled proportionally by an applied voltage, hence the term Voltage-controlled oscillator. The oscillator generates a periodic signal of a specific frequency, and the phase detector compares the phase of that signal with the phase of the input periodic signal, to adjust the oscillator to keep the phases matched.

The PLL bandwidth determines the frequency and phase lock time; lower values of loop bandwidth lead to reduced levels of phase noise (which defines the pectral purity of the PLL), but at the expense of longer lock times and less phase margin.

Carrier-to-Noise ratio

Carrier-to-Noise ratio (CNR or C/N) is the Signal-to-Noise ratio (SNR) of a modulated signal; the term is used to distinguish the CNR of the radio frequency passband signal from the SNR of an analog base band message signal after demodulation.

C/N is the ratio of the relative power level to the noise level in the bandwidth of a system; it allows to analyze if a carrier can still be recognized as such or if it is obliterated by ambient and system noise. C/N Provides a value for the quality of a communication channel.

It is calculated from C/N_0 subtracting the PLL (Phase-locked loop) bandwidth (which first has to be converted from Hz to dB):

$$\frac{C}{N} \text{ [dB]} = \frac{C}{N_0} - \text{PLL} \tag{3.30}$$

Link Margin for Carrier acquisition

Link Margin for carrier Acquisition is evaluated, according to ECSS-E-ST-50-05C, comparing the C/N of the system and the required C/N, which is given by the PLL Acquisition treshold:

$$M_C = \frac{C}{N} - \left(\frac{C}{N}\right)_{\text{req}} \tag{3.31}$$

Link margin value says the effective capability of the communication system:

- If $M < 0$ dB, link is not present between trasmitter and receiver;

- If 0 dB $< M < 3$ dB (6 dB for TC), there is link between trasmitter and receiver, but it is unsatisfactory;

- If $M > 3$ dB (6 dB for TC), link between trasmitter and receiver is 'closed' and communication is guaranteed.

Margins from statistical analysis

From the resulting statistical parameters for each acquisition section, the corresponding margins (which should be > 0 dB) can be calculated:

- Mean Margin - 3σ:

$$M_{3\sigma} = M_{\text{mean}} - 3\sigma \tag{3.32}$$

  M_{mean} is calculated considering triangular distribution

- Nominal Margin - worst case RSS:

$$M_{\text{RSS}} = M_{\text{nom}} - \text{RSS} \tag{3.33}$$

3.3.2 Telecommand and Telemetry acquisition

Demodulation means to extract the original information-bearing signal from a carrier wave; a demodulator is an electronic circuit (or computer program in a software-defined radio) that is used to recover the information content, which is TC in Uplink and TM in Downlink, from the modulated carrier wave.

TC/TM Signal-to-Noise-density ratio

TC/TM S/N_0 is calculated subtracting from basic S/N_0, received at S/C or G/S, the following contributions:

- TC/TM Modulation loss, whose calculation is discussed in Section 4.3:

    1. TC Modulation loss X_{TC}, for TC acquisition by S/C;

    2. TM Modulation loss X_{TM}, for TM acquisition by G/S;

- TC/TM Demodulation Technical loss, which are the Demodulator implementation losses, whose estimation are derived from the Baseband processor analysis and usually we can assume:

    1. TC Demodulation Technical loss $(L_{th})_{TC} = 2$ dB (Uplink)

    2. TM Demodulation Technical loss $(L_{th})_{TM} = 1$ dB (Downlink)

$$\left(\frac{S}{N_0}\right)_{TC/TM} [\text{dBHz}] = \frac{S}{N_0} - X_{TC/TM} - (L_{th})_{TC/TM} \tag{3.34}$$

TC/TM Energy-per-bit-to-Noise-power-density ratio

Energy-per-bit-to-Noise-power-density ratio (E_b/N_0); it is a normalized SNR measure, also known as 'SNR per bit', and it is frequently expressed in dB. It is especially useful when comparing the Bit error rate (BER) performance of different digital modulation schemes without taking bandwidth into account; it directly indicates the power efficiency of the system without regard to modulation type, error correction coding or signal bandwidth (including any use of spread spectrum).

The Energy-per-bit is the signal energy associated with each data bit, so it is equal to the signal power divided by the user Bit rate. Therefore we can calculate E_b/N_0 subtracting from TC/TM S/N_0 the TC/TM Bit rate:

$$\left(\frac{E_b}{N_0}\right)_{TC/TM} [\text{dBHz}] = \left(\frac{S}{N_0}\right)_{TC/TM} - R_{TC/TM} \tag{3.35}$$

Link Margin for TC/TM acquisition

Link Margin for TC/TM Acquisition is evaluated comparing the E_b/N_0 of the system and the required E_b/N_0, which is given by the TC/TM Demodulation treshold (discussed in Section 4.4:

$$M_{TC/TM} = \frac{E_b}{N_0} - \left(\frac{E_b}{N_0}\right)_{req} \tag{3.36}$$

3.3.3 Ranging Tone acquisition

Receivers calculate distances to satellites as a function of the amount of time it takes for satellites' signals to reach the ground. To make such a calculation, the receiver must be able to tell precisely when the signal was transmitted and when it was received.

Ranging baseband signal consist of sine wave (RG Tone) which is radiated from G/S to S/C and then back to the ground. In case of Code Ranging, the tone is phase modulated by a series of codes; each code is synchronised to the tone such that phase transitions due to the code occur when the unmodulated tone phase is 90°. Alternatively, in case of Tone Ranging, the system derives range by measuring the phase shift experienced by two tones (Major Tone and Minor Tone), which are then compared in phase with the ground standard; the phase shift of each tone is proportional to twice the Slant range. Ranging modulation shall be PM.

RG Tone Signal-to-noise-density ratio

RG Tone S/N_0 is calculated subtracting from basic S/N_0, received at S/C or G/S, the following contributions:

- RG Tone Modulation loss, whose calculation is discussed in Section 4.3:

    1. Uplink RG (Major) Tone Modulation loss (X_{MT})$_{up}$, for RG acquisition by S/C;

    2. Uplink RG Minor Tone Modulation loss (X_{mt})$_{up}$, for RG acquisition by S/C in case of Tone RG;

    3. Downlink RG (Major) Tone Modulation loss (X_{MT})$_{dw}$, for RG acquisition by G/S;

    4. Downlink RG Minor Tone Modulation loss (X_{mt})$_{dw}$, for RG acquisition by G/S in case of Tone RG;

- RG Demodulation Technical loss, which are the Ranging Demodulator implementation losses, whose estimation are derived from the Baseband processor analysis and usually we can assume:

    1. Uplink RG Demodulation Technical loss $(L_{th})_{upR} = 1$ dB

    2. Downlink RG Demodulation Technical loss $(L_{th})_{dwR} = 1$ dB

$$\left(\frac{S}{N_0}\right)_{MT/mt} [\text{dBHz}] = \frac{S}{N_0} - X_{MT/mt} - (L_{th})_R \tag{3.37}$$

RG Tone Signal-to-noise ratio in RG video-BW

Similar to what was previously discussed for C/N, S/N is calculated from S/N_0 by subtracting RG Loop bandwidth in Uplink or Downlink (which first has to be converted from Hz to dB):

1. Uplink RG Loop bandwidth BW_{upR}

2. Downlink RG Loop bandwidth BW_{dwR}

$$\left(\frac{S}{N}\right)_{MT/mt} [dB] = \left(\frac{S}{N_0}\right)_{MT/mt} - BW_R \tag{3.38}$$

TC and Total Signal-to-noise ratios in RG video-BW

Uplink RG tones SNRs are important for Downlink PM modulation indexes calculation. In case it is necessary to evaluate the effect of the disturbance caused by TC echo in the backward RG signal, it is required to calculate the TC S/N in RG video-BW as it follows:

$$\left(\frac{S}{N}\right)_{TC} [dB] = \frac{S}{N_0} - X_{TC} - (L_{th})_{upR} - BW_{upR} \tag{3.39}$$

For Downlink PM modulation indexes, it is also necessary to calculate the Uplink Total S/N in RG video-BW, which is a linear quantity given by the previous contributions (which instead are expressed in dB):

$$\left(\frac{S}{N}\right)_{tot} [\text{linear}] = 1 + 10^{\frac{(S/N)_{MT}}{10}} + 10^{\frac{(S/N)_{mt}}{10}} + 10^{\frac{(S/N)_{TC}}{10}} \tag{3.40}$$

Link Margin for RG Tone acquisition

Link Margin for RG Tone Acquisition in Downlink (the signal must make round trip) is evaluated comparing the S/N of the system and the required S/N, also known as Required RG Loop SNR:

$$M_{MT/mt} = \frac{S}{N} - \left(\frac{S}{N}\right)_{req} \tag{3.41}$$

3.3.4 Ranging Measurement accuracy

Margin calculation to determine whether the power of the backward ranging signal is sufficient to ensure a certain accuracy set as a requirement by the user. defined as RG Measurement accuracy requirement σ_R.

RG Measurement accuracy treshold

The S/N required for Measurement accuracy depends on the RG Measurement accuracy requirement σ_R and RG (Major) Tone frequency f_{MT}:

$$\left(\frac{S}{N}\right)_{acc} = -10 \log_{10}(2) + 20 \log_{10}\left(\frac{75000}{\pi f_{MT} \sigma_R}\right) \tag{3.42}$$

RG Code modulation loss

The modulation loss for RG Measurement accuracy depends on the RG Code modulation index, which is the Measurement phase θ_m

$$X_{\text{acc}} = -20 \log_{10} \left[\cos(\theta_m) \right] \tag{3.43}$$

Link Margin for RG Measurement accuracy

Link Margin for RG Measurement accuracy in Downlink is calculated subtracting these two contributions from the Downlink RG (Major) Tone S/N RG video-BW:

$$M_{\text{acc}} = \left(\frac{S}{N} \right)_{\text{MT}} - \left(\frac{S}{N} \right)_{\text{acc}} - X_{\text{acc}} \tag{3.44}$$

Chapter 4

Reference Theories and Standards

In this chapter we discuss in detail the theories and standards which are the references of the script subfunctions for calculating the Slant range, Atmospheric loss, Modulation loss, and Demodulation treshold

4.1 Slant range

Slant range (or slant distance) is the distance along the relative direction between two points; if the two points are at the same level, the Slant distance equals the horizontal distance. The calculation is quite different depending on the mission orbit.

4.1.1 LEO, MEO and LEOP configurations

For Low and Medium Earth orbits (LEO, MEO) the Slant range is calculated from Equatorial Earth radius R, Orbit height h_g (expressed in km) and Antenna min elevation ε:

$$S\,[\text{km}] = \sqrt{(R+h)^2 - R^2 \cos^2(\varepsilon)} - R\sin(\varepsilon) \tag{4.1}$$

Since we are considering the worst case scenario, it is good to choose an Antenna elevation of $\varepsilon = 5°$, in order to maximize the Slant range. in case of Launch and Early orbit phase (LEOP), the process is the same, considering that as orbit height is taken that of the GEO configuration (discussed just ahead).
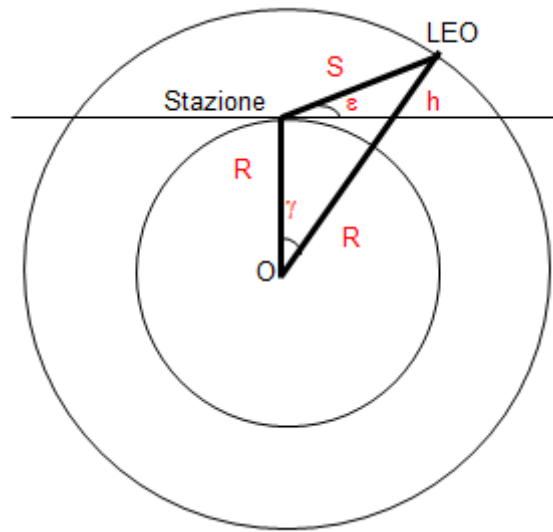
Figure 4.1: *LEO Slant range*

4.1.2 GEO configuration

A Geostationary Earth orbit (GEO) is a circular geosynchronous orbit above the equator and following the direction of Earth's rotation. Communications satellites are often placed in a Geostationary orbit so that Earth-based satellite antennas (located on Earth) do not have to rotate to track them but can be pointed permanently at the position in the sky where the satellites are located. The characteristics of a GEO satellite are:

- S/C latitude $\theta_S = \psi_S = 0°$, because the orbit is equatorial;

- S/C height is fixed at $h_S = 35786.0115$ km

G/S latitude θ_G, G/S height h_G and S/C height h_S are given as geodetic coordinates, for slant range calculation one needs to convert them to geocentric coordinates, taking into account that:

- Hearth equatorial radius is $R_q = 6378.16$ km

- Hearth polar radius is $R_p = 6356.778$ km

Hearth eccentricty is:

$$e = \sqrt{\frac{R_q^2 - R_p^2}{R_q}} \tag{4.2}$$

G/S geocentric longitude:

$$\psi_G \, [\text{deg}] = \arctan\left[\left(R_q(1 - e^2) + h_G\sqrt{1 - \left[e\sin(\theta_G)\right]^2}\right) \frac{\tan(\theta_G)}{R_q + h_G\sqrt{1 - \left[e\sin(\theta_G)\right]^2}}\right] \tag{4.3}$$

G/S height from the center of Hearth:

$$R_G \text{ [km]} = \sqrt{h_G^2 + 2R_q h_G \sqrt{1 - e \sin^2(\theta_G)} + \frac{R_q^2 \left[1 - e^2(2 - e^2)\sin^2(\theta_G)\right]}{1 - \left[e \sin(\theta_G)\right]^2}} \qquad (4.4)$$

S/C height from the center of Hearth:

$$R_S \text{ [km]} = \sqrt{h_S^2 + 2R_q h_S \sqrt{1 - e \sin^2(\theta_S)} + \frac{R_q^2 \left[1 - e^2(2 - e^2)\sin^2(\theta_S)\right]}{1 - \left[e \sin(\theta_S)\right]^2}} \qquad (4.5)$$

G/S longitude ϕ_G and S/C longitude ϕ_S are already expressed in geocentric terms At this point one can calculate the Slant range:

$$\Gamma = \cos(\psi_G)\cos(\psi_S)\cos(\phi_S - \phi_G) + \sin(\psi_G)\sin(\psi_S) \qquad (4.6)$$

$$S \text{ [km]} = \sqrt{R_G^2 + R_S^2 - 2R_G R_S \Gamma} \qquad (4.7)$$

In case of geostationary orbit, Antenna elevation is not entered by the user but depends on Slant range, G/S and S/C positions:

$$\Omega = R_S\big(\cos(\psi_S)\cos(\theta_G)\cos(\phi_S - \phi_G) + \sin(\psi_S)\sin(\theta_G)\big) - R_G\cos(\psi_G - \theta_G) \qquad (4.8)$$

$$\varepsilon = \arcsin\left(\frac{|\Omega|}{S}\right) \qquad (4.9)$$

4.2 Atmospheric loss

While the ionosphere is the primary source of transmission impairments on satellite communications links operating in the frequency bands up to about 1 GHz, many satellite communications links operate in the frequency bands above 1 GHz, where the primary source of transmission impairments is the troposphere. In this chapter, for Atmospheric loss we mean those due to the troposphere and The impairments discussed here are Gaseous attenuation, Cloud attenuation, Rain attenuation and wet surface effects. We focus here on line-of-site link impairments, so additional effects (such as shadowing, blockage and multipath scintillation) are not taken into account.

Total atmospheric loss is calculated from the various contributions (expressed in dB) according to this approximate formula:

$$L_{\text{atm}} \text{ [dB]} = A_g + \sqrt{(A_c + A_r)^2 + A_s^2} \qquad (4.10)$$

Atmospheric model is plagued by uncertainty, which can be assumed to be 25% according to ITU-R P.618-13.

An excellent source to provide predictions of attenuations due to atmosphere are the procedures developed by the ITU-R, which require weather parameters that can be estimated by ITU-R global maps. The various parameters involved will be discussed in the appropriate sections. A database is implemented in the code containing text maps reporting the values of all necessary parameters as a function of latitude and longitude of the GS.

For the extraction of these parameters, a routine was especially created that transforms the latitude and longitude values into indices for moving around in the maps. The maps were derived from 2 years of data with a with a certain spatial resolution in latitude and longitude, so that there is; the latitude grid of the data files is from -90° to +90° , the longitude grid is from -180° to +180°. For a location different from the gridpoints, the data at the desired location is obtained by performing a bilinear interpolation on the values at the four closest grid points.

Listing 4.1: *"importfile" function calling*

```
 1  LAT_frac = (90+LAT)/0.75+1;
 2  LONG_frac = (180+LONG)/0.75+1;
 3  LAT_int = fix(LAT_frac);
 4  LONG_int = fix(LONG_frac);
 5  X1 = map(LAT_int,LONG_int);
 6  X2 = map(LAT_int,LONG_int+1);
 7  X3 = map(LAT_int+1,LONG_int);
 8  X4 = map(LAT_int+1,LONG_int+1);
 9  X = X1*(LAT_int+1—LAT_frac)*(LONG_int+1—LONG_frac) + ...
10      X2*(LAT_int+1—LAT_frac)*(LONG_frac—LONG_int) + ...
11      X3*(LAT_frac—LAT_int)*(LONG_int+1—LONG_frac) + ...
12      X4*(LAT_frac—LAT_int)*(LONG_frac—LONG_int);
```

4.2.1   Gaseous attenuation

A radiowave propagating through the Earth's atmosphere will experience a reduction in signal level due to the gaseous components present in the transmission path. Signal degradation can be minor or severe, depending on frequency, temperature, pressure and water vapor concentration. The principal interaction mechanism involving gaseous constituents and the radiowave is molecular absorption, which results in a reduction in signal amplitude (attenuation) of the signal. The absorption of the radiowave results from a quantum level change in the rotational energy of the molecule, and occurs at a specific resonant frequency or narrow band of frequencies: the resonant frequency of interaction depends on the energy levels of the initial and final rotational energy states of the molecule.

The principal components of the atmosphere, and their approximate percentage by volume, are: oxygen (21%), nitrogen (78%), argon (0.9%), carbon dioxide (0.1%) and water vapor (variable, $\approx$1.7% at sea level and 100% relative humidity). Only oxygen and water vapor have observable resonance frequencies in the

bands of interest for space communications; oxygen absorption involves magnetic dipole changes, whereas water vapor absorption consists of electric dipole transitions between rotational states.
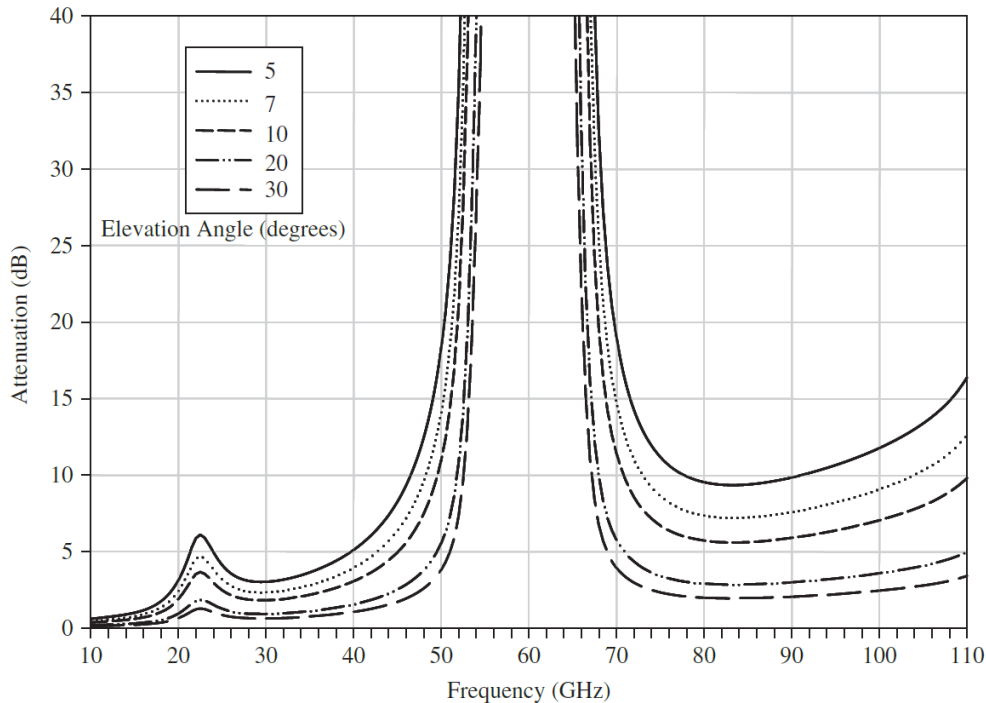
Figure 4.2: *Gas attenuation for Washington DC*

in figure 4.2 the values for the U.S. standard atmosphere were assumed. The stark effect of the oxygen absorption lines at around 60 GHz is seen, while the water vapor absorption line is observed at 22.3 GHz. As the elevation angle decreases, the path length through the troposphere increases, and the resultant total attenuation increases as well.

ITU-R Gaseous Attenuation approximation model

The ITU-R has provided a simplified calculation for a specific range of meteorological conditions and geometrical configurations, that fit our case study. This approximation method, given in Annex 2 of ITU-R P.676-10, provides predictions for frequencies from 1 to 350 GHz, for ground stations from sea level to an altitude of 10 km and for elevation angles from 5° to 90°.

Input parameters required for the calculations:

- Frequency f (GHz);

- Elevation angle θ (deg);

- Surface pressure p = 1013 hPa;

- Air temperature T (K), from global map provided in ITU-R P.836-6;

- Water vapour density ρ (g/m^3), from global map provided in ITU-R P.836-6.

There are two additional adimensional parameters required for the calculations:

$$r_p = \frac{p}{1013} \qquad r_t = \frac{288}{T} \qquad (4.11)$$

Specific attenuation for dry air

The specific attenuation for dry air is determined from an algorithm which depends on the frequency of operation; for $f \leq 54$ GHz:

$$\gamma_0 \text{ [dB/km]} = \left[\frac{7.2 r_t^{2.8}}{f^2 + 0.34 r_p^2 r t^{1.6}} + \frac{0.62 \xi_3}{(54 - f)^{1.16 \xi_1} + 0.83 \xi_2} \right] f^2 r_p^2 \cdot 10^{-3} \qquad (4.12)$$

where:

$$\xi_1 = \varphi(r_p, r_t, 0.0717, -1.8132, 0.0156, -1.6515) \qquad (4.13)$$

$$\xi_2 = \varphi(r_p, r_t, 0.5146, -4.6368, -0.1921, -5.7416) \qquad (4.14)$$

$$\xi_3 = \varphi(r_p, r_t, 0.3414, -6.5851, 0.2130, -8.5854) \qquad (4.15)$$

$$\varphi(r_p, r_t, a, b, c, d) = r_p^a r_t^b \exp[c(1 - r_p) + d(1 - r_t)] \qquad (4.16)$$

Specific attenuation for water vapour

The specific attenuation for water vapour for frequencies from 1 to 350 GHz is determined by:

$$
\begin{aligned}
\gamma_0 \text{ [dB/km]} = \bigg\{ & \frac{3.98 \eta_1 \exp[2.23(1 - r_t)]}{(f - 22.235)^2 + 9.42 \eta_1^2} g(f, 22) + \frac{11.96 \eta_1 \exp[0.7(1 - r_t)]}{(f - 183.31)^2 + 11.41 \eta_1^2} \\
& + \frac{0.081 \eta_1 \exp[6.44(1 - r_t)]}{(f - 321.226)^2 + 6.29 \eta_1^2} + \frac{3.66 \eta_1 \exp[1.6(1 - r_t)]}{(f - 325.153)^2 + 9.22 \eta_1^2} \\
& + \frac{25.37 \eta_1 \exp[1.09(1 - r_t)]}{(f - 380)^2} + \frac{17.4 \eta_1 \exp[1.46(1 - r_t)]}{(f - 488)^2} \\
& + \frac{844.6 \eta_1 \exp[0.17(1 - r_t)]}{(f - 557)^2} g(f, 557) \\
& + \frac{290 \eta_1 \exp[0.41(1 - r_t)]}{(f - 752)^2} g(f, 752) \\
& + \frac{8.3328 \cdot 10^4 \eta_2 \exp[0.99(1 - r_t)]}{(f - 1780)^2} g(f, 1780) \bigg\} f^2 r_t^2 \rho \cdot 10^{-4}
\end{aligned}
\qquad (4.17)
$$

where:

$$\eta_1 = 0.955 r_p r_t^{0.68} + 0.006 \rho \qquad (4.18)$$

$$\eta_2 = 0.735 r_p r_t^{0.5} + 0.0353 r_t^4 \rho \qquad (4.19)$$

$$g(f, f_i) = 1 + \left(\frac{f - f_i}{f + f_i} \right)^2 \qquad (4.20)$$
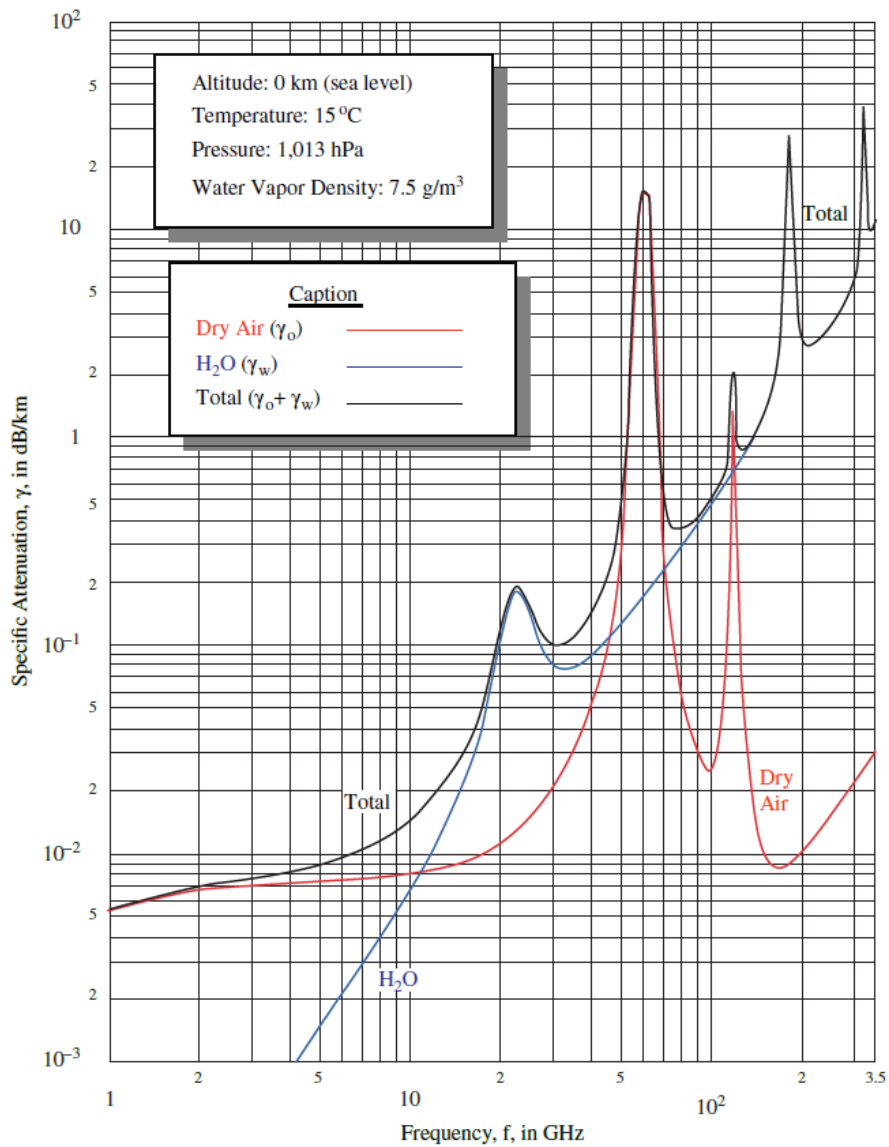
Figure 4.3: *Specific attenuation due to atmospheric gases*

Equivalent height for dry air

The concept of equivalent height is based on the assumption of an exponential atmosphere profile specified by a scale height to describe the decay in density with altitude; The equivalent heights are dependent on pressure, and can be used for altitudes up to about 10 km.

The Equivalent height for dry air is determined from the following:

$$h_0 \, [\text{km}] = \frac{6.1}{1 + 0.17 r_p^{-1.1}} (1 + t_1 + t_2 + t_3) \tag{4.21}$$

where:

$$t_1 = \frac{4.64}{1 + 0.066 r_p^{-2.3}} \exp\left[-\left(\frac{f - 59.7}{2.87 + 12.4 \exp(-7.9 r_p)}\right)\right] \tag{4.22}$$

34

$$t_2 = \frac{0.14 \exp(2.12 r_p)}{(f - 118.75)^2 + 0.031 \exp(2.2 r_p)} \tag{4.23}$$

$$t_3 = \frac{0.0114}{1 + 0.14 r_p^{-2.6}} f \frac{-0.0247 + 0.0001 f + 1.61 \cdot 10^{-6} f^2}{1 - 0.0169 f + 4.1 \cdot 10^{-5} f^2 + 3.2 \cdot 10^{-7} f^3} \tag{4.24}$$

Equivalent height for water vapour

The Equivalent height for water vapour is determined from:

$$
\begin{aligned}
h_w \text{ [km]} = 1.66 \Bigg(1 + & \frac{1.39 \sigma_w}{(f - 22.235)^2 + 2.56 \sigma_w} + \frac{3.37 \sigma_w}{(f - 183.31)^2 + 4.69 \sigma_w} \\
& + \frac{1.58 \sigma_w}{(f - 325.1)^2 + 2.89 \sigma_w} \Bigg)
\end{aligned} \tag{4.25}
$$

where:

$$\sigma_w = \frac{1.013}{[1 + \exp(-8.6(r_p - 0.57))]} \tag{4.26}$$

Total path attenuation

The Total Zenith angle attenuation corresponds to a elevation angle of 90° and is found as:

$$A_z \text{ [dB]} = \gamma_0 h_0 + \gamma_w h_w \tag{4.27}$$

The simple cosecant law can be used to calculate the Total path gaseous attenuation from the Zenith attenuation, for Elevation angles in the range $5° \leq \theta \leq 90°$:

$$A_g \text{ [dB]} = \frac{A_z}{\sin(\theta)} \tag{4.28}$$

4.2.2 Cloud attenuation

Although rain is the most significant hydrometeor affecting radiowave propagation, the influence of clouds and fog can also be present on an earth-space path and must also be considered. Clouds and fog generally consist of hydrosols, which are suspended droplets of liquid water which are typically less than 0.1 mm in diameter, whereas raindrops typically range from 0.1 mm to 10 mm in diameter. Clouds are water droplets, not water vapor, however the relative humidity is usually near 100% within the cloud.

Attenuation due to fog is extremely low for frequencies less than about 100 GHz; since the total path of a satellite link through the fog, even for low elevation angles, is short (on the order of hundreds of meters) the total attenuation caused by fog can be neglected on consideration of links below 100 GHz. We will focus on the effects of clouds in the remainder of this section. The average liquid water content of clouds varies widely, ranging from 0.05 to over 2 g/m^3. Peak values exceeding 5 g/m^3 have been observed in large cumulus clouds associated with thunderstorms; however, peak values for fair weather cumulus are generally less than 1 g/m^3.
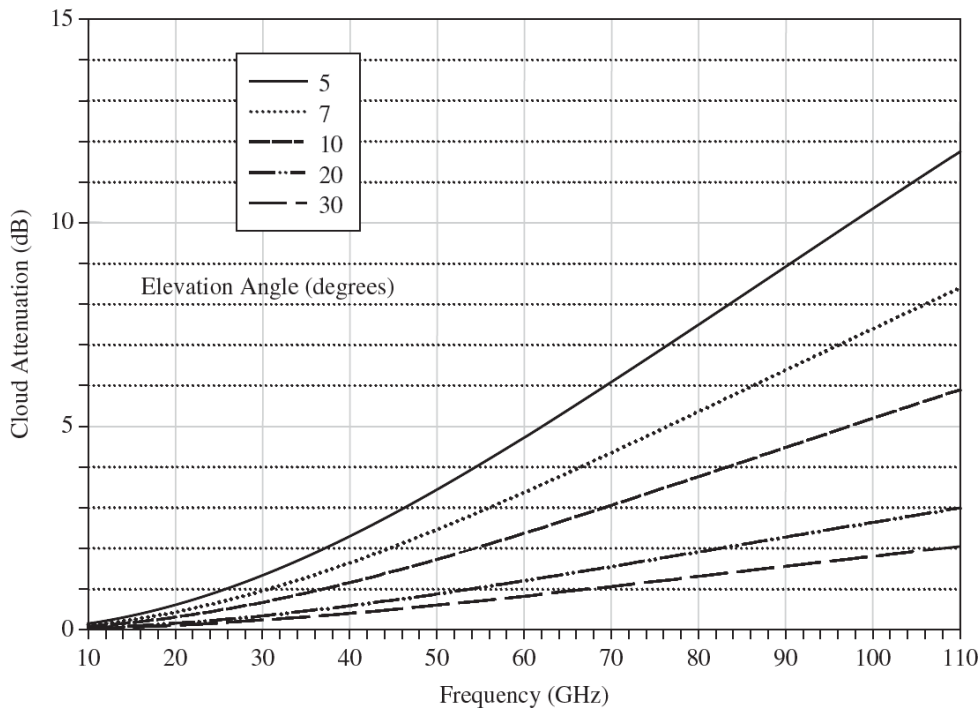
Figure 4.4: *Cloud attenuation for Washington DC*

The calculations for figure 4.4 were based on stratus clouds with a cloud depth of 0.67 km, cloud bottom of 0.33 km, and a liquid water content of 0.29 g/m^3. The cloud attenuation is seen to increase with frequency and with decreasing elevation angle.

The attenuation caused by hydrosols becomes significant particularly for systems operating above 20 GHz. For high margin systems rain attenuation is the dominant impairment, however for low margin systems and higher frequencies, clouds represent an important impairment. Rain occurs less than about 5-8% of the time, whereas clouds are present 50% of the time on average and can have constant coverage for continuous intervals up to several weeks.

ITU-R Cloud attenuation model

The ITU-R provides a model to calculate the attenuation along an Earth-space path for both clouds and fog in Recommendation ITU-R P.840-8; it is valid for liquid water only and is applicable for systems operating at up to 200 GHz.

Input parameters required for the calculations:

- Frequency *f* (GHz);
- Elevation angle *θ* (deg);
- Air temperature *T* (K), which is discussed right after;

- Total columnar liquid water content L (kg/m^2), from global map provided in ITU-R P.836-6;

An intermediate parameter required for the calculation is the Inverse temperature constant:

$$\Phi = \frac{300}{T} \tag{4.29}$$

For cloud attenuation, we assume T = 273.15 K, therefore Φ = 1.098.

Complex Dielectric permittivity

Calculate the Principal and Secondary Relaxation frequencies of the double-Debye model for the dielectric permittivity of water:

$$f_p = 20.09 - 142(\Phi - 1) + 294(\Phi - 1)^2 \tag{4.30}$$

$$f_s = 590 - 1500(\Phi - 1) \tag{4.31}$$

Calculate the Real and Imaginary components of the Complex Dielectric permittivity of water from:

$$\varepsilon''(f) = \frac{f(\varepsilon_0 - \varepsilon_1)}{f_p\left[1 + \left(\frac{f}{f_p}\right)^2\right]} + \frac{f(\varepsilon_1 - \varepsilon_2)}{f_s\left[1 + \left(\frac{f}{f_p}\right)^2\right]} \tag{4.32}$$

$$\varepsilon'(f) = \frac{\varepsilon_0 - \varepsilon_1}{1 + \left(\frac{f}{f_p}\right)^2} + \frac{\varepsilon_1 - \varepsilon_2}{1 + \left(\frac{f}{f_p}\right)^2} + \varepsilon_2 \tag{4.33}$$

where:

$$\varepsilon_0 = 77.6 + 103.3(\Phi - 1) \qquad \varepsilon_1 = 5.48 \qquad \varepsilon_2 = 3.51 \tag{4.34}$$

Specific attenuation coefficient

Calculate the Specific attenuation coefficient from:

$$K_l\left[\frac{\text{dB/km}}{\text{g/m}^3}\right] = \frac{0.819f}{\varepsilon''(1 + \eta)} \tag{4.35}$$

where

$$\eta = \frac{2 + \varepsilon'}{\varepsilon''} \tag{4.36}$$

Total attenuation

Determined the Columnar liquid water content of the cloud from ITU-R global maps, considering a Probability of exceedance of 1%. The Total Cloud attenuation is then found as:

$$A_c\,[\text{dB}] = \frac{LK_l}{\sin(\theta)} \tag{4.37}$$

valid for $5° \le \theta \le 90°$; for elevation angles below about $5°$ the $1/\sin(\theta)$ relationship cannot be employed, since this would assume a cloud of nearly infinite extent.

4.2.3 Rain attenuation

The presence of rain on the transmission path becomes an increasingly important effect as the frequency of operation increases and it is particularly significant for frequencies of above 10 GHz. Raindrops absorb and scatter radiowave energy, resulting in Rain attenuation, a reduction in the transmitted signal amplitude which can degrade the reliability and performance of the communications link; this phenomenon is also called Rain fade.

The attenuating effect of the troposphere is affected by macroscopic and microscopic characteristics of rain systems; the macroscopic characteristics include size, distribution, and movements of rain cells, the height of melting layers, and the presence of ice crystals, while the microscopic characteristics include the size distribution, density, and shape (oblateness) of both raindrops and ice crystals.
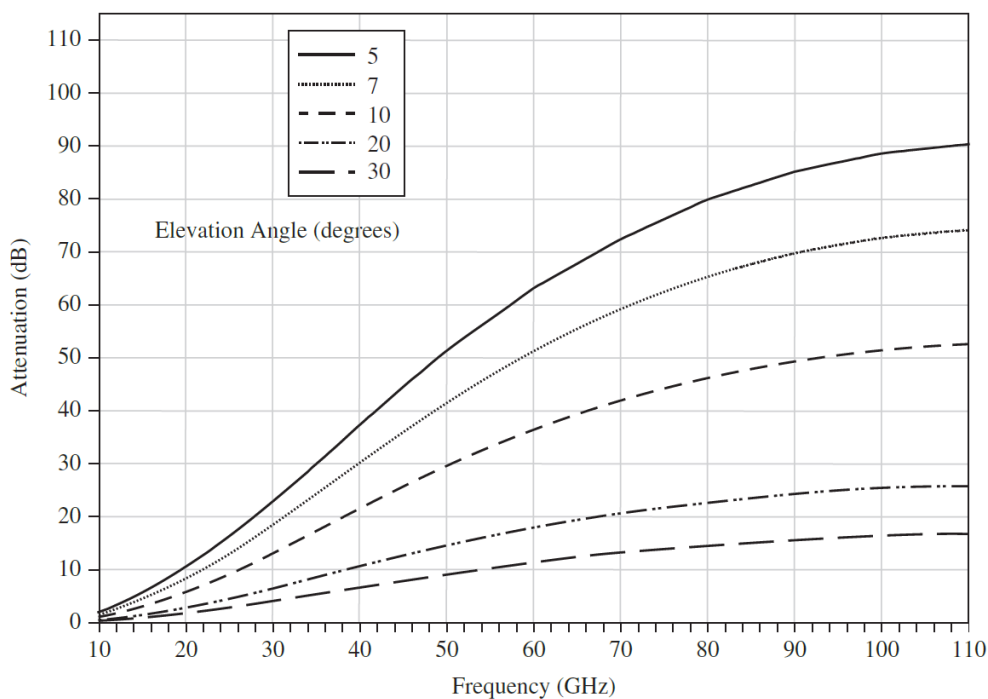
Figure 4.5: *Rain attenuation for Washington DC, Link availability 99%*

Several general characteristics of rain attenuation are seen on figure 4.5. Rain attenuation increases with increasing frequency, and with decreasing elevation angle. These plots are for a 99% annual link availability, which corresponds to a link outage (unavailability) of 1% or about 88 hours per year. Rain attenuation can be very high and, above about 10 GHz, it becomes the dominant impairment to wave propagation through the troposphere.

ITU-R Rain attenuation model

This section describes the ITU-R model as presented in the latest version of recommendation ITU-R P.618-13; other ITU-R reports referred to in the rain model

procedure are ITU-R Recommendations P.837-7, P.838-3, P.839-4, and P.678-3. The ITU-R states that the modeling procedure estimates annual statistics of path attenuation at a given location for frequencies up to 55 GHz.

Input parameters required for the calculations:

- Frequency f (GHz);

- Elevation angle θ (deg);

- Latitude of the ground station φ (deg);

- Polarization tilt angle with respect to the horizontal τ (deg);

- Altitude of the ground station above sea level h_S (km);

- Average annual $0°C$ isotherm height h_0 (km), from global map provided in ITU-R P.839-4;

- Point Rainfall rate for the location of interest for 0.01% of an average year $R_{0.01}$ (mm/h), from global map provided in ITU-R P.837-7.

Rain height at the ground station of interest

Calculate the Rain height at the ground station of interest from:

$$h_R \text{ [km]} = h_0 + 0.36 \tag{4.38}$$

The Average annual $0°C$ isotherm height h_0 is the upper atmosphere altitude at which rain is in the transition state between rain and ice; the rain height is defined in km above sea level.

Slant path length and Horizontal projection

Calculate the Slant path length and Horizontal projection from rain height, elevation angle and altitude of the ground receiver site. Rain attenuation is directly proportional to the Slant path length, which is defined as the length of the satellite-to-ground path that is affected by a rain cell, as shown in Figure 4.6.

The Slant path length, expressed in km, for $\theta \geq 5°$ is determined from:

$$L_S(\theta) \text{ [km]} = \frac{h_R - h_S}{\sin(\theta)} \tag{4.39}$$

The slant path length can result in negative values when the Rain height is smaller than the altitude of the ground receiver site; if a negative value occurs, the slant path length is set to zero.

The Horizontal projection is calculated as:

$$L_G(\theta) \text{ [km]} = L_S \cos(\theta) \tag{4.40}$$

A: frozen precipitation
B: rain height
C: liquid precipitation
D: earth-space path
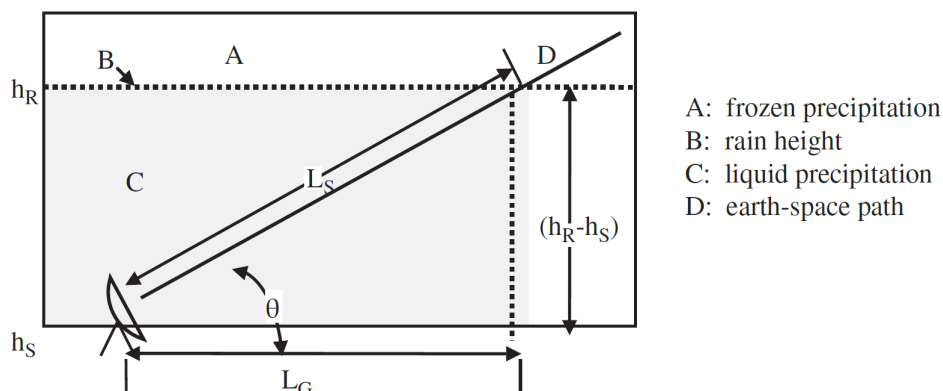
Figure 4.6: *Slant path through rain scheme*

Specific attenuation

Once obtained the Rainfall rate at 0.01% outage from the rain intensity maps for the geographic location of interest, the Specific attenuation is calculated from:

$$\gamma_R \ [\text{dB/km}] = k R_{0.01}^{\alpha} \tag{4.41}$$

where k and α are dependent variables of frequency, elevation angle and polarization tilt angle; they are calculated using Regression coefficients k_H, k_V, α_H and α_V at the frequency of interest, from the following:

$$k = \frac{k_H + k_V + (k_H - k_V)\cos^2(\theta)\cos(2\tau)}{2} \tag{4.42}$$

$$\alpha = \frac{k_H \alpha_H + k_V \alpha_V + (k_H \alpha_H - k_V \alpha_V)\cos^2(\theta)\cos(2\tau)}{2k} \tag{4.43}$$

where $\tau = 45°$ for circular polarization transmissions.

Values for the Regression coefficients are determined as functions of frequency in the range from 1 to 1000 GHz; for linear and circular polarization they can be calculated from the following equations:

$$\log_{10}(k_{H/V}) = \sum_{j=1}^{4}\left(a_j \exp\left[-\left(\frac{\log_{10}(f) - b_j}{c_j}\right)^2\right]\right) + m_k \log_{10}(f) + c_k \tag{4.44}$$

$$\alpha_{H/V} = \sum_{j=1}^{4}\left(a_j \exp\left[-\left(\frac{\log_{10}(f) - b_j}{c_j}\right)^2\right]\right) + m_\alpha \log_{10}(f) + c_\alpha \tag{4.45}$$

Table C.1 in appendix C shows the values for the constants for the coefficients k_H for horizontal polarization, k_V for vertical polarization, α_H for horizontal polarization and C_V for vertical polarization, respectively.

Effective Path length

The Horizontal reduction factor for 0.01% is determined as follows:

$$r_{0.01} = \frac{1}{1 + 0.78\sqrt{\frac{L_G \gamma_R}{f}} - 0.38(1 - e^{-2L})} \qquad (4.46)$$

The Vertical adjustment factor for 0.01% of the time is:

$$v_{0.01} = \frac{1}{1 + \sqrt{\sin(\theta)} \left[31 \left(1 - e^{-\frac{\theta}{1+\chi}} \right) \frac{\sqrt{L_R \gamma_R}}{f^2} - 0.45 \right]} \qquad (4.47)$$

where:

$$L_R \text{ [km]} = \begin{cases} \dfrac{L_G \, r_{0.01}}{\cos(\theta)} & \text{for } \zeta > \theta \\[2mm] \dfrac{h_R - h_S}{\sin(\theta)} & \text{for } \zeta \leq \theta \end{cases} \qquad (4.48)$$

$$\zeta \text{ [deg]} = \arctan \left(\frac{h_R - h_S}{L_G \, r_{0.01}} \right) \qquad (4.49)$$

$$\chi \text{ [deg]} = \begin{cases} 36 - |\varphi| & \text{for } |\varphi| < 36° \\ 0 & \text{for } |\varphi| \geq 36° \end{cases} \qquad (4.50)$$

The Effective path length is determined from:

$$L_E \text{ [km]} = L_R \, v_{0.01} \qquad (4.51)$$

Total attenuation

The predicted Attenuation exceeded for 0.01% of an average year is determined from:

$$A_{0.01} \text{ [dB]} = \gamma_R \, L_E \qquad (4.52)$$

The Attenuation exceeded for other percentages p of an average year, in the range from 0.001% to 5%, can be determined from:

$$A_p \text{ [dB]} = A_{0.01} \left(\frac{p}{0.01} \right)^{-[0.655 + 0.033 \ln(p) - 0.045 \ln(A_{0.01}) - \beta(1-p)\sin(\theta)]} \qquad (4.53)$$

where:

$$\beta = \begin{cases} 0 & \text{if } p \geq 1\% \text{ or } |\varphi| \geq 36° \\ -0.005(|\varphi| - 36) & \text{if } p < 1\% \text{ and } |\varphi| < 36° \text{ and } \theta \geq 25° \\ -0.005(|\varphi| - 36) + 1.8 - 4.25\sin(\theta) & \text{otherwise} \end{cases} \qquad (4.54)$$

This method provides an estimate of long-term statistics due to rain, large year-to-year variability in rainfall statistics can be expected when comparing the predicted results with measured statistics

4.2.4 Tropospheric Scintillation

Scintillation describes the condition of rapid fluctuations of the signal parameters of a radiowave caused by time dependent irregularities in the transmission path; signal parameters affected include amplitude, phase, angle of arrival and polarization. Scintillation effects can be produced in both the ionosphere and in the troposphere.

Tropospheric scintillation is produced by refractive index fluctuations in the first few kilometers of altitude and is caused by high humidity gradients and temperature inversion layers; the effects are seasonally dependent, vary day to day, and vary with the local climate. To a first approximation, the refractive index structure in the troposphere can be considered horizontally stratified, and variations appear as thin layers that change with altitude.

Slant paths at low elevation angles, that is highly oblique to the layer structure, thus tend to be effected most significantly by scintillation conditions, since the path interaction region increases; scintillation effects increase dramatically as the elevation angle drops below $10°$.

ITU-R Scintillation model

ITU-R recommendation P.618-13 provides a quick and effective method to estimate the statistics of tropospheric scintillation from local environmental parameters. This procedure is recommended for applications up to at least 20 GHz and for elevation angles $\theta \geq 4°$.

Input parameters required for the calculations:

- Frequency f (GHz);
- Elevation angle θ (deg);
- Physical diameter of the ground station antenna D (m);
- Antenna efficiency η;
- Altitude of the ground station above sea level h_S (km);
- Average surface ambient temperature T (K) at the site, from global map provided in ITU-R P.836-6;
- Wet term of the radio refractivity N_{wet} (hPa/K^2) at the site, from global map provided in ITU-R P.453-14.

Standard deviation of the signal amplitude

The ITU-R model calculates the standard deviation of the instantaneous signal amplitude (amplitude expressed in dB), which is often referred to as the scintillation intensity. Scintillation intensity increases with increasing frequency, temperature and humidity, and decreases with increasing antenna size and elevation angle as specified by the ITU-R model.

42

The standard deviation of the signal amplitude is determined from the Wet term of the radio refractivity, which incorporates the contibutes of saturation water vapour pressure, temperature and average surface relative humidity:

$$\sigma_{\text{ref}} \text{ [dB]} = 3.6 \cdot 10^{-3} + N_{\text{wet}} \cdot 10^4 \tag{4.55}$$

Antenna averaging factor

The Effective path length L is calculated from:

$$L \text{ [m]} = \frac{2\,h_L}{\sqrt{\sin^2(\theta) + 2.35 \cdot 10^4} + \sin(\theta)} \tag{4.56}$$

where $h_L = 1000$ m is the height of the turbolent layer.

The Effective antenna diameter can be estimated from the geometrical diameter and the antenna efficiency:

$$D_{\text{eff}} \text{ [m]} = \sqrt{\eta} D \tag{4.57}$$

Then it is possible to calculate the Antenna averaging factor:

$$g(x) = \sqrt{3.86(x^2 + 1)^{\frac{11}{12}} \sin\left[\frac{11}{6} \arctan\left(\frac{1}{x}\right)\right] - 7.08 x^{\frac{5}{6}}} \tag{4.58}$$

where

$$x = 1.22 \frac{D_{\text{eff}}^2\, f}{L} \tag{4.59}$$

Scintillation fade depth

the standard deviation of the signal for the period and propagation path is calculated from:

$$\sigma = \sigma_{\text{ref}}\, f^{\frac{7}{12}} \frac{g(x)}{\sin^{1.2}(\theta)} \tag{4.60}$$

The Time percentage factor for the time percentage outage p, of concern in the range $0.01\% < p \leq 50\%$, can be determined by:

$$a(p) = -0.061 \log_{10}^3(p) + 0.072 \log_{10}^2(p) - 1.71 \log_{10}(p) + 3 \tag{4.61}$$

Therefore the Scintillation fade depth for the time percentage p is determined as:

$$A_s(p) \text{ [dB]} = a(p)\, \sigma \tag{4.62}$$

4.2.5 Radio Noise and G/T degradation

Any natural absorbing medium in the atmosphere which interacts with the transmitted radiowave will not only produce a signal amplitude reduction (attenuation), but will also be a source of thermal noise power radiation. The noise associated with these sources, referred to as radio noise, or sky noise, will directly add to the system noise through an increase in the antenna temperature of the receiver. For very low noise communications receivers, radio noise can be the limiting factor in the design and performance of the system. Radio noise is emitted from many sources, both natural (terrestrial and extra-terrestrial origin) and human made.

Sky noise due to rain and clouds

In this section we will discuss only the contributions caused by hydrometeors (rain and clouds); Noise temperature due to rain and cloud can be determined directly from Rain and Cloud attenuations.
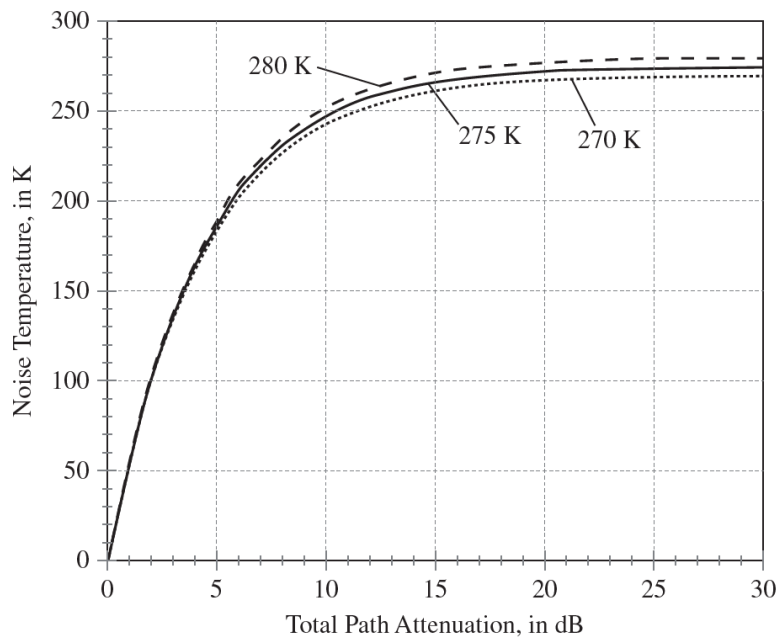
Figure 4.7: *Noise temperature due to rain for various surface temperatures*

Figure 4.7 shows that Noise temperature due to rain (expressed in K) rises quickly with Rain attenuation level and approaches saturation, therefore an asymptote that is precisely the surface temperature, fairly quickly above attenuation values of about 10 dB, below that value the selection of temperature is not very critical.

The Noise temperature introduced by rain and cloud will add directly to the receiver system noise figure, and will degrade the overall performance of the link. The noise power increase occurs coincident with the signal power decrease due to the rain fade; both effects are additive and contribute to the reduction in link Signal-to-Noise ratio.

Thus, the effect we consider is a degradation of G/T, given by an increase in system noise temperature, which we can estimate by an approximate formula that takes into account Rain and Cloud attenuations (expressed in dB):

$$\Delta T_s = -\Delta(G/T) = 279\left(1 - \frac{1}{A_r + A_c}\right) \tag{4.63}$$

4.3 Modulation loss

Various modulation techniques are possible in TT&C environment, which can be classified into two categories:

- Analog modulation, where an analog carrier is continuously modulated by an analog information signal. Analog modulation techniques include:

    1. Phase modulation (PM) with s/c or direct, where the phase shift of the carrier signal is varied in accordance with the instantaneous amplitude of the modulating signal

    2. Frequency modulation (FM) with s/c, where the frequency of the carrier signal is varied in accordance with the instantaneous amplitude of the modulating signal

- Digital modulation, where an analog carrier signal is modulated by a discrete digital signal. Digital modulation methods can be considered as digital-to-analog conversion and the corresponding demodulation or detection as analog-to-digital conversion; the changes in the carrier signal are chosen from a finite number of M alternative symbols. Analog modulation techniques include:

    1. Phase-shift keying (PSK), where a finite number of phases are used.

    2. Frequency-shift keying (FSK), where a finite number of frequencies are used

These are the fundamental modulation techniques of our interest and in this chapter we will discuss their characteristics and the resulting modulation losses, calculated according to CCSDS 401.0-B-32. Other more particular modulations are considered and will be covered in section 4.4, but the associated modulation losses can be related to those discussed below.

Before being modulated on the carrier (or subcarrier) the data, which are analog signals, must be digitized by means of Pulse-code modulation (PCM).

4.3.1 Pulse-code modulation (PCM)

Pulse-code modulation (PCM) is a method used to digitally represent sampled analog signals. In a PCM stream, the amplitude of the analog signal is sampled regularly at uniform intervals, and each sample is quantized to the nearest value within a range of digital steps. PCM process is commonly implemented on a single integrated circuit called an analog-to-digital converter.

Analog data, which are sinusoidal signals, are sampled and quantized through PCM before being appropriately modulated on the carrier for transmission. The sine wave is sampled at regular intervals, shown as vertical lines; for each sample, one of the available values (on the horizontal axis) is chosen. This produces a fully discrete representation of the input signal that can be easily encoded as digital data (decimal numbers are represented as a binary sequence of 0 and 1) for storage or manipulation.
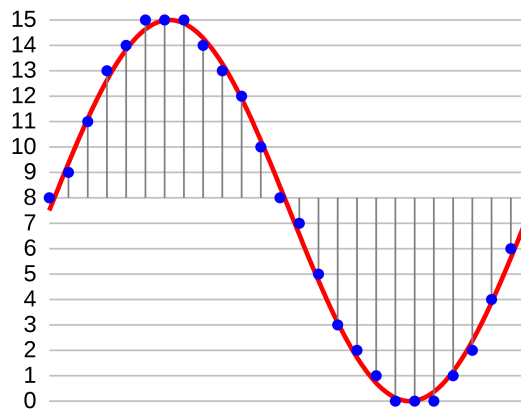
Figure 4.8: *PCM sampling and quantization diagram*

The digital data stream obtained in this way is then line coded as a sequence of pulses to obtain a digital signal. The binary line codes of our interest are:

1. NRZ-L (Non-return to zero - level) is a binary code in which zeros are represented by one significant condition, usually a positive voltage (level A), while ones are represented by some other significant condition, usually a negative voltage (level B);

2. SP-L (Split phase - level) is a binary code in which zeros are represented by level B during the first half-symbol followed by level A during the second half-symbol, while ones are represented by level A during the first half-symbol followed by level B during the second half-symbol.

The difference between these two formats is in the bandwidth of the modulating signal, which is double for SP-L compared to NRZ-L. The requirement of E_b/N_0 for data reception quality is the same for the two cases NRZ-L and SP-L.
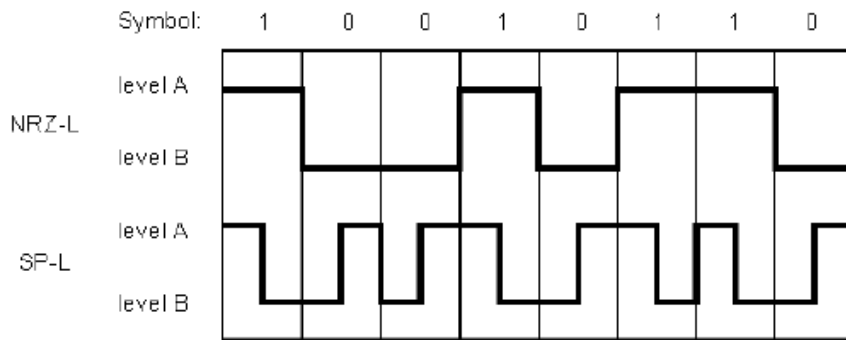
Figure 4.9: *PCM waveforms*

4.3.2 Phase modulation (PM) with subcarriers

Phase modulation (PM) is an Analog modulation technique where the phase of an analog carrier wave is modulated to follow the changing signal level (amplitude) of the analog message (modulating) signal. The amplitude of the carrier wave is maintained constant, but as the amplitude of the message signal changes, the phase of the carrier changes correspondingly. In case of analog signal the phase change is a continuous back and forth movement, while in case of digital signal there is an abrupt change in the phase of the carrier signal.
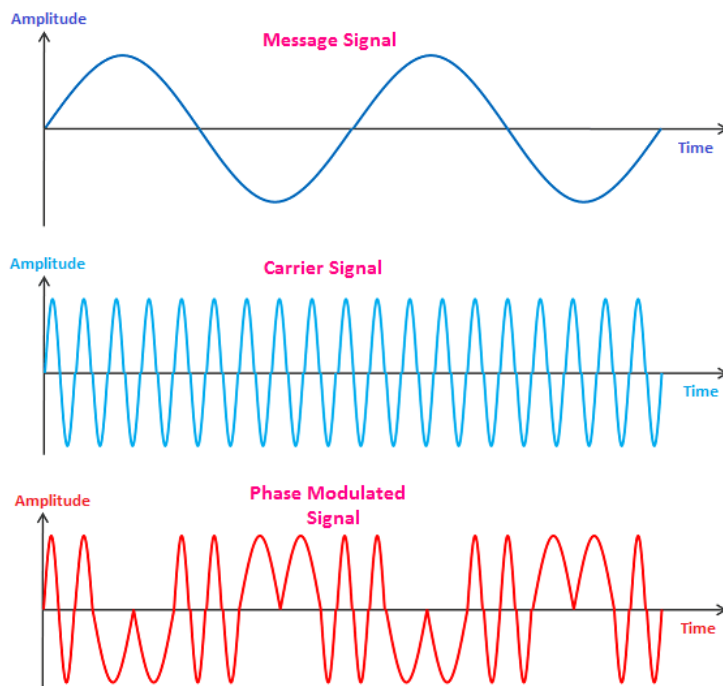
Figure 4.10: *PM signal diagram*

Figure 4.10 shows the low frequency message signal which contains useful information, the high frequency carrier wave which does not contain any information and the resultant phase modulated signal. The phase of both the positive and

47

negative half cycles of the carrier signal varies as per amplitude variations of the modulating signal; during the positive half cycle, the carrier signal phase shifts in one direction, whereas during the negative half cycle, the carrier signal phase shifts in the opposite direction. The phase variation is directly proportional to the amplitude of message signal.

Modulation index

Modulation index (m/i) determines how much the modulated variable changes around its unmodulated level, in other words it makes the phase variations more or less sensitive to the behavior of the baseband signal; it is clear that modulation index of phase modulation is directly proportional to the message signal. It relates to the variations in the phase of the carrier signal through the ralation:

$$m \, [\text{rad}] = \Delta\theta \tag{4.64}$$

where $\Delta\theta$ is the peak phase deviation expressed in rad.

Subcarrier

A subcarrier (s/c) is a sideband of a radio frequency carrier wave, a secondary modulated signal which is modulated into the main carrier to provide an additional channel of transmission. It allows for a single transmission to carry more than one separate signal and each subcarrier is used to carry additional information.

The use of subcarriers allows the separate signals to all be received together as one transmission and then separated out by the receiver. Signals are mixed with lower frequency subcarriers and the resulting signals are then combined with the main carrier, running at a higher frequency, for transmission.

Representation of the carrier signal modulated PM by a sine tone

A sinusoidal carrier $s(t)$ at frequency f_0, modulated PM by a sinusoidal tone at frequency f_1 with modulation index m, is expressible as:

$$s(t) = A_0 \sin[\omega_0 t + m \sin(\omega_1 t)] \tag{4.65}$$

where $\omega = 2\pi f$ is the angular frequency and t is time.

From trigonometry relations:

$$s(t) = A_0 \big(\sin(\omega_0 t) \cos[m \sin(\omega_1 t)] + \cos(\omega_0 t) \sin[m \sin(\omega_1 t)] \big) \tag{4.66}$$

It can be demonstrated that:

$$\sin[m \sin(\omega_1 t)] = \sum_{n=-\infty}^{\infty} J_n(m) \sin(n\omega_1 t) \tag{4.67}$$

$$\cos[m \sin(\omega_1 t)] = \sum_{n=-\infty}^{\infty} J_n(m) \cos(n\omega_1 t) \tag{4.68}$$

Therefore we can write:

$$s(t) = A_0 \sum_{n=-\infty}^{\infty} J_n(m) \sin[2\pi(f_0 + nf_1)t] \tag{4.69}$$

This equation shows that the signal in question consists of a series of tones at frequencies $f_0 + nf_1$ of amplitude proportional to the corresponding Bessel function of order n having the modulation index as its argument.
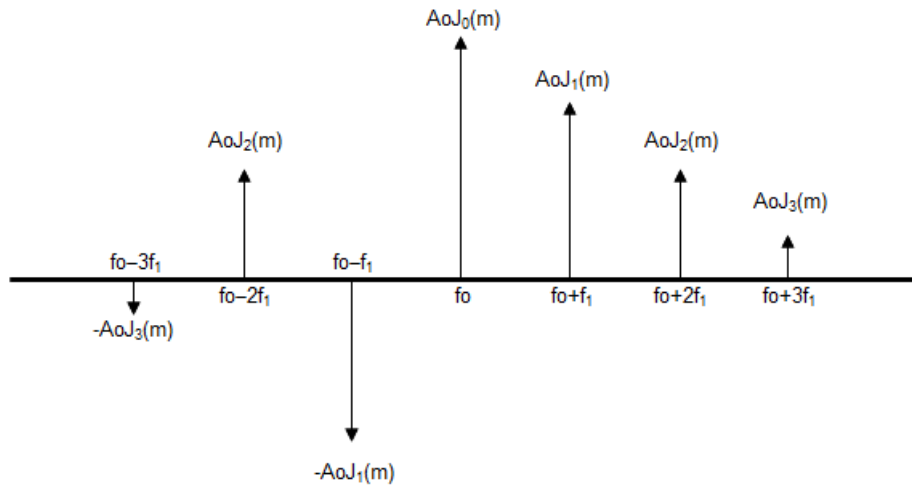
Figure 4.11: *PM signal representation as a series of tones*

Carrier compression

Total power of unmodulated carrier:

$$P_{\text{tot}} = \frac{A_0^2}{2} \tag{4.70}$$

Residual carrier power after direct modulation:

$$P_c = \frac{A_0^2 J_0^2(m)}{2} \tag{4.71}$$

Carrier compression (in dB) is:

$$\Delta\,[\text{dB}] = 10\log_{10}\left(\frac{P_c}{P_{\text{tot}}}\right) = 10\log_{10}\left[J_0^2(m)\right] \tag{4.72}$$

Case of multiple modulating tones

In case of two sinusoidal modulating tones with frequencies f_1 and f_2, and modulation indices m_1 and m_2, the signal is composed by the following tones reported in the table 4.1

	Frequency	**Amplitude**
Residual carrier	f_0	$A_0 J_0(m_1) J_0(m_2)$
Sidebands due to tone f_1	$f_0 \pm n f_1$	$A_0 J_n(m_1) J_0(m_2)$
Sidebands due to tone f_2	$f_0 \pm n f_1$	$A_0 J_0(m_1) J_n(m_2)$
Intermodulation tones	$f_0 \pm n f_1 \pm m f_2$	$A_0 J_n(m_1) J_m(m_2)$

Table 4.1: *Multiple modulating tones*

Modulation loss (Carrier PM modulated by one or more tones)

Given a signal v(t), its total energy relative to the time interval [0,T] is by definition:

$$E(t) = \int_0^T v^2(t)\,\mathrm{dt} \tag{4.73}$$

and its average power is given by:

$$P = \frac{E(T)}{T} \tag{4.74}$$

For a sinusoidal signal $v(t) = A$, considering $T = \frac{1}{f} \to \omega = \frac{2\pi}{T}$, we have:

$$P = \frac{1}{T} \int_0^T v^2(t)\,\mathrm{dt} = \frac{A^2}{2T} \left[t - \frac{\sin(\omega t)\cos(\omega t)}{\omega} \right]_0^T = \frac{A^2}{2} \tag{4.75}$$

Thus the modulated signal (4.65) has total power $P_t = A_0^2/2$,
while each component of its development (4.69) has power $P_n = A_0^2 J_n^2(m)/2$.
The same is applicable to the case with multiple modulants, but with product of multiple $J(m_i)$.

With reference to carrier recovery, the useful power is only that P_0 associated with the remaining carrier (the component at frequency f_0) so in case of 'K' modulating tones, it is:

$$\text{Carrier loss [dB]} = 10\log_{10}(P_{\text{tot}}) - 10\log_{10}(P_0) = -10\log_{10}\left(\frac{P_0}{P_{\text{tot}}}\right)$$

$$= -10\log_{10}\left[\frac{A_0^2 J_0^2(m_1) J_0^2(m_2) \dots J_0^2(m_k)/2}{A_0^2/2} \right] \tag{4.76}$$

$$= -10\log_{10}\left[J_0^2(m_1) J_0^2(m_2) \dots J_0^2(m_k) \right]$$

Similarly, for the recovery of the i-th modulant, assuming that the frequencies of the individual modulating tones are sufficiently spaced to filter out only the main lobes related to it, we have:

$$\text{i-modulation loss [dB]} = -10\log_{10}\left[2J_i^2(m_i) J_0^2(m_1) J_0^2(m_2) \dots J_0^2(m_k) \right] \tag{4.77}$$

This applies if subcarriers are PSK modulated by a PCM stream data (PCM/PSK/PM signal): this is the case of our interest, in which carrier suppression occurs, so that all the power useful for data recovery is that associated with the subcarrier, given by the i-modulation loss mentioned above.

PCM/PSK/PM Modulation loss summary

	Carrier	$-10\log_{10}\left[J_0^2(m_{TC})J_0^2(M_{up})J_0^2(m_{up})\right]$
	TC	$-10\log_{10}\left[2J_1^2(m_{TC})J_0^2(M_{up})J_0^2(m_{up})\right]$
UP	RG Carrier	$-10\log_{10}\left[J_0^2(M_{up})J_0^2(m_{up})\right]$
	RG Mj tone	$-10\log_{10}\left[2J_0^2(m_{TC})J_1^2(M_{up})J_0^2(m_{up})\right]$
	RG Mn tone	$-10\log_{10}\left[2J_0^2(m_{TC})J_0^2(M_{up})J_1^2(m_{up})\right]$
	Carrier	$-10\log_{10}\left[J_0^2(m_{TM})J_0^2(\mu_{MT})J_0^2(\mu_{mt})J_0^2(\mu_{TC})\exp(-\mu_N^2)\right]$
	TM	$-10\log_{10}\left[2J_1^2(m_{TM})J_0^2(\mu_{MT})J_0^2(\mu_{mt})J_0^2(\mu_{TC})\exp(-\mu_N^2)\right]$
DW	RG Mj tone	$-10\log_{10}\left[2J_0^2(m_{TM})J_1^2(\mu_{MT})J_0^2(\mu_{mt})J_0^2(\mu_{TC})\exp(-\mu_N^2)\right]$
	RG Mn tone	$-10\log_{10}\left[2J_0^2(m_{TM})J_0^2(\mu_{MT})J_1^2(\mu_{mt})J_0^2(\mu_{TC})\exp(-\mu_N^2)\right]$

Table 4.2: *PCM/PSK/PM Modulation loss table*

The modulation indices shown above will be discussed in subsection 4.3.4.

4.3.3 Phase modulation (PM) direct

In the absence of subcarriers, the carrier is PM modulated directly by a PCM data stream, with the possible presence of other modulating tones.

Tone PM modulated by PCM data

By modulating PM a sine tone with PCM data, the power of the composite signal is distributed between the residual of the modulated tone and the component of the modulating code according to $\cos^2$ and $\sin^2$, respectively, of the modulation index β, so:

$$P_{tone} = P_{tot}\cos^2(\beta) \qquad\qquad P_{code} = P_{tot}\sin^2(\beta) \tag{4.78}$$

$$\text{Tone loss [dB]} = -10\log_{10}\left(\frac{P_{tone}}{P_{tot}}\right) = -10\log_{10}\left[\cos^2(\beta)\right] \tag{4.79}$$

$$\text{Code loss [dB]} = -10\log_{10}\left(\frac{P_{code}}{P_{tot}}\right) = -10\log_{10}\left[\sin^2(\beta)\right] \tag{4.80}$$

The above applies regardless of the format of the PCM data (NRZ-L or SP-L).

If a subcarrier is PM modulated, there would be subcarrier residual, so only part of the power related to the component in question is useful for data retrieval; it would therefore be necessary to add the $\cos^2(\beta)$ and $\cos^2(\beta)$ terms to the i-modulation loss already considered, but this is not our case.

Modulation loss (Carrier PM modulated directly by PCM data)

In the presence of only PCM data directly modulating the carrier in PM (PCM/PM signal), the loss is that due to power sharing between carrier and modulating code:

$$\text{Carrier loss [dB]} = -10 \log_{10} \left[\cos^2(\beta) \right] \tag{4.81}$$

$$\text{Data modulation loss [dB]} = -10 \log_{10} \left[\sin^2(\beta) \right] \tag{4.82}$$

If other modulating tones (themselves eventually modulated by codes) are also present, losses should be calculated taking into account both the components due to the modulating tones and the power repartition that the data determine between modulation and carrier residual:

$$\text{Carrier loss [dB]} = -10 \log_{10} \left[\cos^2(\beta) J_0^2(m_1) J_0^2(m_2) \dots J_0^2(m_k) \right] \tag{4.83}$$

$$\text{Data modulation loss [dB]} = -10 \log_{10} \left[\sin^2(\beta) J_0^2(m_1) J_0^2(m_2) \dots J_0^2(m_k) \right] \tag{4.84}$$

$$\text{i-tone loss [dB]} = -10 \log_{10} \left[2 J_i^2(m_i) J_0^2(m_1) J_0^2(m_2) \dots J_0^2(m_k) \cos^2(\beta) \right] \tag{4.85}$$

PCM/PM Modulation loss summary

UP	Carrier	$-10 \log_{10} \left[\cos^2(m_{TC}) J_0^2(M_{up}) J_0^2(m_{up}) \right]$
	TC	$-10 \log_{10} \left[\sin^2(m_{TC}) J_0^2(M_{up}) J_0^2(m_{up}) \right]$
	RG Carrier	$-10 \log_{10} \left[J_0^2(M_{up}) J_0^2(m_{up}) \right]$
	RG Mj tone	$-10 \log_{10} \left[2 \cos^2(m_{TC}) J_1^2(M_{up}) J_0^2(m_{up}) \right]$
	RG Mn tone	$-10 \log_{10} \left[2 \cos^2(m_{TC}) J_0^2(M_{up}) J_1^2(m_{up}) \right]$
DW	Carrier	$-10 \log_{10} \left[\cos^2(m_{TM}) J_0^2(\mu_{MT}) J_0^2(\mu_{mt}) J_0^2(\mu_{TC}) \exp(-\mu_N^2) \right]$
	TM	$-10 \log_{10} \left[\sin^2(m_{TM}) J_0^2(\mu_{MT}) J_0^2(\mu_{mt}) J_0^2(\mu_{TC}) \exp(-\mu_N^2) \right]$
	RG Mj tone	$-10 \log_{10} \left[2 \cos^2(m_{TM}) J_1^2(\mu_{MT}) J_0^2(\mu_{mt}) J_0^2(\mu_{TC}) \exp(-\mu_N^2) \right]$
	RG Mn tone	$-10 \log_{10} \left[2 \cos^2(m_{TM}) J_0^2(\mu_{MT}) J_1^2(\mu_{mt}) J_0^2(\mu_{TC}) \exp(-\mu_N^2) \right]$

Table 4.3: *PCM/PM Modulation loss table*

The modulation indices shown above will be discussed in subsection 4.3.4.

4.3.4 Modulation indices combination

Here are described the modulation indices for PM in Uplink and Downlink and how to combine their maximum and minimum values of the modulation indices for calculating losses in the favourable and adverse cases.

Uplink PM Modulation indices

m/i	Min	Nom	Max
TC	m_{TC}^-	m_{TC}	m_{TC}^+
RG Mj tone	M_{up}^-	M_{up}	M_{up}^+
RG Mn tone	m_{up}^-	m_{up}	m_{up}^+

Table 4.4: *Uplink modulation indices values*

To combine modulation indexes take into consideration that:

- Modulation components subtract power to the carrier, so the worst case is when all modulation indexes are max and viceversa for best case;

- Best case is when power on TC tone is maximized, so TC m/i has to be max and min as far as RG, and viceversa for worst case.

- Best case is when power on RG major tone is maximized, so RG major tone m/i has to be max and min as far as TC and RG minor tone, and viceversa for worst case.

- Best case is when power on RG minor tone is maximized, so RG minor tone m/i has to be max and min as far as TC and RG major tone, and viceversa for worst case.

Carrier		TC		RG Mj tone		RG Mn tone	
Fav	Adv	Fav	Adv	Fav	Adv	Fav	Adv
m_{TC}^-	m_{TC}^+	m_{TC}^+	m_{TC}^-	m_{TC}^-	m_{TC}^+	m_{TC}^-	m_{TC}^+
M_{up}^-	M_{up}^+	M_{up}^-	M_{up}^+	M_{up}^+	M_{up}^-	M_{up}^-	M_{up}^+
m_{up}^-	m_{up}^+	m_{up}^-	m_{up}^+	m_{up}^-	m_{up}^+	m_{up}^+	m_{up}^-

Table 4.5: *Uplink modulation indices combinations*

Downlink PM Modulation indices

Downlink PM Effective modulation indexes are calculated from Nominal modulation indexes and the Uplink RG tones, TC in RG video-BW and Total SNRs; the last one is linear, while the other must first be converted from dB to linear through $10^{S/N}$.

m/i	Min	Nom	Max
TM RG tones	m^-_{TM} m^-_{dw}	m_{TM} m_{dw}	m^+_{TM} m^+_{dw}
RG Mj tone	$\mu^-_{MT} = m^-_{dw}\sqrt{\frac{(S/N)^-_{MT}}{(S/N)^-_{tot}}}$	$\mu_{MT} = m_{dw}\sqrt{\frac{(S/N)_{MT}}{(S/N)_{tot}}}$	$\mu^+_{MT} = m^+_{dw}\sqrt{\frac{(S/N)^+_{MT}}{(S/N)^+_{tot}}}$
RG Mn tone	$\mu^-_{mt} = m^-_{dw}\sqrt{\frac{(S/N)^-_{mt}}{(S/N)^-_{tot}}}$	$\mu_{mt} = m_{dw}\sqrt{\frac{(S/N)_{mt}}{(S/N)_{tot}}}$	$\mu^+_{mt} = m^+_{dw}\sqrt{\frac{(S/N)^+_{mt}}{(S/N)^+_{tot}}}$
TC echo	$\mu^-_{TC} = m^-_{dw}\sqrt{\frac{(S/N)^-_{TC}}{(S/N)^-_{tot}}}$	$\mu_{TC} = m_{dw}\sqrt{\frac{(S/N)_{TC}}{(S/N)_{tot}}}$	$\mu^+_{TC} = m^+_{dw}\sqrt{\frac{(S/N)^+_{TC}}{(S/N)^+_{tot}}}$
Noise	$\mu^-_N = \frac{m^+_{dw}}{\sqrt{2(S/N)^+_{tot}}}$	$\mu_N = \frac{m_{dw}}{\sqrt{2(S/N)_{tot}}}$	$\mu^+_N = \frac{m^-_{dw}}{\sqrt{2(S/N)^-_{tot}}}$

Table 4.6: *Downlink modulation indices values*

To combine modulation indexes take into consideration that:

- Modulation components subtract power to the carrier, so worst case is when tones modulation indexes are max while noise m/i is min, and viceversa for best case;

- Best case is when power on TM tone is maximized, so TM (and also noise) m/i has to be max and min as far as effective RG and TC echo, and viceversa for worst case;

- Best case is when power on RG tone is maximized, so TM (and also noise) m/i has to be min and max as far as effective RG and TC echo, and viceversa for worst case.

Carrier		TM		RG Mj tone		RG Mn tone	
Fav	Adv	Fav	Adv	Fav	Adv	Fav	Adv
m^-_{TM} m^-_{dw}	m^+_{TM} m^+_{dw}	m^+_{TM} m^-_{dw}	m^-_{TM} m^+_{dw}	m^-_{TM} m^+_{dw}	m^+_{TM} m^-_{dw}	m^-_{TM} m^+_{dw}	m^+_{TM} m^-_{dw}
μ^-_{MT} μ^-_{mt} μ^-_{TC} μ^+_N	μ^+_{MT} μ^+_{mt} μ^+_{TC} μ^-_N	μ^-_{MT} μ^-_{mt} μ^-_{TC} μ^+_N	μ^+_{MT} μ^+_{mt} μ^+_{TC} μ^-_N	μ^+_{MT} μ^+_{mt} μ^+_{TC} μ^-_N	μ^-_{MT} μ^-_{mt} μ^-_{TC} μ^+_N	μ^+_{MT} μ^+_{mt} μ^+_{TC} μ^-_N	μ^-_{MT} μ^-_{mt} μ^-_{TC} μ^+_N

Table 4.7: *Downlink modulation indices combinations*

4.3.5 Phase-shift keying (PSK)

Phase-shift keying (PSK) is a digital modulation process which conveys data by changing (modulating) the phase of a constant frequency reference signal (the carrier wave). Any digital modulation scheme uses a finite number of distinct signals to represent digital data; PSK uses a finite number of phases, each assigned a unique pattern of binary digits. Usually, each phase encodes an equal number of bits; each pattern of bits forms the symbol that is represented by the particular phase. Various forms of PSK are discussed in the subsection 4.4.1
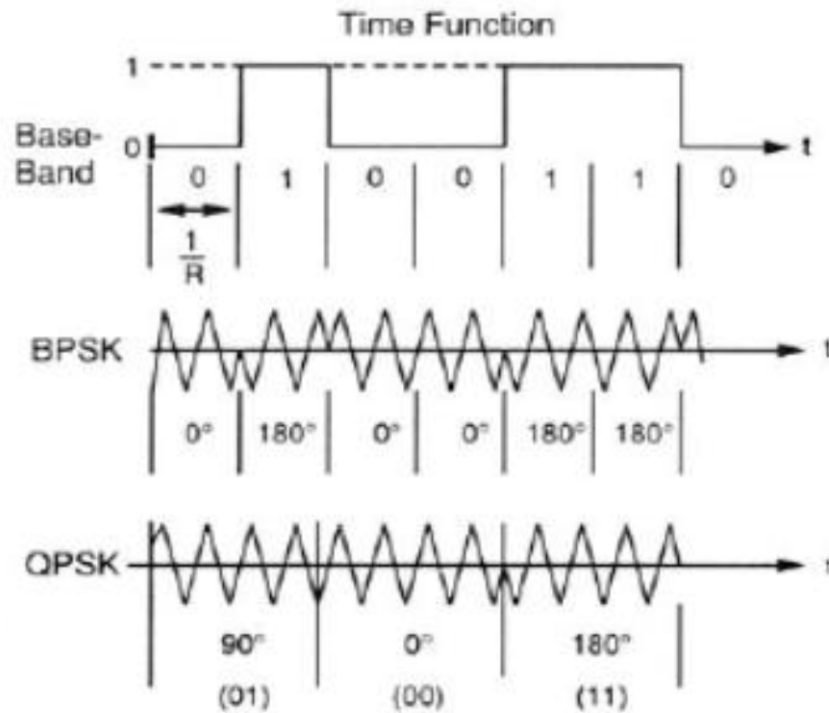
Figure 4.12: *PSK signal diagram*

This is a special case of the previous one when $\beta = \frac{\pi}{2}$ and thus all the signal power goes on the modulator and the residual tone component disappears altogether. In this case the modulation loss on data recovery is theoretically zero, except to bring into account the effect of the in-band limitation of the signal with respect to the theoretical bandwidth, which is unlimited.

Roll-off factor

This limitation is defined by the value assigned to the roll-off factor α, which varies in a range from 0 to 5:

- for $\alpha = 0$ the band coincides with the Nyquist band and loss is maximized; the value of Nyquist frequency corresponds to one-half of the rate of the discrete signal;

- for $\alpha = 1$ the band corresponds to the first lobe (one-side band);

- $\alpha = 5$ corresponds to a band theoretically unlimited with zero loss

Roll-off factor is generally assumed to be in the range from 0.2 to 0.5.

Case of PCM(NRZ-L)/PSK signal

Representation in the time domain: $x(t) = \text{rect}_T(t)$, where $\text{rect}(t)$ is the rectangular function.
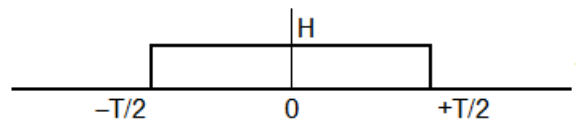
Figure 4.13: *NRZ-L signal diagram*

It can be demonstrated that the representation in the time domain results:

$$X(f) = HT \frac{\sin(\pi f T)}{\pi f T} \tag{4.86}$$

Signal power spectrum:

$$S(f) = |X(f)|^2 = H^2 T^2 \frac{\sin^2(\pi f T)}{(\pi f T)^2} = E_b \frac{\sin^2(\pi f T)}{(\pi f T)^2} \tag{4.87}$$

where:

- T is the bit duration (period)
- $R = \frac{1}{T}$ is the bit rate
- H is the bit level, which can be expressed ad $H = R\sqrt{E_b}$
- $E_b = H^2 T^2$ is the energy per bit
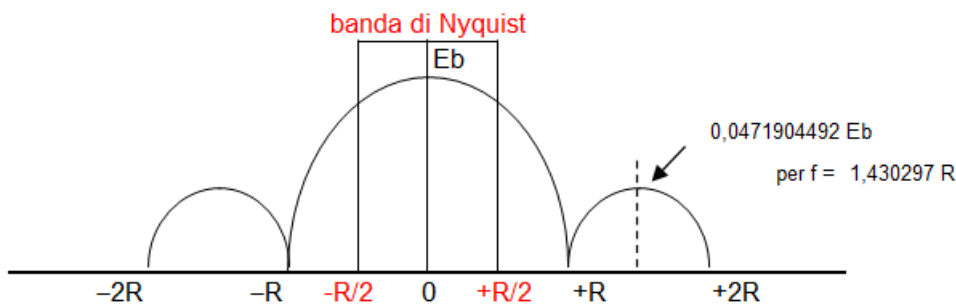
Figure 4.14: *NRZ power spectrum diagram*

The total signal power is: $P_{\text{tot}} = E_b/T$

Considering the assumed modulated tone of amplitude A_0, it is also: $P_{\text{tot}} = \frac{A_0^2}{2}$

P_{tot} refers to the entire spectrum of the signal, which is theoretically infinite. In practice, the used band of the signal is bounded between -B and +B with reference to the band center. B is usually defined with respect to the Bit rate, the frequency value of which corresponds to the first null in the spectrum and thus delimits the main lobe of the spectrum (equal to twice the Nyquist band, which instead ranges from $-\frac{R}{2}$ to $+\frac{R}{2}$). Therefore the total bandwidth is given by:

$$BW = 2B = 2 \cdot (1 + \alpha)\frac{R}{2} = (1 + \alpha)R \tag{4.88}$$

56

The loss due to band limitation, expressed in dB, is given by:

$$\text{Mod. loss [dB]} = 10\log_{10}(P_{\text{tot}}) - 10\log_{10}\left(P_{[\text{-B,+B}]}\right) = -10\log_{10}\left(\frac{P_{[\text{-B,+B}]}}{P_{\text{tot}}}\right)$$

(4.89)

$$= -10\log_{10}\left(\int_{-B}^{B} S(f)\text{df}\right) = -10\log_{10}(A)$$

$$A = \frac{2}{\pi}\left[\text{Si}[\pi(1+\alpha)] - \frac{\sin^2[\frac{\pi}{2}(1+\alpha)]}{\frac{\pi}{2}(1+\alpha)}\right]$$

(4.90)

where Si is the sine integral function.
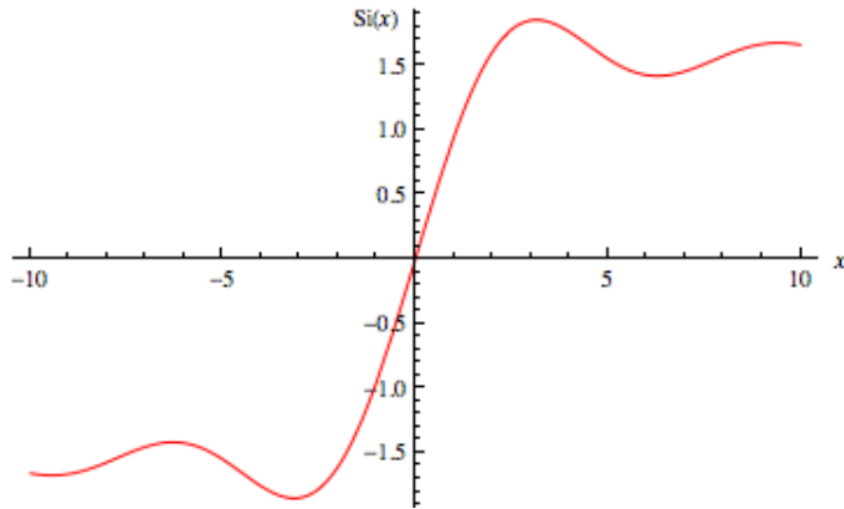
Figure 4.15: *Sine integral function*

Case of PCM(SP-L)/PSK signal

Representation in the time domain: $x(t) = -H\text{rect}_{T/2}(t) + H\text{rect}_{T/2}\left(t-\frac{T}{4}\right)$
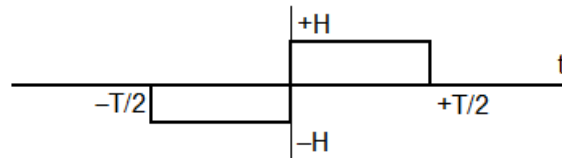
Figure 4.16: *SP-L signal diagram*

It can be demonstrated that the representation in the time domain results:

$$X(f) = -jHT\frac{\sin^2(\pi f\frac{T}{2})}{\pi f\frac{T}{2}}$$

(4.91)

Signal power spectrum:

$$S(f) = |X(f)|^2 = H^2T^2\frac{\sin^4\left(\pi f\frac{T}{2}\right)}{\left(\pi f\frac{T}{2}\right)^2} = E_b\frac{\sin^4\left(\pi f\frac{T}{2}\right)}{\left(\pi f\frac{T}{2}\right)^2}$$

(4.92)
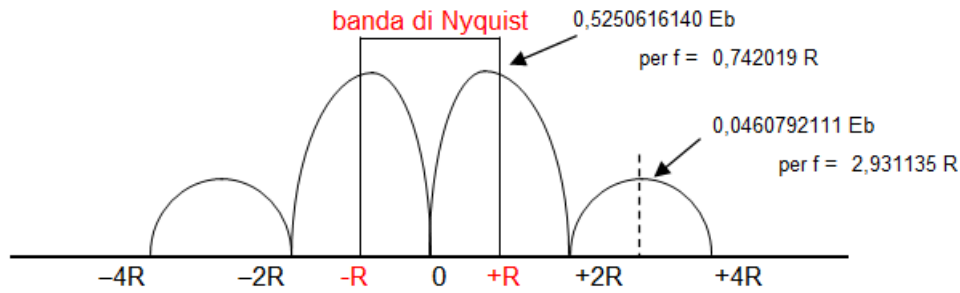
Figure 4.17: *SP-L power spectrum diagram*

We observe that the level transition within the bit waveform is equivalent to twice as many symbols physically transmitted over the channel, and thus a doubling of the bandwidth compared with the NRZ-L case. In fact, the first null of the spectrum now falls at distance 2R (and the Nyquist band is also doubled going from -R to +R). In this case the total bandwidth is given by:

$$BW = 2B = 2 \cdot (1 + \alpha)R = (1 + \alpha)2R \tag{4.93}$$

The loss due to band limitation, expressed in dB, is now given by:

$$\text{Mod. loss [dB]} = 10 \log_{10}(P_{\text{tot}}) - 10 \log_{10}(P_{[-B,+B]}) = -10 \log_{10}\left(\frac{P_{[-B,+B]}}{P_{\text{tot}}}\right)$$
$$= -10 \log_{10}\left(\int_{-B}^{B} S(f) df\right) = -10 \log_{10}(2A - B) \tag{4.94}$$

$$A = \frac{2}{\pi}\left[\text{Si}[\pi(1 + \alpha)] - \frac{\sin^2[\frac{\pi}{2}(1 + \alpha)]}{\frac{\pi}{2}(1 + \alpha)}\right] \tag{4.95}$$

$$B = \frac{2}{\pi}\left[\text{Si}[2\pi(1 + \alpha)] - \frac{\sin^2[\pi(1 + \alpha)]}{\pi(1 + \alpha)}\right] \tag{4.96}$$

PSK Modulation loss summary

	PCM(NRZ-L)/PSK	PCM(SP-L)/PSK
TC/TM	$-10 \log_{10}(A)$	$-10 \log_{10}(2A - B)$
A	$\frac{2}{\pi}\left[\text{Si}[\pi(1 + \alpha)] - \frac{\sin^2[\frac{\pi}{2}(1+\alpha)]}{\frac{\pi}{2}(1+\alpha)}\right]$	
B	$\frac{2}{\pi}\left[\text{Si}[2\pi(1 + \alpha)] - \frac{\sin^2[\pi(1+\alpha)]}{\pi(1+\alpha)}\right]$	

Table 4.8: *PSK Modulation loss table*

In this case the carrier is suppressed, so there is no budget for carrier recovery; moreover, ranging is not possible.

4.3.6   Frequency modulation (FM) with subcarriers

Frequency modulation (FM) is an Analog modulation technique where the information is transmitted over a carrier wave by varying its frequency in accordance with the amplitude of the message signal. The frequency of the carrier signal is varied continously whereas the amplitude of the carrier signal remains constant.
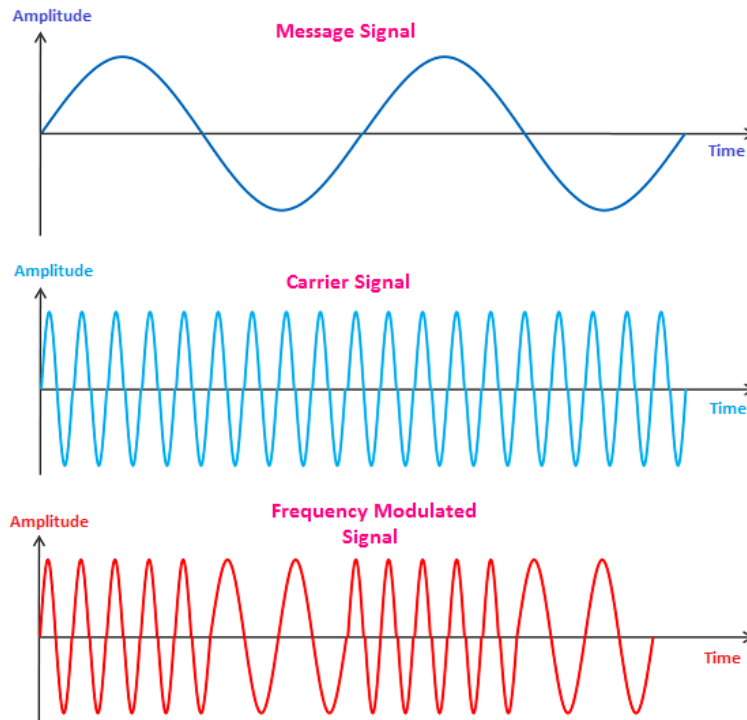
Figure 4.18: *FM signal diagram*

Figure 4.10 shows that the resultant frequency modulated signal, where the frequency of both the positive and negative half cycles of the carrier wave is varied in accordance with the instant amplitude of the modulating signal.

The carrier wave does not contain any information so even if we change the frequency of the carrier wave, there will be no information loss. However, if we change the frequency of the modulating signal, a certain amount of information loss will occur because the modulating signal contains the information. So the frequency of the modulating signal should not be changed.

Frequency deviation

In FM, the amount of change in frequency of the carrier signal is determined by the amplitude of the message signal. For example, let's assume that the carrier signal has a maximum frequency deviation of $\Delta f = \pm 4$ kHz. In such case, the carrier signal will move up and down by 4 kHz. The frequency of the modulated wave is high when the message signal reaches its maximum amplitude.

Representation of the carrier signal modulated FM by a sine tone

Given the modulating signal $m(t) = \cos(2\pi f_m t)$, which is a tone at frequency f_m, which for convenience is represented by cosine; this does not change the substance of subsequent developments, because sine and cosine are the same waveform translated by $\frac{\pi}{2}$. The sinusoidal carrier s(t) at frequency fo, FM modulated by m(t), can be expressed as:

$$s(t) = A_0 \sin\left[2\pi f_0 t + 2\pi \Delta f \int_0^t m(\tau)\mathrm{d}\tau\right] \tag{4.97}$$

$$\int \cos(at)\mathrm{dt} = \frac{1}{a}\sin(at) \quad \Longrightarrow \quad \int_0^t m(\tau)\mathrm{d}\tau = \frac{\sin(2\pi f_m t)}{2\pi f_m t} \tag{4.98}$$

$$s(t) = A_0 \sin[\omega_0 t + \beta \sin(\omega_m t)] \tag{4.99}$$

expression that is analogous to 4.65 for PM modulation, identifying the modulation index with the ratio:

$$\beta = \frac{\Delta f}{f_m} \tag{4.100}$$

Thus, what has already been seen in the PM case, with s/c with β instead of m, applies; in particular, we refer to the same type of spectrum with spaced components of fm and with amplitude proportional to Bessel functions.

Modulation loss (Carrier FM modulated by a tones)

On the other hand, the discussion changes for FM modulation losses: in the PM case, the receiving demodulation process basically corresponds to filtering the main component at the frequency of the modulating tone, in the FM case it happens that the whole received signal concurs to the recovery of the modulant (that is, in practice, all components that fall within an however finite band that is calculated by Carson's rule).

In FM therefore, the Carson's bandwidth (B_c) is defined as that portion of the RF spectrum that encloses 98% of the total transmitted power. It is given by:

$$B_c = 2(\Delta f + f_m) = 2(\beta + 1)f_m \tag{4.101}$$

The number of spectral components that fall within B_c depends on β: in addition to the carrier residual, the components to be brought into account (unilaterally) are equal to the integer part of $\beta + 1$.

β	$\beta + 1$	f_0	$+f_m$	$+2f_m$	$+3f_m$	$+4f_m$	% of Power
		$J_0^2(\beta)$	$2J_1^2(\beta)$	$2J_2^2(\beta)$	$2J_3^2(\beta)$	$2J_4^2(\beta)$	
0.5	1.5	x	x				0.998113591
1	2	x	x	x			0.999222153
1.5	2.5	x	x	x			0.99228324
2	3	x	x	x	x		0.99758677
3	4	x	x	x	x	x	0.996024168

Table 4.9: *FM modulation loss components*

FM with s/c works only in Uplink. Modulation losses can be calculated in this way for TC and RG tones (calculating β from Δf), while carrier modulation loss is zero.

4.3.7 Frequency-shift keying (FSK)

Frequency-shift keying (FSK) is a digital modulation scheme in which digital information is transmitted through discrete frequency changes of a carrier signal. The simplest FSK is binary FSK (BFSK), which uses a pair of discrete frequencies to transmit binary (zeros and ones) information; with this scheme, the 1 is called the mark frequency and the 0 is called the space frequency.
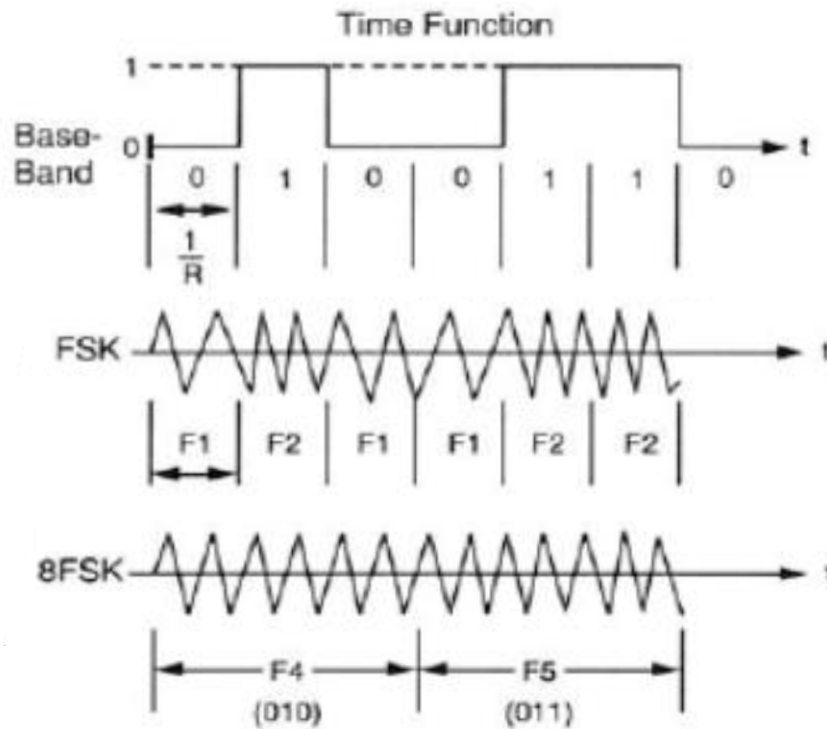
Figure 4.19: *FSK signal diagram*

As in the PSK case, the loss is related to the signal bandwidth limitation, defined according to Carson's rule as a function of frequency deviation.

Representation of the carrier signal FSK modulated by PCM data

Given the modulating signal $m(t)$ consisting of a PCM signal representing the sequence of information logic symbols 0 and 1, the sinusoidal carrier $s(t)$ at frequency f_0, FSK modulated by $m(t)$, is expressible by 4.97, so its instantaneous frequency is:

$$f(t) = f_0 + \Delta f\, m(t) \tag{4.102}$$

Case of PCM(NRZ-L)/FSK signal

In other words, if m is associated with amplitude +1 at logical symbol 1 and amplitude -1 at logical symbol 0, the modulated signal corresponds to the carrier whose frequency jumps between the two different values associated with the two logic symbols 0 and 1.

$$\text{FSK}(t) = \begin{cases} A_0 \sin(2\pi f_0 + \Delta f)t & \text{for bit 1} \\ A_0 \sin(2\pi f_0 - \Delta f)t & \text{for bit 0} \end{cases} \tag{4.103}$$

The power spectrum of the NRZ-L signal is of the type:

$$S(f) = E_b \frac{\sin^2(\pi f T_b)}{(\pi f T_b)^2} \tag{4.104}$$

In the case under consideration, given T_b the period of the bit, the frequency of the waveform is:

$$f_m = \frac{1}{T_b} = R_b \tag{4.105}$$

which is the information bit rate, and the equivalent modulation index is expressible as:

$$\beta = \frac{\Delta f}{f_m} = \frac{\Delta f}{R_b} \tag{4.106}$$

The corresponding Carson's Bandwidth then results as:

$$B_c = 2(\Delta f + R_b). \tag{4.107}$$

We can therefore calculate the modulation loss relative to a receiving bandwidth equal to B_c, assuming we have Δf and R_b as inputs. From what we have seen for PSK modulation loss and since $B_c T_b = 2(\beta + 1)$ it results:

$$\text{Mod. loss [dB]} = -10\log_{10}\left(\frac{P_{[-B_{C/2}, +B_{C/2}]}}{P_{\text{tot}}}\right) \tag{4.108}$$
$$= -10\log_{10}(A)$$

$$A = \frac{2}{\pi}\left[\text{Si}[2\pi(1+\beta)] - \frac{\sin^2[\pi(1+\beta)]}{\pi(1+\beta)}\right] \tag{4.109}$$

Case of PCM(SP-L)/FSK signal

The difference from the NRZ-L case is in is that, for SP-L, a level transition is associated with each symbol, so the frequency of the modulating waveform is double:

$$f_m = \frac{1}{T_s} = R_s = 2R_b \quad \Longrightarrow \quad \beta = \frac{\Delta f}{f_m} = \frac{\Delta f}{2R_b} \quad \Longrightarrow \quad B_c = 2(\Delta f + 2R_b) \tag{4.110}$$

The power spectrum of the SP-L signal is of the type:

$$S(f) = E_b \frac{\sin^4(\pi f T_b)}{(\pi f T_b)^2} \tag{4.111}$$

$$\text{Mod. loss [dB]} = -10 \log_{10}\left(\frac{P_{[-B_{C/2}, +B_{C/2}]}}{P_{\text{tot}}}\right) \tag{4.112}$$

$$= -10 \log_{10}(2A - b)$$

$$A = \frac{2}{\pi}\left[\text{Si}[2\pi(1+\beta)] - \frac{\sin^2[\pi(1+\beta)]}{\pi(1+\beta)}\right] \tag{4.113}$$

$$B = \frac{2}{\pi}\left[\text{Si}[4\pi(1+\beta)] - \frac{\sin^2[2\pi(1+\beta)]}{2\pi(1+\beta)}\right] \tag{4.114}$$

FSK Modulation loss summary

	PCM(NRZ-L)/FSK	PCM(SP-L)/FSK
TC/TM	$-10\log_{10}(A)$	$-10\log_{10}(2A - B)$
β	$\beta = \frac{\Delta f}{R_{\text{TC/TM}}}$	$\beta = \frac{\Delta f}{2R_{\text{TC/TM}}}$
A	$\frac{2}{\pi}\left[\text{Si}[2\pi(1+\beta)] - \frac{\sin^2[\pi(1+\beta)]}{\pi(1+\beta)}\right]$	
B	$\frac{2}{\pi}\left[\text{Si}[4\pi(1+\beta)] - \frac{\sin^2[2\pi(1+\beta)]}{2\pi(1+\beta)}\right]$	

Table 4.10: *FSK Modulation loss table*

In this case, as for PSK, the carrier is suppressed, so there is no budget for carrier recovery; moreover, ranging is not possible.

4.4 TC and TM Demodulation treshold

In this section we aim to determine the correspondence between data transmission quality requirements (Bit error rate) and the corresponding theoretical required Eb/No levels (necessary to calculate TC/TM link margins); this depends on the modulation modulation with which the PCM data stream is modulated on the carrier (or subcarrier).

First of all, we will discuss the relationship that determines the theoretical required Eb/N0 for various digital modulations, and then how this varies according to the type of encoding that is applied to data.

4.4.1 BER relationships

Binary phase-shift keying (BPSK)

BPSK is the simplest form of PSK and uses two phases which are separated by $180°$, so can also be termed 2-PSK.

The BER of BPSK under Additive white Gaussian noise (AWGN) can be calculated as:

$$\text{BER} = P_b = \frac{1}{2}\text{erfc}\left(\sqrt{\frac{E_b}{N_0}}\right) \tag{4.115}$$

Since there is only one bit per symbol, the BER is also the Symbol error rate (SER).

The Complementary error function erfc is defined as:

$$\text{erfc}(x) = \frac{2}{\sqrt{\pi}}\int_x^\infty e^{-t^2}\text{dt} \tag{4.116}$$
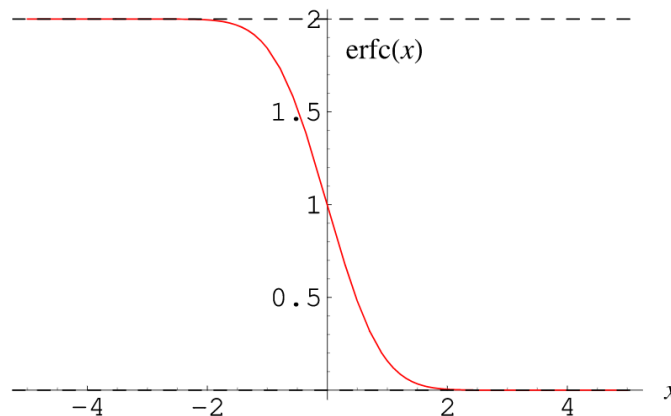
Figure 4.20: *erfc function*

We are interested in inverting this expression to derive theoretical required E_b/N_0 from the BER level. Since E_b/N_0 is expressed as a linear quantity in the expression, we must then convert it to dB.

Quadrature phase-shift keying (QPSK)

QPSK uses four phases which are separated by 90°, so can also be termed 4-PSK. With four phases, QPSK can encode two bits per symbol; so a QPSK symbol does not represent 0 or 1, but 00, 01, 10, or 11.

Conceptual transmitter structure for QPSK: the binary data stream is split into the in-phase (I channel) and quadrature-phase (Q channel) components; these are then separately modulated onto two orthogonal basis functions. Afterwards the two signals are superimposed and the resulting signal is the QPSK signal.

The mathematical analysis shows that QPSK can be used either to double the data rate compared with a BPSK system while maintaining the same bandwidth of the signal, or to maintain the data rate of BPSK but halving the bandwidth needed. In this latter case, the BER of QPSK is exactly the same as the BER of BPSK.

Although QPSK can be viewed as a quaternary modulation, it is easier to see that it is is characterized by two independently modulated carriers. The even (or odd)

bits are used to modulate the in-phase component of the carrier, while the odd (or even) bits are used to modulate the quadrature-phase component. BPSK is used on both carriers and they can be independently demodulated. As a result, the probability of bit error for QPSK is the same as for BPSK (while SER can be approximated as twice the BER).

Offset QPSK (OQPSK)

Taking four values of the phase (two bits) at a time to construct a QPSK symbol can allow the phase of the signal to jump by as much as 180° at a time; these phase-shifts result in large amplitude fluctuations, an undesirable quality in communication systems.

By offsetting the timing of the odd and even bits (thus introducing an offset between I and Q channels) by one bit-period (or half a symbol-period), the in-phase and quadrature components will never change at the same time (only one bit of the symbol is changed at a time). This will limit the phase-shift to no more than 90° at a time, so it yields much lower amplitude fluctuations than non-offset QPSK. This is why OQPSK is sometimes preferred in practice, while BER remains the same.
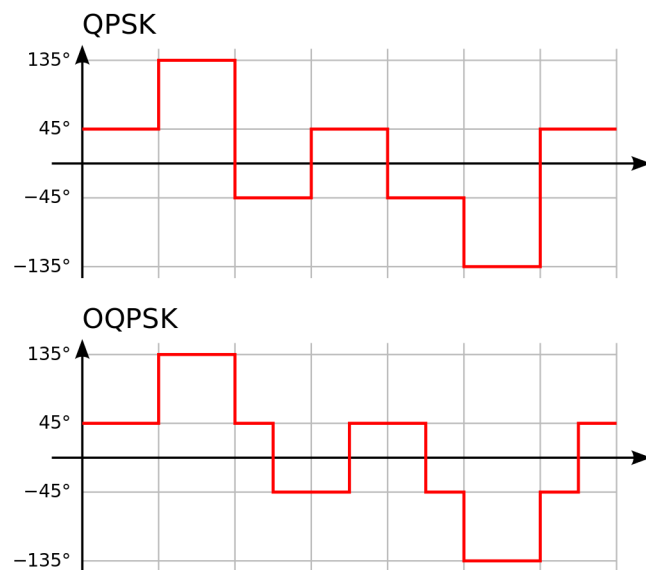
Figure 4.21: *Phase difference between QPSK and OQPSK*

Higher-order PSK

Any number of phases may be used to construct a PSK constellation but 8-PSK is usually the highest order PSK constellation deployed, because with more than 8 phases, the error-rate becomes too high. Although any number of phases may be used, the fact that the constellation must usually deal with binary data means that the number of symbols is usually a power of 2 to allow an integer number of bits per symbol.

For the general M-PSK, The BER can be estimated as:

$$\text{BER} = P_b = \frac{1}{m}\text{erfc}\left[\sqrt{\frac{mE_b}{N_0}}\sin\left(\frac{\pi}{M}\right)\right] \tag{4.117}$$

where:

- M are the number of phase used in the modulation
- $m = \log_2(M)$

Gaussian minimum-shift keying (GMSK)

Minimum-shift keying (MSK) is a type of Continuous-phase frequency-shift keying (CPFSK) with a frequency separation of one-half the bit rate. In contrast to other digital phase modulation techniques where the carrier phase abruptly resets to zero at the start of every symbol (e.g. M-PSK), with CPM the carrier phase is modulated in a continuous manner. Phase continuity yields high spectral efficiency.

Similar to OQPSK, MSK is encoded with bits alternating between quadrature components, with the Q component delayed by half the symbol period. However, instead of square pulses as OQPSK uses, MSK encodes each bit as a half sinusoid. This results in a constant-modulus signal (constant envelope signal), i.e., the transmitted carrier power is constant. This yields to excellent power efficiency and reduces problems caused by non-linear distortion.

Gaussian minimum-shift keying (GMSK) is similar to standard minimum-shift keying (MSK); however, the digital data stream is first shaped with a Gaussian filter before being applied to a frequency modulator, and typically has much narrower phase shift angles than most MSK modulation systems. This has the advantage of reducing sideband power, which in turn reduces out-of-band interference between signal carriers in adjacent frequency channels. GMSK has high spectral efficiency, but it needs a higher power level than QPSK, for instance, in order to reliably transmit the same amount of data:

$$\text{BER} = P_b = \frac{1}{2}\text{erfc}\left(\sqrt{\frac{\alpha E_b}{N_0}}\right) \tag{4.118}$$

where α =0.68 is the factor indicating the increase in power level.

Binary Frequency-shift keying (BFSK)

For analyzing the bit error rate with coherent FSK demodulation, let us compare the signaling waveform used by BFSK (or 2-FSK) when compared with BPSK. We can see how the distance between the energy of the signaling waveform:

- for BPSK it is $4E_b$, because it uses antipodal signaling
- for BFSK it is $2E_b$, because it uses orthogonal signaling
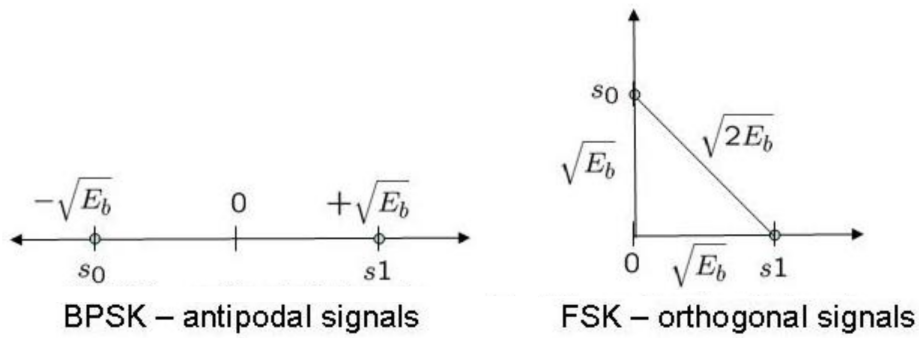
Figure 4.22: *Antipodal and orthogonal signaling diagram*

Using similar mathematical formulation used for BPSK, but with the distance between the signals reduced by half, the bit error probability for coherent binary frequency shift keying is:

$$\text{BER} = P_b = \frac{1}{2}\text{erfc}\left(\sqrt{\frac{E_b}{2N_0}}\right) \tag{4.119}$$

For obtaining the same bit error rate as BPSK, binary frequency shift keying requires around 3dB more power.
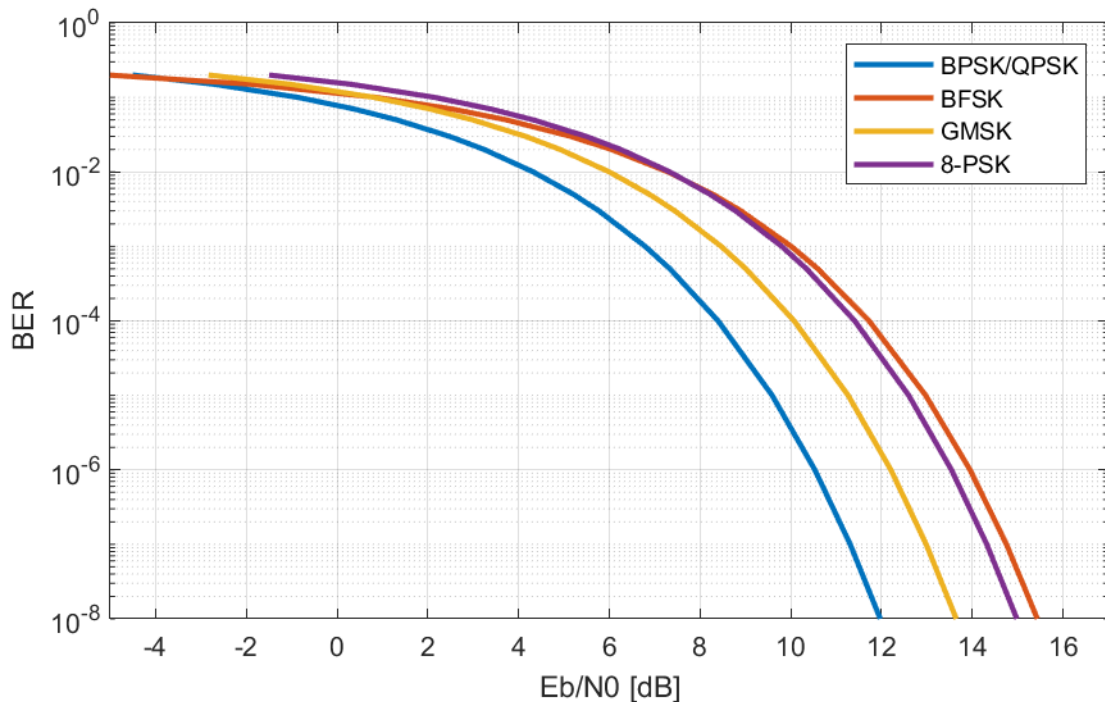
Figure 4.23: *BER performance for different modulation techniques*

Figure 4.23 shows BER variation as a function of E_b/N_0 for the modulation techniques discussed above and how it tends to increase, generally speaking, going from BPSK to 8-PSK and BFSK, passing through GMSK.

4.4.2 CCSDS Communications protocol

The Consultative Committee for Space Data Systems (CCSDS) is an agency that develops recommended standards for space communications; these standards, among other things, specify possible communications protocols designed to be used over a space link. A communication protocol is a system of rules that allows two or more entities of a communications system to transmit information via any kind of variation of a physical quantity; it defines the rules, syntax, semantics and synchronization of communication, well-defined formats for exchanging various messages and possible error recovery methods.

Here we will analyze only those aspects of the protocol that are involved in calculating the Link Budget, starting with modulation: the modulation techniques provided are precisely those previously discussed: PM and FM for analog modulation, BPSK, QPSK, OQPSK, 8-PSK, GMSK, and BFSK for digital modulation.

In addition to the choice of modulation technique, for the calculation of demodulation treshold, it is important to consider the encoding applied to the data. In general, this generates a coding gain over the theoric threshold, which will improve the quality of communication. Figure 4.24 shows how the demodulation treshold for a Baseband can vary due to the effect of encoding.
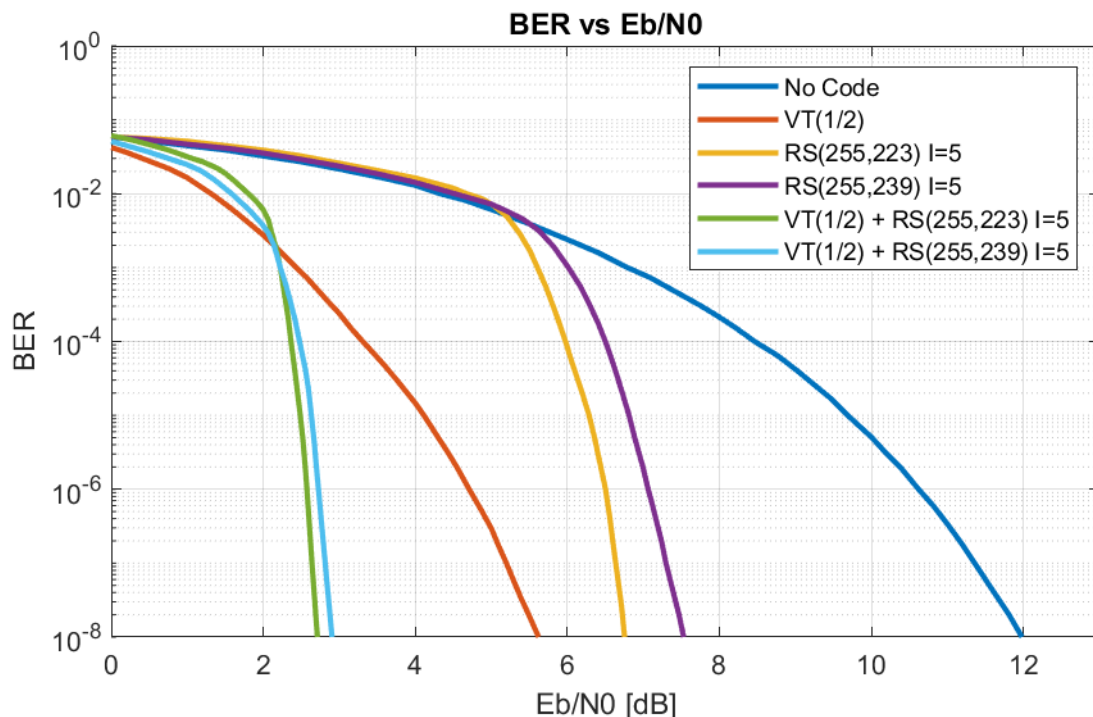
Figure 4.24: *BER performance for different encodings*

No encoding other than the implicit Hamming encoding is usually applied to Telecommand, so the TC acquisition threshold coincides with the theoric threshold calculated only as function of the modulation applied to the Uplink carrier. Hamming code is a binary linear error-correcting code which can detect one-bit and two-bit errors, or correct one-bit errors without detection of uncorrected

errors. Hamming codes are perfect codes, which means that they achieve the highest possible rate for codes with their block length and minimum distance of three (i.e. the minimal number of bit changes needed to go from any code word to any other code word is three). Due to the limited redundancy that Hamming codes add to the data, they can only detect and correct errors when the error rate is low.

For Telemetry. CCSDS protocol foresees two possible encodings:

- Viterbi (VT) decoding is an algorithm used for decoding a bitstream that has been encoded using a Convolutional code; Convolutional codes are a family of error-correcting codes that generates parity symbols via the sliding application of a boolean polynomial function to a data stream. Each m-bit information symbol (string) to be encoded is transformed into an n-bit symbol, where m/n is the base code rate ($n \geq m$); the transformation is a function of the last k information symbols, where k is the depth (or memory) of the encoder, which is often called the constraint length.

- Reed-Solomon (R-S) are a group of nonbinary error-correcting codes which are based on oversampling a polynomial that is constructed from the data to be transmitted; this means that this polynomial is computed at more points than would be sufficient to identify it univocally, then the value of these points is transmitted and at reception it is possible to reconstruct the original polynomial, and consequently the data, even in presence of errors. R-S codes operate on a block of data treated as a set of finite-field elements called symbols and are able to detect and correct multiple symbol errors; by adding $t = n - k$ check symbols to the data (where n is the block length and k the message length), a Reed–Solomon code can detect (but not correct) any combination of up to t erroneous symbols, or locate and correct up to $t/2$ erroneous symbols at unknown locations.

Based on the presence on TM of Viterbi, Reed-Solomon or a Concatenated scheme with both codes, according to the selection of Convolutional code rate and R-S block length, there will be a certain coding gain to be subtracted from the theoric demodulation treshold; these values can be deduced from the graphs provided in CCSDS 130.1-G-3. This graphs are reported in appendix C and we can observe a performance degradation as the VT code rate increases (there is a gap of about 2.4 dB between the case of rate 1/2 and the case of rate 7/8).

69

4.4.3   DVB-S2 Communications protocol

Digital Video Broadcasting - Satellite - Second Generation (DVB-S2) is the second generation specification for satellite broadcasting and consists of a communications protocol which benefits from more recent developments in channel coding (LDPC codes) combined with four modulation formats (QPSK, 8PSK, 16APSK and 32APSK). QPSK and 8PSK are typically proposed for broadcast applications, while 16APSK and 32APSK (Amplitude and phase-shift keying) modes are mainly targeted at professional applications and require a higher level of available C/N. It is regulated by the European Telecommunications Standards Institute (ETSI).

Low density parity check codes (LDPC) are a class of high-performance forward error correction (FEC) codes. The central idea is that the sender encodes the message in a redundant way, allowing the receiver to detect a limited number of errors that may occur anywhere in the message. Errors that are encountered can be not simply detected, but also corrected, and there is no need of a reverse channel to request retransmission of data when an error occurs; the downside is that there is a fixed overhead that is added to the message, thereby requiring a higher forward-channel bandwidth. The selected LDPC codes use very large block lengths (64800 bits) and Code rates from 1/4 to 9/10 are available, depending on the selected modulation and the system requirements; coding rates 1/4, 1/3 and 2/5 have been introduced to operate, in combination with QPSK, under exceptionally poor link conditions, where the signal level is below the noise level.

Error performance can be evaluated from tables given in ETSI EN 302 307-1 V1.4.1 and reported in appendix **??**, which reports Spectral efficiency and ideal E_s/N_0 for the various possible MODCOD combination and fixed PER = 10^{-7}:

- Spectral efficiency η_s is a measure of the performance of channel coding methods, and it refers to the ability of a given channel encoding method to utilize bandwidth efficiently; it is defined as the average number of bits per unit of time (bit rate) that can be transmitted per unit of bandwidth;

- E_s/N_0 is the required energy per symbol to noise power spectral density (in dB);

- PER is the ratio between the useful transport stream packets (188 bytes) correctly received and affected by errors, after FEC.

Required E_b/N_0 can be calculated as:

$$\frac{E_b}{N_0} \, [\text{dB}] = \frac{E_s}{N_0} - 10 \log_{10}(\eta_s) \tag{4.120}$$

It is also necessary to mention the AX.25 communications protocol, which does not involve any encoding for either telecommand or telemetry.

Chapter 5

SROC Mission and Communication

After analyzing the theories and developing the Link Budget Calculator, this was adapted for SROC mission and employed to study its communications system and design a possible configuration of GSN for support, trying to meet the mission needs as best as possible with a low cost and efficient solution, but also able to improve some aspects of the mission that might turn out to be tricky. The mission informations are taken from reference [6] and only the necessary ones are summarized in this chapter.

5.1 Mission overview

The Space Rider Observer Cube (SROC) mission is led by ESA and has been thought as an add-on to complement the Space Rider project; it aims at demonstrating critical capabilities and technologies required for successfully executing a rendezvous & docking mission in a safety-sensitive context. The SROC space system is constituted by a 12U CubeSat, which will be launched as payload of Space Rider (the launch is planned at the end of 2024) and deployed from the cargo bay, and a deployment and retrieval system. SROC will fly in formation with Space Rider taking observation of the vehicle from close distance (with a multispectral camera) before docking and reentering Earth with the mothership.

5.1.1 Mission statement and Main objectives

> **SROC mission statement**
>
> To operate a CubeSat in LEO to demonstrate capabilities in the close-proximity operations domain in a safety-critical context, including rendezvous and docking with another operational spacecraft.

These are the main mission objectives that have been derived considering the identified stakeholders' needs:

- To demonstrate critical technologies and functions related to formation flight missions, in terms of:

    - Proximity Navigation

    - Guidance and Control capabilities

    - Communication architecture

    - Autonomous operations

- To demonstrate critical technologies and functions related to deployment, docking and retrieval of CubeSats:

    - Guidance, navigation and control algorithms for close approach up to docking

    - Deployment and retrieval mechanisms

    - Docking systems

- To observe Space Rider with unprecedented imaging for engineering and outreach purposes:

    - Imaging capabilities

5.1.2 Concept of operations

Because this is an innovative and complex mission, multiple mission scenarios are required to be planned with an incremental level of complexity. Here we will analyze the baseline scenario, which involves an Observe & Retrieve mission: The spacecraft is deployed from Space Rider, observes the vehicle from close distance, and eventually approaches Space Rider, performs docking and it is retrieved and stowed into the cargo bay for re-entry on Earth.

Mission phase	Mission subphases
Integration & Pre-Launch Phase (IPLP)	Integration phase (SROC in SR, SR in Vega C) Pre-Launch phase
Launch & Early Operations Phase (LEOP)	Launch phase Deployment phase
Commissioning and Performance Verification Phase (CPVP)	Commissioning phase Verification phase
Proximity Operations Phase (POP)	Rendezvous phase (to start formation flight) SR Observation phase (orbiting around SR)
Docking & Retrieval Phase (DRP)	Closing phase Final Approach phase Mating phase Retrieval phase
End of Mission Phase (EMP)	Re-entry phase Post-landing phase Post-flight phase

Table 5.1: *SROC Observe* & *Retrieve scenario ConOps*

An Observe mission is also provided, in which SROC is not retrieved in the SR cargo bay at the end of its mission. This scenario can represent an alternative option in case of time and/or cost costrains, or it serves as off-nominal scenario of the baseline one, should any failure occur that prevents docking.

The maximum mission duration is about 30 days from deployment to completion of retrieval in the cargo bay, while the nominal duration is less than 15 days. In case of a disposal in orbit (i.e. no retrieval), the SROC spacecraft will lower its orbit and disintegrate in Earth upper atmosphere in less than 1.5 years.
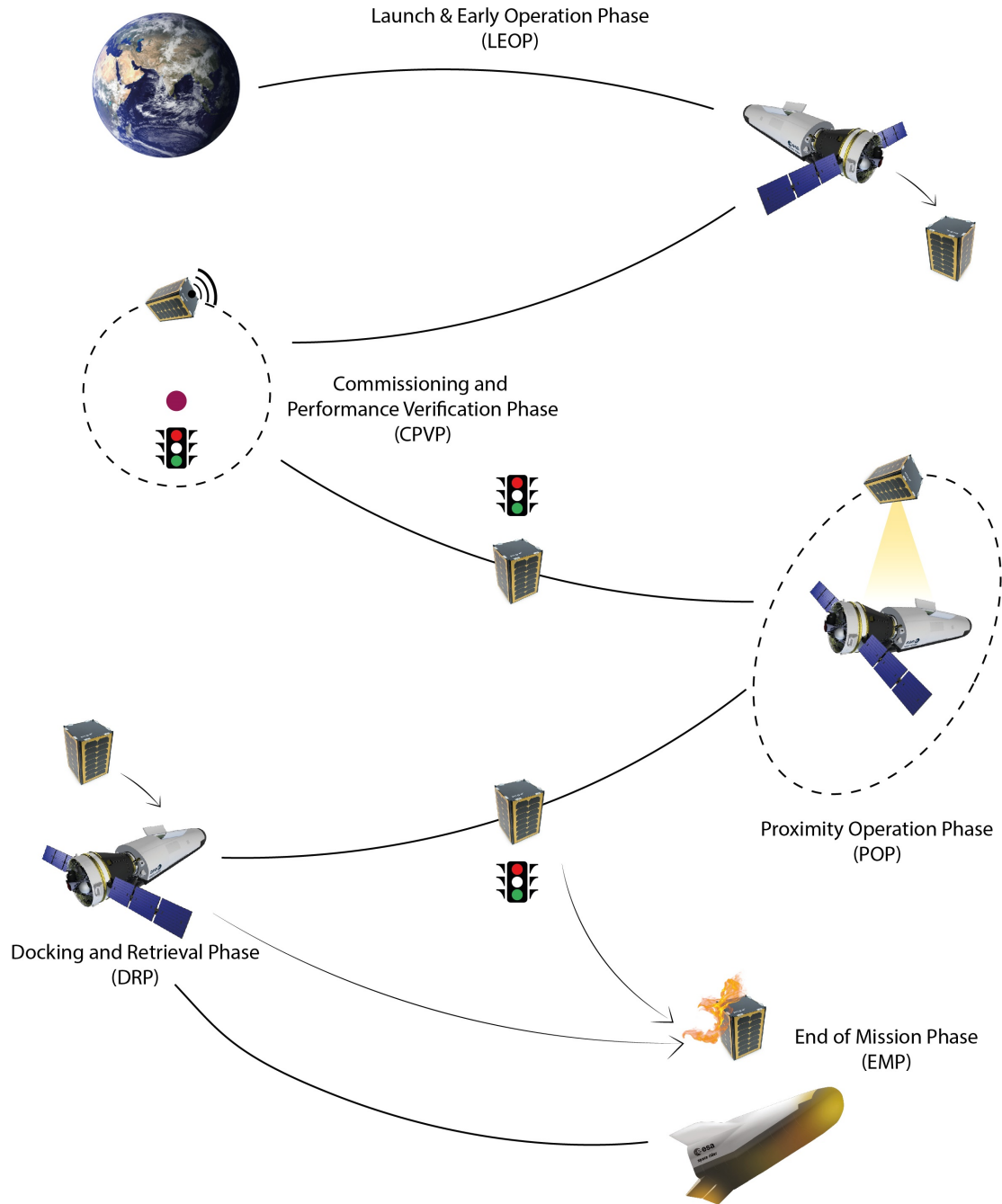
Figure 5.1: *SROC mission phases*

5.1.3   Mission architecture

The SROC Mission architecture summarise and briefly describes the mission elements. The main objectives of the mission are related with the demonstration of advanced capabilities in the area of proximity operations; novel technology is being developed for this purpose and it needs to be tested in orbit in different phases of the mission.

Mission element	Description of baseline	Options / comments
Subject	Space Rider observations	Visual observations are considered for the baseline design with the objective of achieving 1 cm spatial resolution
	Close Proximity Operations	Execution of manoeuvres for acquisition of hold points, for insertion into rendezvous trajectories with respect to SR, for insertion into observation trajectories. Determination of relative distance from Space Rider with different sensors and techniques
	Docking & Retrieval demonstration	Single deployment and retrieval of SROC (no reuse within the same mission)
Payload	Visual camera	The baseline solution for the payload is a visual camera based on Tyvak detector (the same used for the navigation cameras) with ad-hoc optics
	ProxOps technlogy	6 DOF propulsion system, navigation & control algorithms, deployment & retrieval system, docking system
Space Segment	1 CubeSat (SROC)	12U form factor, based on Tyvak Phoenix platform, with body mounted solar arrays and cold gas propulsion sys
	Multi-Purpose CubeSat Dispenser	MPCD design is compliant with the Observe & Retrieve scenario
	Docking System	DOCKS is the interface between SROC and the MPCD. It includes the sensors suite for supporting the navigation function for relative distance < 1m and the mechanisms needed to guarantee SROC docking to SR
Orbit & Constellations	LEO circular 400 km	Quasi-equatorial orbit (i = 6.2°) assumed as baseline
	Formation flight with SR	Rendezvous: passively safe in-plane + out-of-plane segments. SR observation: Walking Safety Ellipse with relative inclination change and variable geometry. Docking: along the in-track axis
Comm Architecture	Store & Forward architecture	Direct link to Earth for communication. Crosslink between SROC spacecraft and MPCD is an option for supporting navigation function
Ground Segment	Ground station network	Network of UHF and S-band ground stations. Compatibility with Estrack network is guaranteed
	Mission Control Centre	SROC MCC in Torino. The SROC MCC shall be in contact with the SR MCC for specific mission phases and/or needs
Operations	Mission Planning Spacecraft Control Flight dynamics	Drivers for Ops design: safety, reliability & autonomy. Compliance with ESA standards. Coordination with SR operations
Launch Segment	CSG spaceport + Vega C + SR	Launch assumed Q4 2024 (baseline, target: SR maiden flight). Other late launch dates are considered

Table 5.2: *SROC mission architecture*

5.1.4 Mission analysis

In this section we analyze the orbit trajectory, which is an important element in the study of communications through link budget and visibility analysis. To continue with the study we will simply approximate the orbit of SROC by simply considering that of Space Rider.

Space Rider features a variety of scenarios, depending on mission phase (LEOP, routine, de-orbit) and orbital configuration (near-equatorial orbit, mid-inclination orbit). Our analysis, however, takes place entirely in the routine phase and we will consider only the near-equatorial orbit.

The first Space Rider System reference envision a Near-Equatorial Orbit at 400 km altitude and 6.2 deg inclination. In table 5.3 are reported the initial orbital parameters for the propagation of the orbital phase, which are the ones at the Injection condition and are obtained from the Space Segment analysis. The orbital parameters are osculating and expressed in the True of Date Earth Equator reference frame, and also the topocentric geodetic coordinates are provided.

Injection Epoch (UTC)	1 Jan 2025 09:47:20.61
Semimajor axis a (km)	6778.129
Eccentricity e	0.000
Inclination i (deg)	6.200
Longitude of the ascending node Ω (deg)	118.824
Argument of periapsis ω (deg)	1.990
True anomaly θ (deg)	235.364
Latitude (deg)	107.90
Longitude (deg)	-5.250
Height h (km)	400.176

Table 5.3: *Injection Orbital Parameters of the Near-Equatorial Orbit*

Starting from this initial condition, the two-month mission is simulated concerning the reference mission timeline based on payload activities, and adopting a dynamic model which as perturbative forces takes into account Earth gravity, atmospheric drag and Luni-solar third body attraction. The corresponding propagated orbit order is critical to compute the Ground Stations coverage for the mission.

In the link budget, it should also be taken into account that, during the formation flight for the observational phase, there is a 200 m keep-out zone between Space Rider and SROC to ensure the safety of operations

5.2 Communication system

SROC Telecommunications are handled through two radios:

- an S-Band radio, baselined for high data-rate downlink of Payload Scientific data;

- and a UHF transceiver baselined for TT&C needs (TC and TM Housekeeping data).

Each radio can operate simultaneously and independently. Both can Downlink telemetry and mission data if needed. A third optional radio is under evaluation to provide Intersatellite link (or Data relay) between SROC and the MPCD, and could either be a dedicated module or the TT&C transceiver itself.

Two antennas are mounted on the CubeSat:

- a V Dipole omnidirectional deployable antenna for the Space-Ground and Space-Space UHF links;

- a Patch antenna with Left-handed circular polarization (LHCP) for the Space-Ground S-band link

Communication is characterized by a Store & Forward architecture: each data packet must first be totally acquired, then it is temporarily stored, its integrity is verified, and lastly it is transmitted downlink. The communication architecture provides two options and both are viable:

- SROC can communicate via interlink with SR (in UHF);

- SROC can communicate via direct link with ground station with autonomy level (in S-band or UHF).

	UHF	**S-band**
Frequency Band (MHz)	400-470 800-930	2200-2400
Data Rate (kbps)	1.2-250	100-4000
Modulation Scheme	FSK, GMSK	BPSK
Encoding	AX.25	CCSDS
Encription	AES-GCM	AES-GCM
Antenna Type	V dipole	Patch
Polarization	Linear	Circular (LHCP)
Antenna Gain (dB)	1.9	5-7
Max RF Tx Power (W)	1-2	1-2
Line loss (dB)	0.5	0.5
System G/T (dB/K)	-25.98	-22.88

Table 5.4: *SROC Communication system characteristics*

The daily amount of data from the payload to be transmitted is 100 MB/day and this is a major drive for the design of the GSN. To understand whether this satisfies the data download capability, a visibility analysis is required, which is discussed in subsection 6.2.1.

5.3 GSN for SROC support

Direct communication with SROC is handled by Politecnico di Torino, but external support may be required. Telespazio could provide a Ground Station Network to support the baseline one, but here it will be designed to be completely independent from the latter and to ensure full communication with SROC even on its own. The main drivers considered in the GSN design are:

- The selection of a well-consolidated set and operationally-proven S-Band and UHF Ground Stations already used in the past by Telespazio for several other missions;

- The re-use of the existing infrastuctures, with the purpose of minimizing implementation costs and efforts as much as possible;

- The provision of a quality service with multiple options (when possible) and once the actual performance has been evaluated, where the low-cost solution is not completely satisfactory, the proposal of alternative solutions;

- The achievement of a visibility window as wide as possible to provide a greater margin of time in the docking phase.

5.3.1 GSN functions

The GSN implements the following functions:

- Access to the Spacecraft
    - Satellite tracking
    - Telemetry downlink (Housekeeping and Payload scientific data)
    - Telecommand uplink (Backup)
- Networking
    - Data connectivity with internal entity
    - Data connectivity with external entity

Satellite tracking

Antennas has three tracking modes

- Manual

- Auto-track (Mono-pulse)

- Program-track (TLE)

For the spacecraft to be acquired, it is necessary to know its position when it rises on the horizon; this condition depends on the physical limits of antenna motion and the circular horizon of the site, but it is a good estimate to consider a value of 5° elevation as the cut-off angle.

A Two-line element set (TLE) is a data format encoding a list of orbital elements of an Earth-orbiting object for a given point in time, noted as epoch. Using a suitable prediction formula, the state (position and velocity) at any point in the past or future can be estimated to some accuracy.
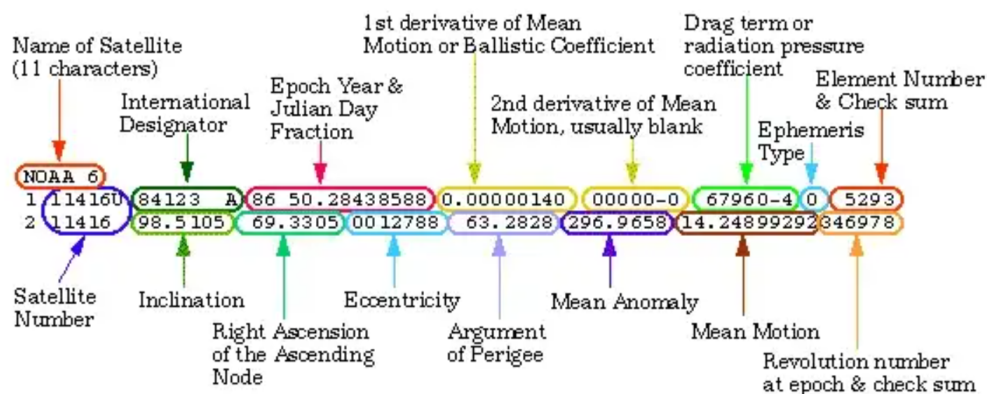
Figure 5.2: *TLE file scheme*

The TLE file is loaded into the antenna and, at the appropriate time, it can be set in Program-track so that the TLE is processed by the Antenna control unit (ACU), which moves the antenna to point to the predicted position, where the satellite is expected to be. However, in case the antenna is not pointing the signal mainlobe, the offsets can be adjusted manually on both axis (aziumth and elevation) to improve the signal level.

The feed of each Ground Stations is equipped with Auto-track capability using the single-channel mono-pulse technique, which is an electronic scan network of switches that samples the incoming RF from the tracking channel and the data channel; due to the positioning of the tracking channel, the received RF signals are not at the same power level. A Tracking signal is created and passed to the ACU, which creates positioning commands, so that the antenna moves to where the signal is strongest.

Telemetry downlink

Telemetry function characteristics:

- The Ground station waits for Satellite visibility start, i.e the Acquisition of signal (AOS);

79

- As soon as the Baseband Unit (BBU) have a Telemetry lock, the TM frames are sent to the Network Control Centre (NCC) and if necessary, a protocol conversion is performed, so that the NCC can deal with them and transfer data to users;

- By means of the BB Manager, it is possible to connect on the BBU to check:

  - BB configuration (according to the mission characteristics)

  - Bit error rate

  - Synchronization errors

  - Decoding errors

  - lost frames

- This occurs ideally (if there are no unforeseen contingencies) up to the satellite visibility end, i.e. the Loss of signal (LOS).

Downlink data can be of two types:

- Housekeeping (HK) TM, which are the spacecraft onboard data, are received in UHF (as baseline) with low data rate.

- Payload scientific data, which are the mission data to fulfill the objectives, are received in S-band (as baseline) with high data rate.

Telecommand uplink

Telecommand function characteristics:

- The Ground station waits for Satellite visibility start (AOS);

- At $5°$ of elevation, the command carrier will be raised up and sweep is started so, once the onboard lock is obtained, sweep is stopped and command activity will start;

- The Ground System commands and controls the spacecraft based on requests from the users to the control centres;

- This occurs ideally (if there are no unforeseen contingencies) up to the satellite visibility end (LOS);

- The Telecommand function performed by Telespazio is intended as a redundancy backup, since the spacecraft will be controlled primarily by Politecnico di Torino;

TC is received only in UHF with low data rate so, as we will see soon, only some ground stations have command capabilities.

5.3.2   Selected Ground Stations

Three Ground Stations has been selected to support SROC mission in all frequency bands. Stations were selected only from those close to the equator, preferably with a latitude $< 10°$, to prevent passages of little or no duration.

Station	Country	Latitude	Longitude	Height	Supported bands
Singapore	Singapore	1.3961° N	103.8343° E	25.6 m	UHF / S-band
Malindi	Kenya	2.9963° S	40.1938° E	17.0 m	S-band
Sri Lanka	Sri Lanka	7.2742° N	80.7248° E	462.0 m	UHF / S-band

Table 5.5: *Selected Ground stations for SROC support*

In figure 5.3, the SR/SROC Ground track is illustrated for the first day of the mission together with the selected Ground Stations network:

Figure 5.3: *SR/SROC Ground track and GSN*

Malindi and Singapore Ground stations are selected directly from the Space Rider Network for routine phase with quasi-equatorial orbit. They can do simultaneous TM reception in S-band. Since they are designed for Space Rider data acquisition (2 GB per day) they can easily manage SROC data acquisition on their own: the downside is that these stations will have to handle communications with SROC and Space Rider concurrently. For TC transmission in UHF, A Yagi-Uda antenna has also been identified in Singapore.

81

In order to give an alternative to the coexistence of SROC and Space Rider links, and to provide another site for UHF communication, the Sri Lanka ground station was also included; it belongs to another network specifically dedicated to nano, micro and small satellites. It is suitable for SROC mission, because it allows both UHF and S-band communication and it is geolocated roughly halfway between the other two stations (useful to obtain continuous visibility).

G/S antennas are parabolic dishes for S-band and Yagi-Uda for UHF. They can transmit and receive in RHCP and/or LHCP: for TC Uplink it is possible to switch between the two polarizations, while for TM Downlink the two channels can be in operation simultaneously.

Parameters	Singapore		Malindi	Sri Lanka	
Frequency Band	S-band	UHF	S-band	S-band	UHF
Diameter (m)	9.1	–	10	3.7	–
Tx Frequency (MHz)	2025-2120	401-403	2025-2120	2020-2120	401-403
Rx Frequency (MHz)	2200-2300	399-402	2200-2300	2200-2300	399-402
Antenna Gain (dB)	43.7	14.6	44.52	35.89	14.6
Max EIRP (dBW)	59	34	68	50	34
System G/T (dB/K)	20.5	-11.6	21.6	12.8	-11.6

Table 5.6: *Ground stations specifications*

Singapore Ground Station

SI1 antenna was installed in August 2011, and it is located in Singapore, about 137 km north of the equator, off the southern tip of the Malay Peninsula. Two distinct antennas are selected in this site:

- A 3.7 m parabolic dish provides S-band capabilities for payload scientific data reception;
- A 16-element Yagi-Uda antenna provides UHF capabilities for TT&C needs.

The station is characterized by uninterruptable power and high level of security.

Logistic parameters		
Site	Singapore	
Antenna name	SI1	
Diameter (m)	9.1	
Latitude	1.3961° N	
Longitude	103.8343° E	
Height	25.6 m	
Technical parameters		
Band	S-band	UHF
Tx Frequency (MHz)	2025-2120	401-403
Rx Frequency (MHz)	2200-2300	399-402
Antenna Gain (dB)	43.7	14.6
Max EIRP (dBW)	59	34
System G/T (dB/K)	20.5	-11.6
Uplink polarization	Circular (RHCP or LHCP) selectable	
Downlink polarization	Circular (RHCP or LHCP) simultaneously	
Axial ratio (dB)	1.0	
Tracking mode	Mono-pulse, Program-track (TLE) and manual	
Travel range	0° ± 360° (azimuth), −2° to +182° (elevation)	
Max speed	15°/sec (azimuth), 7°/sec (elevation)	
Pointing accuracy	0.08° (max error)	
Tx Line loss (dB)	1 + 1 (HPA + U/C)	
Rx Line loss (dB)	1 + 1 (LNA + D/C)	

Table 5.7: *Singapore G/S specifications*

Malindi Ground Station

MAL-2A antenna is located 145 Km North of Mombasa (Kenya); the station site is the Broglio Space Centre, which is a complex of facilities situated near the Equator in 'Ngwana Bay near Malindi. It consists of a 10 m parabolic dish and it provides S-band capabilities for Payload data reception only. Considering the mission baseline , TT&C needs are not fulfilled by this station.

Logistic parameters		
Site	Malindi	
Antenna name	MAL-2A	
Diameter (m)	10	
Latitude	2.9963° S	
Longitude	40.1938° E	
Height	17.0 m	
Technical parameters		
Band	S-band
Tx Frequency (MHz)	2025-2120
Rx Frequency (MHz)	2200-2300
Antenna Gain (dB)	44.52
Max EIRP (dBW)	68
System G/T (dB/K)	21.6
Uplink polarization	Circular (RHCP or LHCP) selectable
Downlink polarization	Circular (RHCP or LHCP) simultaneously
Axial ratio (dB)	1.0
Tracking mode	Mono-pulse, Program-track (TLE) and manual
Travel range	0° ± 360° (azimuth)
Max speed	19.75°/sec (azimuth), 5.16°/sec (elevation)
Pointing accuracy	0.01° (max error)
Tx Line loss (dB)	1 + 1 (HPA + U/C)
Rx Line loss (dB)	1 + 1 (LNA + D/C)

Table 5.8: *Malindi G/S specifications*

Sri Lanka Ground Station

AS-01 antenna is located in Sri Lanka, off the south-eastern coast of the Indian subcontinent, specifically in a major city of the central area called Kandy. The antenna is composed by two subsystems (integrated into the same structure):

- A 3.7 m parabolic dish provides S-band capabilities for payload scientific data reception;

- A 16-element Yagi-Uda antenna provides UHF capabilities for TT&C needs.

This station has been designed to minimize external needs in terms of land, electronics storage and human support, but it has rather poor performance.

Logistic parameters		
Site	Sri Lanka	
Antenna name	AS-01	
Diameter (m)	3.7	
Latitude	7.2742° N	
Longitude	80.7248° E	
Height	462.0 m	
Technical parameters		
Band	S-band	UHF
Tx Frequency (MHz)	2025-2120	401-403
Rx Frequency (MHz)	2200-2300	399-402
Antenna Gain (dB)	35.89	14.6
Max EIRP (dBW)	50	34
System G/T (dB/K)	12.8	-11.6
Uplink polarization	Circular (RHCP or LHCP) selectable	
Downlink polarization	Circular (RHCP or LHCP) simultaneously	
Axial ratio (dB)	1.0	
Tracking mode	Mono-pulse, Program-track (TLE) and manual	
Travel range	0° ± 270° (azimuth), 0° to 90° (elevation)	
Max speed	20°/sec (azimuth), 2°/sec (elevation)	
Pointing accuracy	0.1° (max error)	
Tx Line loss (dB)	1 + 1 (HPA + U/C)	
Rx Line loss (dB)	1 + 1 (LNA + D/C)	

Table 5.9: *Sri Lanka G/S specifications*

5.3.3   Ground Stations architecture

The typical architecture of a Ground Station operated by Telespazio provides 4 chains, 2 for Uplink and 2 for Downlink. Each one can operate on both LHCP or RHCP, since it is possible, by means of switches, to invert the connection between the various equipments and/or with the antenna (useful in case of failure in one of the channels).
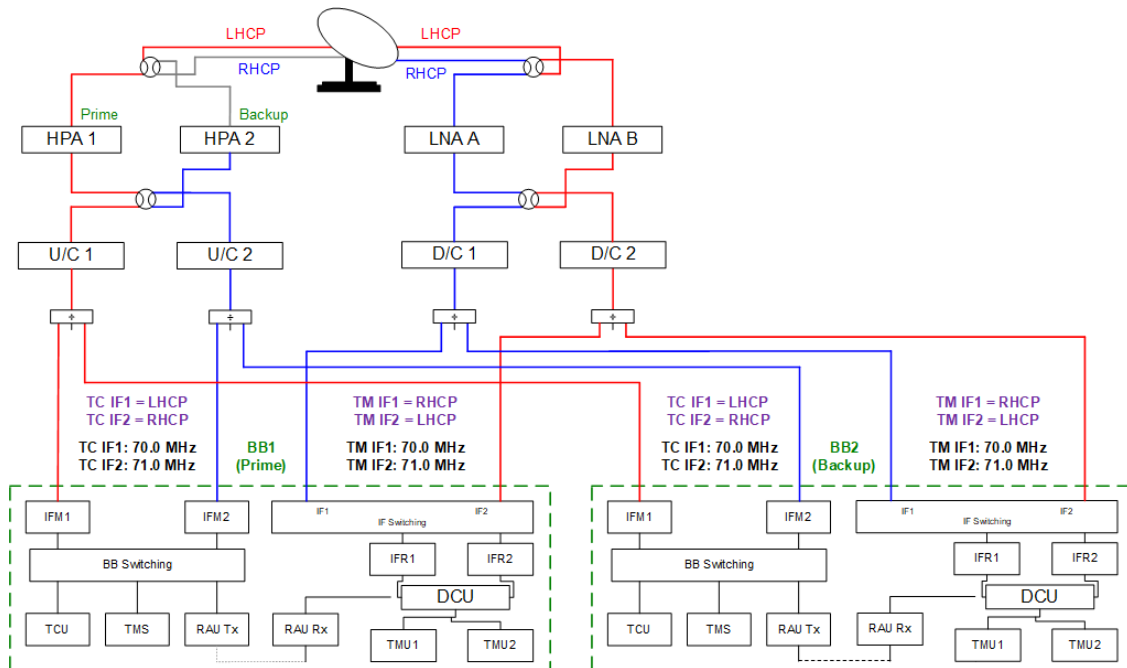
Figure 5.4: *Ground Station typical architecture*

For Uplink, a Prime and a Backup chain are foreseen, working in redundancy configuration. The Uplink signal transmitted by BBU, which is in IF level (in a range from 60 to 78 MHz, which are the operational frequencies of U/C and D/C considered models), is converted in RF by the Up Converter (U/C 1 and U/C 2) and then passes through the High Power Amplifier (HPA 1 and HPA 2) which generates a Tx Power to be radiated by the antenna feed. For TC transmission, one of the channel must be selected, with either LHCP or RHCP.

For Downlink as well, there are a Primary and a Backup chain in redundancy. Low Noise Amplifier (LNA 1 and LNA 2) converts Rx Power to RF, which are converted in IF level by Down Converter (D/C 1 and D/C 2), to be fed to BBU input. Both channels can operate at the same time on both LHCP and RHCP.

For Uplink, BBU is equipped with two modulators (IFM1 and IFM2), that permit the transmission of the carrier modulated by TC data coming from Telecommand Unit (TCU) output, in either LHCP or RHCP.

For Downlink BBU is equipped with 2 IF receiver (IFR1 and IFR2), that permit the reception of the carrier modulated by TM data, feeding to Telemetry unit (TMU1 and TMU2). With this configuration BBU is capable to receive both polarization at the same time.

Both U/C and both D/C are connected to the Prime BBU (BB1) but also to a Backup BBU (BB2), which runs concurrently and serves as redundancy in case BB 1 fails.

Concurrent communication configuration

Malindi and Singapore stations are part of the Space Rider network and consequently, according to the philosophy adopted, the same antenna (Singapore SI1 and Malindi MAL-2A) should be able to communicate with Space Rider and SROC using the same G/S configuration. Since Uplink with SROC is only in UHF, the Uplink chain is dedicated to Space Rider only, while Downlink needs to be shared between the two spacecraft, so that Payload scientific data can be received from both SROC and Space Rider simultaneously. This is possible by applying one of these two strategies:

- BB 2 is dedicated to SROC while BB 1 is dedicated to Space Rider. This is possible by assuming that SROC operates in similar frequencies as Space Rider, in a range of 14 MHz ($\pm$7 MHz from D/C reference frequency), so that the same D/C can operate on both signals, considering a Carrier bandwidth of 4 MHz; the D/C frequency needs to be setted according to the spacecrafts frequencies, which however, to avoid any interference, must have an offset of at least 4 MHz. The disadvantage, in addition to the frequency constraint, is that in this way the redundancy of Space Rider BBU is lost; if a failure happens to BB 1, it would be replaced by BB 2 and SROC would be left without support.

- LHCP channel is dedicated to SROC (which supports only LHCP) while RHCP channel is dedicated to Space Rider (which supports both polarizations). In this way, there would be no frequency constraint and BBU redundancy would be maintained, but redundancy on the channels would be lacking instead; if a failure happens in the RHCP channel or if, for some other reason, it becomes necessary to dedicate LHCP channel to Space Rider, SROC would be left without support.

In both cases, the lack of redundancy of one element rather than another threatens the safety philosophy for both Space Rider and SROC. Obviously, the safest and most expensive solution is to locate on both sites a dedicated antenna for SROC, having to take into account, however, that the on-site antennas might all be already employed in other activities and, at that point, a new one would have to be built from scratch, exponentially increasing cost and effort of implementation. A cheaper but still reliable alternative is to consider the same antenna and equip it with a receiver chain (LNA, D/C and BBU) dedicated to SROC.

Chapter 6

SROC Link Budget and Visibility

This chapter discusses the results of the communications analysis for the GSN proposed for SROC support. The link budget analysis is critical to understand whether the GSN so designed provides a satisfactory link with each station for each case. This leads to the following final considerations and proposed improvements.

6.1 Link Budget analysis

The link budget was calculated for all selected Ground stations, in both Uplink and Downlink, to assess the quality of their performance and the ability to ensure robust communication capacity in the worst-case scenario.

These are the preliminary considerations and assumptions made in order to calculate the link budget:

- Extreme longitude satellite position is assumed with an elevation angle of 5° (worst case);

- Link availability assumed 99.99 % for conservative reasons;

- Atmospheric model uncertainty assumed $\pm\,25\,\%$;

- S/C transmitting at nominal Tx Power of 1 W, while Max Tx Power of 2 W is considered for the favourable case;

- S/C Axial Ratio value is assumed in a way to obtain consistent value of polarization loss;

- S/C TC Demodulation Technical loss assumed 2 dB from experience and conservative reasons;

- G/S TM Demodulation Technical loss assumed 1 dB from BBU tests;

- Roll-off factor is assumed variable in the range 0.2-0.5.

All link budget tables are reported in annex A; they are calculated for available sites based on the links considered:

- S-band Downlink budget with High data rate (HDR)

- UHF Uplink budget

- UHF Downlink Budget with Low data rate (LDR)

For each case, the estimated margins and resulting considerations are reported in the tables below. Note that margins in the nominal case must be at least:

- Uplink > 6 dB

- Downlink > 3 dB

S-band Downlink with HDR

We can notice that:

- S-band antennas selected in Singapore and Malindi Ground stations are large in size (9.1 m and 10 m diameter, respectively), with excellent EIRP and G/T values; margins are very high even in the worst case scenario, ensuring high-performance communication.

- S-band antenna in Sri Lanka is less performant but still guarantees closed link even in the worst case scenario;

- The antennas point Space Rider but must also communicate with SROC, so they are affected by an offset distance of 200 m; however the signal loss it causes is absolutely negligible ($< 10^{-3}$ dB).

Station	PL data acquisition margin (dB)		
	Nominal	Adverse	Favourable
Singapore	12.467	11.009	18.686
Malindi	14.621	13.403	20.600
Sri Lanka	4.951	3.520	11.142

Table 6.1: *Payload data acqusition margins for S-band Downlink budget*

UHF Uplink

Here are some considerations

- Since the TC bit rate was unknown, a value of 64 kbps was considered for conservative reasons. it is in fact, one of the highest values among the conventional ones handled by Telespazio;

- The UHF antennas selected in Singapore and Sri Lanka has Uplink performance that manages to provide high margins and thus a definitely closed link;

- Pointing error losses are neglectable for a UHF-antenna, whose HPBW is assumed to be 30°.

Station	TC acquisition margin (dB)		
	Nominal	Adverse	Favourable
Singapore	23.146	22.308	23.735
Sri Lanka	23.227	22.409	23.795

Table 6.2: *TC acqusition margins for UHF Uplink budget*

UHF Downlink with LDR

We can notice that:

- Margins are > 3 dB only in the favourable case, while for nominal and adverse case they are > 0 dB but < 3 dB;

- HK TM bit rate is more demanding than the TC one, and if SROC transmits at the nominal power of 1 W, the Yagi-Uda antenna allows link establishment but its downlink performance is too poor to ensure that this is satisfactory;

- To ensure a closed link, SROC should transmit in Downlink at the maximum power of 2 W.

Station	TM acquisition margin (dB)		
	Nominal	Adverse	Favourable
Singapore	1.392	0.555	4.989
Sri Lanka	1.473	0.656	5.050

Table 6.3: *TM acquisition margins for UHF Downlink budget*

To ensure a closed link without needing Max Tx power from SROC, an alternative solution could be to install on both sites an UHF Helix antenna with at least 11 turns, to improve the Gain by about 2 dB and thus ensure > 3 dB margins.

Frequency (MHz)	400
Wavelegth (mm)	750
Turns	11
Helix legth (mm)	2062.5
helix diameter (mm)	238.73
Gain (dB)	16.19
G/T (dB/K)	-7.334

Table 6.4: *UHF Helix antenna design*

6.2 Visibility analysis

Visibility analysis is essential to understand whether the GSN is able to allow all data to be downloaded from the Spacecraft and to provide support for a satisfactory duration during critical phases, for example the docking.

6.2.1 Daily visibility

First, we want to study the AOS and LOS of SROC/SR to understand whether the daily visibility time in a day allows the download of all the data. The daily amount of data from the payload to be transmitted is 100 MB/day.

Assuming to transmit always at the max data rate, to guarantee the download of all these data, the requirement for GSN design is to provide, in the routine phase, a minimum daily visibility window of at least:

$$\text{Required visibility (best)} = \frac{100 \text{ MB/day}}{4 \text{ Mbps}} = 200 \text{ s/day} = 3 \text{ m } 20 \text{ s /day} \tag{6.1}$$

Considering instead the minimum data rate, the time window that should be obtained would be:

$$\text{Req. visibility (worst)} = \frac{100 \text{ MB/day}}{0.1 \text{ Mbps}} = 8000 \text{ s/day} = 2 \text{ h } 13 \text{ m } 20 \text{ s /day} \tag{6.2}$$

From Space Rider state vector and the geographical characteristics of the GSN, it is possible to obtain an access summary report, which is the basis of the visibility analysis study. The analyses have been executed considering a G/S cut-off angle of both 2° and 5° of elevation, but only the results for the 5° case, that are more conservative, are reported. An exemple of Access summary report is reported in appendix B, along with the Global statistics of the passes for every station.

Table 6.5 shows a summary of visibility data for each station, averaged over all days considered, from January 2 to February 3.

Station	Passes	Min time	Max time	Mean time	Daily time
Singapore	15	2m 57.46s	8m 20.74s	6m 36.93s	1h 55m 2.07s
Malindi	15	6m 6.51s	8m 23.9s	7m 32.5s	1h 53m 7.54s
Sri Lanka	15	2m 43.5s	8m 15.83 s	6m 26.08s	1h 36m 32.33s
Total	45	–	–	21m 28.73s	5h 24m 40.95s

Table 6.5: *GSN coverage for SROC*

As can be seen, the total coverage is greater than 5 hours, which is definitely enough to provide the coverage needed to download data even at the lowest data rate. This makes sense when we consider that the Singapore and Malindi stations

alone can guarantee Space Rider's data download, which is far more demanding than SROC's (2GB at a max data rate of 2 Mbps).

By carefully analyzing the access report, some interesting considerations can be made:

- Since the Malindi and Singapore stations are at approximately zero latitude, thus very close to the equator, the visibility durations of the two stations are very similar,With passages lasting even more than 8 minutes;

- For the same reason, the visibility for these stations does not have much variability even as the passes change during the day; in fact, the difference between the durations of the shortest and longest passes is always less than 2 minutes, and the passes never last less than 6 minutes;

- The matter is quite different for the Sri lanka station, which instead, is farther from the equator; therefore, while having passages of similar maximum duration as the other stations, this time can shorten consistently over the course of the day, from more than 8 minutes to less than 3 minutes.

The figure 6.1 shows the SROC/SR visibility for the first mission day considered (January 2), representing the elevation in function of time for each of the two selected Ground for the Routine phase.
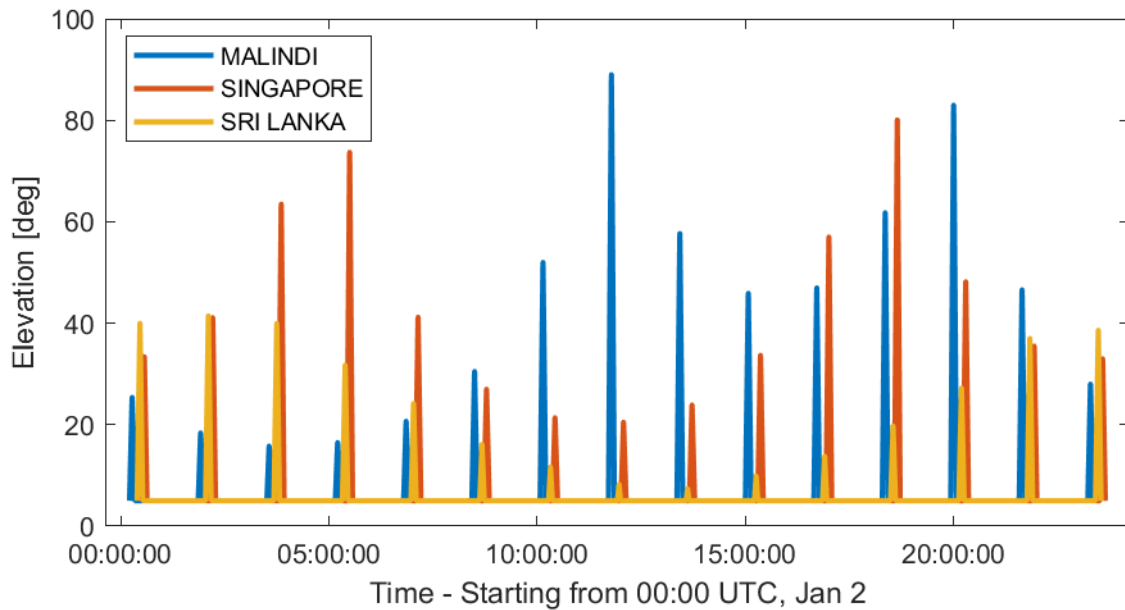
Figure 6.1: *SROC Visibility plot for the first day of mission*

6.2.2   Sri Lanka - Singapore Overlap

One of the main demands for the GSN for support is to obtain a continuous visibility window greater than the typical single station window (of about 8 minutes). The way the mission is structured, it is impossible to achieve this with a single station, so the choice is to focus on the possibility of obtaining continuous visibility from combining two stations.

In the first instance, the stations considered were Malindi, Bangalore, Sri Lanka, Singapore and Biak (listed in order of longitude from east to west). Analyzing the access report And focusing on a single day (for example January 2), it turns out that:

- Bangalore and Sri Lanka stations are located at very similar longitudes (77.58° E and 80.72° E respectively) so it is not necessary to consider them both;

- Bangalore station is located at high latitude (12.97° N) and is not suitable to track SROC; in fact, the result is that there is overlap with Singapore for only a few passes, and in addition there is a whole part of the day in which SROC passes are not visible from Bangalore, so it was discarded from the analysis;

- Between Malindi and Sri Lanka stations and between Singapore and Biak stations there is never overlap, so the Malindi and Biak stations are not fit for purpose;

The station in Sri Lanka is the only one useful for the purpose, and the temporal characteristics of the combination between Sri Lanka and Singapore stations are given in table 6.6.

	Sri Lanka	Singapore	Overlap	Total
Min coverage	5m 51.18s	8m 14.16s	52.63s	13m 12.71s
Max coverage	8m 4.81s	7m 57.38s	1m 50.43s	14m 24.4s
Mean coverage	–	–	1m 27.75s	13m 59.4s

Table 6.6: *Sri Lanka - Singapore overlap characteristics*

In this way, it is possible to obtain a total visibility variable from 13 minutes to over 14 minutes, going almost double the visibility of a single station; this is a considerable improvement, providing a greater time margin to carry out docking.

The complete report of visibility of Sri Lanka and Singapore station combination for January 2 can be found in appendix B

Attention must be paid to the presence of a portion of the day in which this overlap is not present; this issue should be added to the drives to be considered when the docking phase will be scheduled.

6.3 Conclusions

Link Budget and Visibility analysis have shown how this low-cost proposal of GSN for SROC support is vaible for achieving the set goals and almost entirely meets the requirements, except for a few issues, which basically are:

- Coexistence of SROC and Space Rider links in Singapore and Malindi stations for S-band Downlink, with lack of redundancy which reduces the safety level of operations;

- Poor Downlink performance of the UHF Yagi-Uda antenna selected in Singapore and Sri Lanka stations;

- Overlap not always present between Sri Lanka and Singapore, with presence of unfavorable daily time window to perform the docking phase.

However, this is a preliminary proposal, designed with the goal of achieving maximum results with minimum effort. Should this turn into an actual offer, taking into consideration the analysis done, it does not seem difficult to file down the imperfections, keeping in mind, however, that any improvement will necessarily result in a large investment of cost and labor. At present, the most effective and efficient migiorative solutions would seem to be:

- Installation of equipment to create one or two Downlink chains dedicated to SROC for S-band antennas in Singapore and Malindi stations (Space Rider network);

- Installation in Singapore and Sri Lanka stations of a Helix antenna specially designed for SROC UHF Downlink;

- Design and implementation of a mobile Ground Station between Malindi and Singapore, replacing Sri Lanka station, capable of both S-band and UHF communication, with the purpose of further increasing the duration of continuous visibility.

Appendix A

Link Budget tables

A.1 S-band Downlink with HDR

A.1.1 S-band Downlink budget for Singapore G/S

LINK BUDGET ID:		SROC - S-Band Donwlink - Singapore		
Spaceraft		SROC		
Location		SINGAPORE		
Ground Station		SI1		
DOWNLINK		**NOMINAL**	**ADVERSE**	**FAVOURABLE**
Satellite				
S/C Axial Ratio	dB	2.90	4.75	1.00
S/C Crosspolar diS/Crimination	dB	15.63	11.48	24.81
S/C Transmitted power	W	1.0	1.0	2.0
S/C TX Line losses	dB	0.5	0.5	0.5
S/C TX Antenna Gain	dBi	5.0	5.0	7.0
S/C EIRP	dBW	**4.50**	**4.50**	**9.51**
Link				
Slant Range	km	1804.519		
Power flux density at G/S in Free Space	dBW/m^2	-131.62	-131.62	-126.61
Downlink frequency	GHz	**2.250**		
Downlink Wavelength	m	0.133		
Free Space Loss	dB	164.613		
Pointing Offset	°	0.006	0.006	0.006
Pointing Offset Loss	dB	0.000	0.000	0.000
Polarisation Mismatch Loss	dB	0.132	0.447	0.000
Ionospehric Loss	dB	0.0	0.0	0.0
Atmospheric model uncertainty	%	0	25	-25
Atmospheric Loss	dB	3.940	4.925	2.955
Total Propagation losses	dB	168.684	169.985	167.568
Ground Station				
G/S Axial Ratio	dB	1.00	1.00	1.00
G/S Crosspolar discrimination	dB	24.81	24.81	24.81
G/S DL Half power beamwidth	°	1.067		
G/S Pointing Accuracy	°	0.080	0.080	0.080

		NOMINAL	ADVERSE	FAVOURABLE
G/S Pointing Accuracy	°	0.080	0.080	0.080
G/S Pointing Accuracy Loss	dB	0.097	0.097	0.097
G/S Rx Antenna G/T	dB/K	**20.50**	**20.50**	**20.50**
Boltzman's Constant	W/Hz/K	1.38E-23		
Power Flux Density at G/S	dBW/m²	-135.789	-137.089	-129.662
Downlink S/No	dB/Hz	**84.818**	**83.517**	**90.945**
Telemetry acquisition				
TM Carrier Modulation loss	dB	0.604	0.761	0.512
G/S TM Demodulation Technical loss	dB	1.0	1.0	1.0
Telemetry S/No	dBHz	83.21	81.76	89.43
TM Bit Rate	kb/s	**4000**		
TM Bit Rate	dBHz	66.021		
TM Eb/No	dB	17.19	15.74	23.41
Required Eb/No for 1e-6 FER	dB	4.726	4.726	4.726
Margin for TM acquisition (>3dB)	dB	**12.467**	**11.009**	**18.686**
Mean Margin - 3*sigma (>0dB)	dB	10.823		
Nom Margin - Worst Case RSS (>0dB)	dB	11.421		

A.1.2 S-band Downlink budget for Malindi G/S

LINK BUDGET ID:		SROC - S-Band Donwlink - Malindi		
Spaceraft		SROC		
Location		MALINDI		
Ground Station		MAL-2A		
DOWNLINK		NOMINAL	ADVERSE	FAVOURABLE
Satellite				
S/C Axial Ratio	dB	2.90	4.75	1.00
S/C Crosspolar diS/Crimination	dB	15.63	11.48	24.81
S/C Transmitted power	W	1.0	1.0	2.0
S/C TX Line losses	dB	0.5	0.5	0.5
S/C TX Antenna Gain	dBi	5.0	5.0	7.0
S/C EIRP	dBW	**4.50**	**4.50**	**9.51**
Link				
Slant Range	km	1804.519		
Power flux density at G/S in Free Space	dBW/m²	-131.62	-131.62	-126.61
Downlink frequency	GHz	**2.250**		
Downlink Wavelength	m	0.133		
Free Space Loss	dB	164.613		
Pointing Offset	°	0.006	0.006	0.006
Pointing Offset Loss	dB	0.001	0.001	0.001
Polarisation Mismatch Loss	dB	0.132	0.447	0.000
Ionospehric Loss	dB	0.0	0.0	0.0
Atmospheric model uncertainty	%	0	25	-25
Atmospheric Loss	dB	2.982	3.727	2.236
Total Propagation losses	dB	167.726	168.787	166.849
Ground Station				
G/S Axial Ratio	dB	1.00	1.00	1.00
G/S Crosspolar discrimination	dB	24.81	24.81	24.81
G/S DL Half power beamwidth	°	0.971		
G/S Pointing Accuracy	°	0.01	0.01	0.01

		NOMINAL	ADVERSE	FAVOURABLE
G/S Pointing Accuracy Loss	dB	0.002	0.002	0.002
G/S Rx Antenna G/T	dB/K	**21.600**	**21.600**	**21.600**
Boltzman's Constant	W/Hz/K	1.38E-23		
Power Flux Density at G/S	dBW/m²	-134.735	-135.796	-128.848
Downlink S/No	dB/Hz	**86.972**	**85.911**	**92.859**
Telemetry acquisition				
TM Carrier Modulation loss	dB	0.604	0.761	0.512
G/S TM Demodulation Technical loss	dB	1.0	1.0	1.0
Telemetry S/No	dBHz	85.37	84.15	91.35
TM Bit Rate	kb/s	**4000**		
TM Bit Rate	dBHz	66.021		
TM Eb/No	dB	19.35	18.13	25.33
Required Eb/No for 1e-6 FER	dB	4.726	4.726	4.726
Margin for TM acquisition (>3dB)	dB	**14.621**	**13.403**	**20.600**
Mean Margin - 3*sigma (>0dB)	dB	13.029		
Nom Margin - Worst Case RSS (>0dB)	dB	13.797		

A.1.3   S-band Downlink budget for Sri Lanka G/S

LINK BUDGET ID:		SROC - S-Band Downlink - Sri Lanka		
Spaceraft		SROC		
Location		SRI LANKA		
Ground Station		AS-01		
DOWNLINK		**NOMINAL**	**ADVERSE**	**FAVOURABLE**
Satellite				
S/C Axial Ratio	dB	2.90	4.75	1.00
S/C Crosspolar diS/Crimination	dB	15.63	11.48	24.81
S/C Transmitted power	W	1.0	1.0	2.0
S/C TX Line losses	dB	0.5	0.5	0.5
S/C TX Antenna Gain	dBi	5.0	5.0	7.0
S/C EIRP	dBW	**4.50**	**4.50**	**9.51**
Link				
Slant Range	km	1804.519		
Power flux density at G/S in Free Space	dBW/m²	-131.62	-131.62	-126.61
Downlink frequency	GHz	2.250		
Downlink Wavelength	m	0.133		
Free Space Loss	dB	164.613		
Pointing Offset	°	0.000	0.000	0.000
Pointing Offset Loss	dB	0.000	0.000	0.000
Polarisation Mismatch Loss	dB	0.132	0.447	0.000
Ionospehric Loss	dB	0.0	0.0	0.0
Atmospheric model uncertainty	%	0	25	-25
Atmospheric Loss	dB	3.829	4.787	2.872
Total Propagation losses	dB	168.574	169.847	167.485
Ground Station				
G/S Axial Ratio	dB	1.00	1.00	1.00
G/S Crosspolar discrimination	dB	24.81	24.81	24.81
G/S DL Half power beamwidth	°	2.623		
G/S Pointing Accuracy	°	0.10	0.10	0.10

		NOMINAL	ADVERSE	FAVOURABLE
G/S Pointing Accuracy Loss	dB	0.025	0.025	0.025
G/S Rx Antenna G/T	dB/K	**12.800**	**12.800**	**12.800**
Boltzman's Constant	W/Hz/K	1.38E-23		
Power Flux Density at G/S	dBW/m²	-135.605	-136.878	-129.506
Downlink S/No	dB/Hz	**77.301**	**76.028**	**83.401**
Telemetry acquisition				
TM Carrier Modulation loss	dB	0.604	0.761	0.512
G/S TM Demodulation Technical loss	dB	1.0	1.0	1.0
Telemetry S/No	dBHz	75.70	74.27	81.89
TM Bit Rate	kb/s	**4000**		
TM Bit Rate	dBHz	66.021		
TM Eb/No	dB	9.68	8.25	15.87
Required Eb/No for 1e-6 FER	dB	4.73	4.73	4.73
Margin for TM acquisition (>3dB)	dB	**4.951**	**3.520**	**11.142**
Mean Margin - 3*sigma (>0dB)	dB	3.313		
Nom Margin - Worst Case RSS (>0dB)	dB	3.931		

A.2   UHF Uplink

A.2.1   UHF Uplink budget for Singapore G/S

LINK BUDGET ID:		**SROC - UHF Uplink - Singapore**		
Spaceraft		SROC		
Location		SINGAPORE		
Ground Station		SI1		
UPLINK		**NOMINAL**	**ADVERSE**	**FAVOURABLE**
Ground Station				
G/S Axial Ratio	dB	1.0	1.0	1.0
G/S Crosspolar discrimination	dB	24.81	24.81	24.81
G/S TX Antenna Gain	dBi	14.20	14.20	14.20
G/S UL Half power beamwidth	°	30.00		
G/S Pointing Accuracy	°	0.00	0.00	0.00
G/S Pointing Accuracy Loss	dB	0.000	0.000	0.000
G/S EIRP	dBW	**34.00**	**34.00**	**34.00**
Link				
Slant Range	km	1804.519		
Power flux density at S/C in Free Space	dBW/m²	-102.119	-102.119	-102.119
Uplink frequency	GHz	**0.402**		
Uplink Wavelength	m	0.746		
Free Space Loss	dB	149.654	149.654	149.654
Pointing Offset	°	0.000	0.000	0.000
Pointing Offset Loss	dB	0.000	0.000	0.000
Polarisation Mismatch Loss	dB	0.132	0.447	0.000
Ionospehric Loss	dB	0.3	0.3	0.3
Atmospheric model uncertainty	%	0	25	-25
Atmospheric Loss	dB	1.460	1.825	1.095
Total losses	dB	151.545	152.226	151.048
Satellite				
S/C Axial Ratio	dB	2.90	4.75	1.00

98

		NOMINAL	ADVERSE	FAVOURABLE
S/C Crosspolar discrimination	dB	15.63	11.48	24.81
SC RX Line losses	dB	0.5	0.5	0.5
S/C RX Antenna Gain	dB	1.9	1.9	1.9
S/C RX Antenna G/T	dB/K	**-25.98**	**-25.98**	**-25.98**
Boltzman's Constant	W/Hz/K	1.38E-23		
Power Flux Density at S/C	dBW/m²	-104.011	-104.691	-103.514
Uplink S/No	dBHz	**85.074**	**84.394**	**85.571**
Telecommand acquisition				
TC Carrier Modulation loss	dB	0.604	0.761	0.512
S/C TC Demodulation Technical loss	dB	2.00	2.00	2.00
Telecommand S/No	dB	82.47	81.63	83.06
TC Bit rate	kb/s	**64**		
TC Bit rate	dBHz	48.06		
TC Eb/No	dB	34.409	33.571	34.997
Required Eb/No for 1e-5 BER	dB	11.263	11.263	11.263
Margin for TC acquisition (>3dB)	dB	**23.146**	**22.308**	**23.735**
Mean Margin - 3*sigma (>0dB)	dB	22.467		
Nom Margin - Worst Case RSS (>0dB)	dB	22.639		

A.2.2   UHF Uplink budget for Sri Lanka G/S

LINK BUDGET ID:		**SROC - UHF Uplink - Sri Lanka**		
Spaceraft		SROC		
Location		SRI LANKA		
Ground Station		AS-01		
UPLINK		**NOMINAL**	**ADVERSE**	**FAVOURABLE**
Ground Station				
G/S Axial Ratio	dB	1.0	1.0	1.0
G/S Crosspolar discrimination	dB	24.81	24.81	24.81
G/S TX Antenna Gain	dBi	14.20	14.20	14.20
G/S UL Half power beamwidth	°	30.00		
G/S Pointing Accuracy	°	0.00	0.00	0.00
G/S Pointing Accuracy Loss	dB	0.000	0.000	0.000
G/S EIRP	dBW	**34.00**	**34.00**	**34.00**
Link				
Slant Range	km	1804.519		
Power flux density at S/C in Free Space	dBW/m²	-102.119	-102.119	-102.119
Uplink frequency	GHz	**0.402**		
Uplink Wavelength	m	0.746		
Free Space Loss	dB	149.654	149.654	149.654
Pointing Offset	°	0.000	0.000	0.000
Pointing Offset Loss	dB	0.000	0.000	0.000
Polarisation Mismatch Loss	dB	0.132	0.447	0.000
Ionospehric Loss	dB	0.3	0.3	0.3
Atmospheric model uncertainty	%	0	25	-25
Atmospheric Loss	dB	1.379	1.724	1.034
Total losses	dB	151.464	152.124	150.988
Satellite				
S/C Axial Ratio	dB	2.90	4.75	1.00
S/C Crosspolar discrimination	dB	15.63	11.48	24.81
SC RX Line losses	dB	0.5	0.5	0.5

		NOMINAL	ADVERSE	FAVOURABLE
S/C RX Antenna Gain	dB	1.9	1.9	1.9
S/C RX Antenna G/T	dB/K	**-25.98**	**-25.98**	**-25.98**
Boltzman's Constant	W/Hz/K	1.38E-23		
Power Flux Density at S/C	dBW/m²	-103.930	-104.590	-103.453
Uplink S/No	dBHz	**85.155**	**84.495**	**85.632**
Telecommand acquisition				
TC Carrier Modulation loss	dB	0.604	0.761	0.512
S/C TC Demodulation Technical loss	dB	2.00	2.00	2.00
Telecommand S/No	dB	82.55	81.73	83.12
TC Bit rate	kb/s	**64**		
TC Bit rate	dBHz	48.06		
TC Eb/No	dB	34.490	33.672	35.058
Required Eb/No for 1e-5 BER	dB	11.263	11.263	11.263
Margin for TC acquisition (>3dB)	dB	**23.227**	**22.409**	**23.795**
Mean Margin - 3*sigma (>0dB)	dB	22.561		
Nom Margin - Worst Case RSS (>0dB)	dB	22.734		

A.3 UHF Downlink with LDR

A.3.1 UHF Downlink budget for Singapore G/S

LINK BUDGET ID:		**SROC - UHF Downlink - Singapore**		
Spaceraft		SROC		
Location		SINGAPORE		
Ground Station		SI1		
DOWNLINK		**NOMINAL**	**ADVERSE**	**FAVOURABLE**
Satellite				
S/C Axial Ratio	dB	2.90	4.75	1.00
S/C Crosspolar diS/Crimination	dB	15.63	11.48	24.81
S/C Transmitted power	W	1.0	1.0	2.0
S/C TX Line losses	dB	0.5	0.5	0.5
S/C TX Antenna Gain	dBi	1.9	1.9	1.9
S/C EIRP	dBW	**1.40**	**1.40**	**4.41**
Link				
Slant Range	km	1804.519		
Power flux density at G/S in Free Space	dBW/m²	-134.72	-134.72	-131.71
Downlink frequency	GHz	**0.400**		
Downlink Wavelength	m	0.750		
Free Space Loss	dB	149.610		
Pointing Offset	°	0.000	0.000	0.000
Pointing Offset Loss	dB	0.000	0.000	0.000
Polarisation Mismatch Loss	dB	0.132	0.447	0.000
Ionosphehric Loss	dB	0.3	0.3	0.3
Atmospheric model uncertainty	%	0	25	-25
Atmospheric Loss	dB	1.455	1.819	1.091
Total Propagation losses	dB	151.497	152.176	151.002
Ground Station				
G/S Axial Ratio	dB	1.000	1.000	1.000
G/S Crosspolar discrimination	dB	24.81	24.81	24.81

		NOMINAL	ADVERSE	FAVOURABLE
G/S Rx Antenna Gain	dBi	14.2	14.2	14.2
G/S DL Half power beamwidth	°	30.00		
G/S Pointing Accuracy	°	0.00	0.00	0.00
G/S Pointing Accuracy Loss	dB	0.000	0.000	0.000
G/S System Noise Temperature	dBK	23.524	23.524	23.524
G/S Rx Antenna G/T	dB/K	**-9.324**	**-9.324**	**-9.324**
Boltzman's Constant	W/Hz/K	1.38E-23		
Power Flux Density at G/S	dBW/m²	-136.606	-137.286	-133.100
Downlink S/No	dB/Hz	**69.180**	**68.500**	**72.685**
Telemetry acquisition				
TM Carrier Modulation loss	dB	0.604	0.761	0.512
G/S TM Demodulation Technical loss	dB	1.0	1.0	1.0
Telemetry S/No	dBHz	67.58	66.74	71.17
TM Bit Rate	kb/s	**250**		
TM Bit Rate	dBHz	53.979		
TM Eb/No	dB	13.60	12.76	17.19
Required Eb/No for 1e-6 FER	dB	12.20	12.20	12.20
Margin for TM acquisition (>3dB)	dB	**1.392**	**0.555**	**4.989**
Mean Margin - 3*sigma (>0dB)	dB	0.462		
Nom Margin - Worst Case RSS (>0dB)	dB	0.885		

A.3.2   UHF Downlink budget for Sri Lanka G/S

LINK BUDGET ID:		SROC - UHF Downlink - Sri Lanka		
Spaceraft		SROC		
Location		SRI LANKA		
Ground Station		AS-01		
DOWNLINK		**NOMINAL**	**ADVERSE**	**FAVOURABLE**
Satellite				
S/C Axial Ratio	dB	2.90	4.75	1.00
S/C Crosspolar diS/Crimination	dB	15.63	11.48	24.81
S/C Transmitted power	W	1.0	1.0	2.0
S/C TX Line losses	dB	0.5	0.5	0.5
S/C TX Antenna Gain	dBi	1.9	1.9	1.9
S/C EIRP	dBW	**1.40**	**1.40**	**4.41**
Link				
Slant Range	km	1804.519		
Power flux density at G/S in Free Space	dBW/m²	-134.72	-134.72	-131.71
Downlink frequency	GHz	**0.400**		
Downlink Wavelength	m	0.750		
Free Space Loss	dB	149.610		
Pointing Offset	°	0.000	0.000	0.000
Pointing Offset Loss	dB	0.000	0.000	0.000
Polarisation Mismatch Loss	dB	0.132	0.447	0.000
Ionospehric Loss	dB	0.3	0.3	0.3
Atmospheric model uncertainty	%	0	25	-25
Atmospheric Loss	dB	1.374	1.718	1.031
Total Propagation losses	dB	151.416	152.075	150.941
Ground Station				
G/S Axial Ratio	dB	1.000	1.000	1.000
G/S Crosspolar discrimination	dB	24.81	24.81	24.81

G/S Rx Antenna Gain	dBi	-9.324		-9.324		-9.324		
G/S DL Half power beamwidth	°	30.00						
G/S Pointing Accuracy	°	0.00		0.00		0.00		
G/S Pointing Accuracy Loss	dB	0.000		0.000		0.000		
G/S System Noise Temperature	dBK	23.524		23.524		23.524		
G/S Rx Antenna G/T	dB/K	**-9.324**		**-9.324**		**-9.324**		
Boltzman's Constant	W/Hz/K	1.38E-23						
Power Flux Density at G/S	dBW/m²	-136.525		-137.185		-133.040		
Downlink S/No	dB/Hz	**69.260**		**68.601**		**72.746**		
Telemetry acquisition								
TM Carrier Modulation loss	dB	0.604		0.761		0.512		
G/S TM Demodulation Technical loss	dB	1.0		1.0		1.0		
Telemetry S/No	dBHz	67.66		66.84		71.23		
TM Bit Rate	kb/s	**250**						
TM Bit Rate	dBHz	53.979						
TM Eb/No	dB	13.68		12.86		17.25		
Required Eb/No for 1e-6 FER	dB	12.20		12.20		12.20		
Margin for TM acquisition (>3dB)	dB	**1.473**		**0.656**		**5.050**		
Mean Margin - 3*sigma (>0dB)	dB	0.546						
Nom Margin - Worst Case RSS (>0dB)	dB	0.980						

Appendix B

Visibility report

B.1   Access summary report for January 2

```
04 Oct 2022 17:11:47
Satellite-SR_2025_01_01_6_2_long-To-Facility-Bangalore, Facility-Biak, Facility-Malindi,
Facility-Singapore, Facility-Sri_Lanka:  Access Summary Report


SR_2025_01_01_6_2_long-To-Bangalore
-----------------------------------
            Access       Start Time (UTCG)         Stop Time (UTCG)        Duration (sec)
            ------    ------------------------  ------------------------  --------------
                 1    2 Jan 2025 00:23:10.860   2 Jan 2025 00:30:22.325        431.465
                 2    2 Jan 2025 02:01:37.223   2 Jan 2025 02:08:53.825        436.601
                 3    2 Jan 2025 03:40:13.208   2 Jan 2025 03:47:15.827        422.620
                 4    2 Jan 2025 05:19:02.800   2 Jan 2025 05:25:25.312        382.512
                 5    2 Jan 2025 06:58:15.698   2 Jan 2025 07:03:15.487        299.788
                 6    2 Jan 2025 08:38:25.255   2 Jan 2025 08:40:17.538        112.283
                 7    2 Jan 2025 18:30:22.381   2 Jan 2025 18:33:35.827        193.446
                 8    2 Jan 2025 20:07:47.794   2 Jan 2025 20:13:16.763        328.969
                 9    2 Jan 2025 21:45:44.105   2 Jan 2025 21:52:19.732        395.627
                10    2 Jan 2025 23:23:56.684   2 Jan 2025 23:31:03.556        426.872


SR_2025_01_01_6_2_long-To-Biak
------------------------------
            Access       Start Time (UTCG)         Stop Time (UTCG)        Duration (sec)
            ------    ------------------------  ------------------------  --------------
                 1    2 Jan 2025 00:38:54.192   2 Jan 2025 00:46:36.862        462.670
                 2    2 Jan 2025 02:17:18.528   2 Jan 2025 02:25:26.245        487.717
                 3    2 Jan 2025 03:55:47.083   2 Jan 2025 04:04:08.219        501.136
                 4    2 Jan 2025 05:34:23.550   2 Jan 2025 05:42:42.756        499.206
                 5    2 Jan 2025 07:13:06.623   2 Jan 2025 07:21:14.269        487.646
                 6    2 Jan 2025 08:51:50.774   2 Jan 2025 08:59:48.580        477.806
                 7    2 Jan 2025 10:30:30.199   2 Jan 2025 10:38:28.681        478.482
                 8    2 Jan 2025 12:09:03.760   2 Jan 2025 12:17:11.902        488.142
                 9    2 Jan 2025 13:47:35.637   2 Jan 2025 13:55:52.124        496.487
                10    2 Jan 2025 15:26:11.634   2 Jan 2025 15:34:24.936        493.302
                11    2 Jan 2025 17:04:55.103   2 Jan 2025 17:12:50.687        475.584
                12    2 Jan 2025 18:43:44.331   2 Jan 2025 18:51:14.487        450.157
                13    2 Jan 2025 20:22:32.351   2 Jan 2025 20:29:43.969        431.619
                14    2 Jan 2025 22:01:11.355   2 Jan 2025 22:08:24.326        432.971
                15    2 Jan 2025 23:39:39.673   2 Jan 2025 23:47:13.168        453.495
```

SR_2025_01_01_6_2_long-To-Malindi

Access	Start Time (UTCG)	Stop Time (UTCG)	Duration (sec)
1	2 Jan 2025 00:12:37.402	2 Jan 2025 00:20:04.310	446.908
2	2 Jan 2025 01:51:34.287	2 Jan 2025 01:58:25.035	410.748
3	2 Jan 2025 03:30:26.338	2 Jan 2025 03:36:55.748	389.410
4	2 Jan 2025 05:09:04.295	2 Jan 2025 05:15:41.971	397.676
5	2 Jan 2025 06:47:28.480	2 Jan 2025 06:54:38.705	430.225
6	2 Jan 2025 08:25:47.319	2 Jan 2025 08:33:35.010	467.691
7	2 Jan 2025 10:04:09.361	2 Jan 2025 10:12:23.429	494.068
8	2 Jan 2025 11:42:39.113	2 Jan 2025 11:51:03.014	503.901
9	2 Jan 2025 13:21:16.124	2 Jan 2025 13:29:37.590	501.465
10	2 Jan 2025 14:59:56.048	2 Jan 2025 15:08:12.349	496.301
11	2 Jan 2025 16:38:34.041	2 Jan 2025 16:46:50.080	496.039
12	2 Jan 2025 18:17:08.903	2 Jan 2025 18:25:28.823	499.920
13	2 Jan 2025 19:55:44.064	2 Jan 2025 20:04:03.601	499.538
14	2 Jan 2025 21:34:24.749	2 Jan 2025 21:42:30.719	485.970
15	2 Jan 2025 23:13:14.105	2 Jan 2025 23:20:50.736	456.631

SR_2025_01_01_6_2_long-To-Singapore

Access	Start Time (UTCG)	Stop Time (UTCG)	Duration (sec)
1	2 Jan 2025 00:30:00.236	2 Jan 2025 00:37:46.855	466.620
2	2 Jan 2025 02:08:32.046	2 Jan 2025 02:16:31.063	479.017
3	2 Jan 2025 03:47:00.966	2 Jan 2025 03:55:14.728	493.763
4	2 Jan 2025 05:25:33.349	2 Jan 2025 05:33:52.332	498.983
5	2 Jan 2025 07:04:13.742	2 Jan 2025 07:12:22.692	488.949
6	2 Jan 2025 08:43:02.003	2 Jan 2025 08:50:49.506	467.503
7	2 Jan 2025 10:21:52.419	2 Jan 2025 10:29:19.593	447.173
8	2 Jan 2025 12:00:36.767	2 Jan 2025 12:07:58.698	441.930
9	2 Jan 2025 13:39:10.989	2 Jan 2025 13:46:46.238	455.249
10	2 Jan 2025 15:17:38.502	2 Jan 2025 15:25:35.135	476.633
11	2 Jan 2025 16:56:06.333	2 Jan 2025 17:04:18.078	491.745
12	2 Jan 2025 18:34:39.884	2 Jan 2025 18:42:52.576	492.692
13	2 Jan 2025 20:13:20.153	2 Jan 2025 20:21:21.527	481.374
14	2 Jan 2025 21:52:03.217	2 Jan 2025 21:59:51.028	467.812
15	2 Jan 2025 23:30:42.754	2 Jan 2025 23:38:26.475	463.722

SR_2025_01_01_6_2_long-To-Sri_Lanka

Access	Start Time (UTCG)	Stop Time (UTCG)	Duration (sec)
1	2 Jan 2025 00:23:31.483	2 Jan 2025 00:31:39.465	487.982
2	2 Jan 2025 02:02:04.493	2 Jan 2025 02:10:13.898	489.404
3	2 Jan 2025 03:40:38.696	2 Jan 2025 03:48:46.582	487.886
4	2 Jan 2025 05:19:17.207	2 Jan 2025 05:27:13.999	476.793
5	2 Jan 2025 06:58:05.375	2 Jan 2025 07:05:32.844	447.469
6	2 Jan 2025 08:37:07.371	2 Jan 2025 08:43:42.868	395.497
7	2 Jan 2025 10:16:22.045	2 Jan 2025 10:21:48.669	326.624
8	2 Jan 2025 11:55:37.770	2 Jan 2025 12:00:02.062	264.292
9	2 Jan 2025 13:34:31.637	2 Jan 2025 13:38:41.685	250.048
10	2 Jan 2025 15:12:53.850	2 Jan 2025 15:17:50.456	296.607
11	2 Jan 2025 16:51:00.697	2 Jan 2025 16:57:06.543	365.846
12	2 Jan 2025 18:29:07.688	2 Jan 2025 18:36:13.034	425.346
13	2 Jan 2025 20:07:21.984	2 Jan 2025 20:15:05.397	463.413
14	2 Jan 2025 21:45:45.026	2 Jan 2025 21:53:46.356	481.329
15	2 Jan 2025 23:24:14.481	2 Jan 2025 23:32:21.266	486.785

B.2   Global statistics

```
04 Oct 2022 17:11:47
Satellite-SR_2025_01_01_6_2_long-To-Facility-Malindi, Facility-Singapore, Facility-Sri_Lanka:
Access Summary Report


SR_2025_01_01_6_2_long-To-Malindi
---------------------------------
Global Statistics
-----------------
Min Duration     397    28 Jan 2025 12:15:00.387    28 Jan 2025 12:21:06.905        366.518
Max Duration       2     1 Jan 2025 12:41:49.774     1 Jan 2025 12:50:15.625        505.851
Mean Duration                                                                       452.503
Total Duration                                                                   222631.566


SR_2025_01_01_6_2_long-To-Singapore
-----------------------------------
Global Statistics
-----------------
Min Duration       1     1 Jan 2025 09:47:00.610     1 Jan 2025 09:49:58.070        177.460
Max Duration     106     8 Jan 2025 14:12:19.725     8 Jan 2025 14:20:40.465        500.741
Mean Duration                                                                       460.138
Total Duration                                                                   226847.985


SR_2025_01_01_6_2_long-To-Sri_Lanka
-----------------------------------
Global Statistics
-----------------
Min Duration     488     3 Feb 2025 17:01:08.648     3 Feb 2025 17:03:52.149        163.502
Max Duration     166    12 Jan 2025 18:12:18.202    12 Jan 2025 18:20:34.041        495.839
Mean Duration                                                                       386.089
Total Duration                                                                   189955.620
```

B.3   Sri Lanka - Singapore overlap for January 2

Access	Sri Lanka (s)	Singapore (s)	Overlap (s)	Total (s)
1	482.638	480.569	97.704	865.503
2	470.642	486.358	92.725	864.275
3	442.999	478.808	73.406	848.401
4	393.83	459.57	37.525	815.875
5	325.912	439.717		
6	258.643	433.881	No overlap	
7	234.341	448.067		
8	277.327	473.27		
9	351.181	494.167	52.630	792.718
10	418.184	500.487	92.791	825.880
11	463.144	491.584	110.432	844.296
12	485.175	475.709	109.875	851.009
13	491.013	465.113	102.438	853.688
14	489.354	467.06	98.021	858.393
15	484.817	477.388	97.804	864.401

Appendix C

Reference tables and graphs

C.1   Constants for Regression coefficient

	j	a_j	b_j	c_j	$m_{k/\alpha}$	$c_{k/\alpha}$
k_H	1	−5.33980	−0.10008	1.13098	−0.18961	0.71147
	2	−0.35351	1.26970	0.45400		
	3	−0.23789	0.86036	0.15354		
	4	−0.94158	0.64552	0.16817		
k_V	1	−3.80595	0.56934	0.81061	−0.16398	0.63297
	2	−3.44965	−0.22911	0.51059		
	3	−0.39902	0.73042	0.11899		
	4	0.50167	1.07319	0.27195		
α_H	1	−0.14318	1.82442	−0.55187	0.67849	−1.95537
	2	0.29591	0.77564	0.19822		
	3	0.32177	0.63773	0.13164		
	4	−5.37610	−0.96230	1.47828		
	5	16.1721	−3.29980	3.43990		
α_V	1	−0.07771	2.33840	−0.76284	−0.053739	0.83433
	2	0.56727	0.95545	0.54039		
	3	−0.20238	1.14520	0.26809		
	4	−48.2991	0.791669	0.116226		
	5	48.5833	0.791459	0.116479		

Table C.1: *Constants to calculate Regression coefficient for Rain attenuation*

C.2   Error performance for DVB-S2

MODCOD	Modulation	LDPC code	Spectral efficiency	E_s/N_0 (dB)
1	QPSK	1/4	0.490243	-2.35
2	QPSK	1/3	0.656448	-1.24
3	QPSK	2/5	0.789412	-0.30
4	QPSK	1/2	0.988858	1.00
5	QPSK	3/5	1.188304	2.23
6	QPSK	2/3	1.322253	3.10
7	QPSK	3/4	1.487473	4.03
8	QPSK	4/5	1.587196	4.68
9	QPSK	5/6	1.654663	5.18
10	QPSK	8/9	1.766451	6.20
11	QPSK	9/10	1.788612	6.42
12	8PSK	3/5	1.779991	5.50
13	8PSK	2/3	1.980636	6.62
14	8PSK	3/4	2.228124	7.91
15	8PSK	5/6	2.478562	9.35
16	8PSK	8/9	2.646012	10.69
17	8PSK	9/10	2.679207	10.98
18	16APSK	2/3	2.637201	8.97
19	16APSK	3/4	2.966728	10.21
20	16APSK	4/5	3.165623	11.03
21	16APSK	5/6	3.300184	11.61
22	16APSK	8/9	3.523143	12.89
23	16APSK	9/10	3.567342	13.13
24	32APSK	3/4	3.703295	12.73
25	32APSK	4/5	3.951571	13.64
26	32APSK	5/6	4.119540	14.28
27	32APSK	8/9	4.397854	15.69
28	32APSK	9/10	4.453027	16.05

Table C.2: *Error performance at PER* $= 10^{-7}$ *(AWGN channel)*
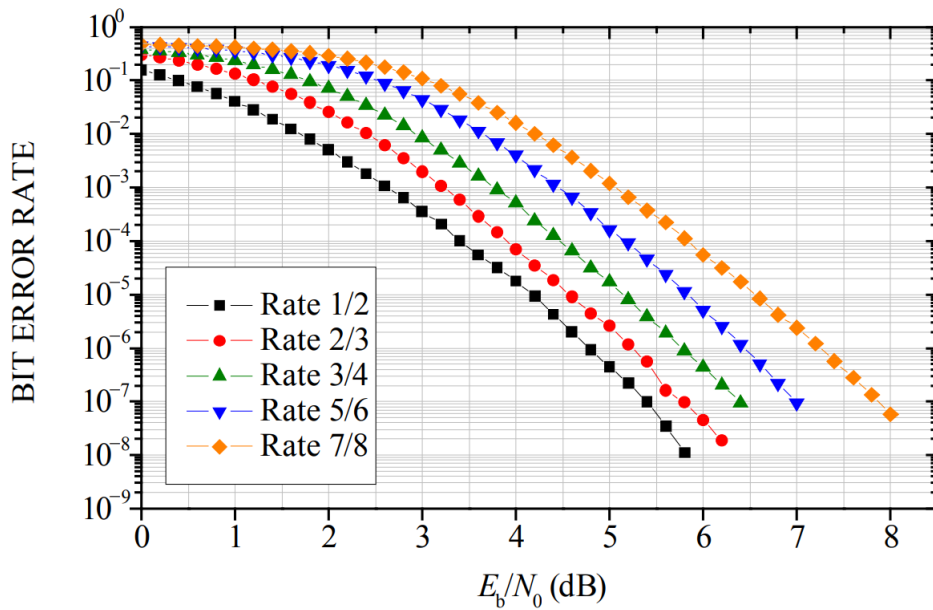
C.3 Error performance for CCSDS

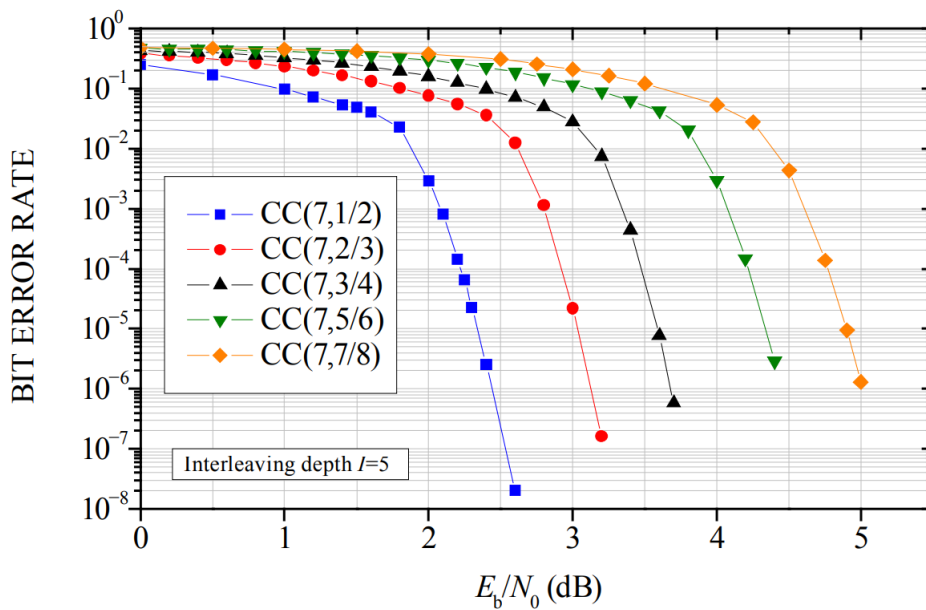Figure C.1: *BER performance of CCSDS Convolutional Codes*

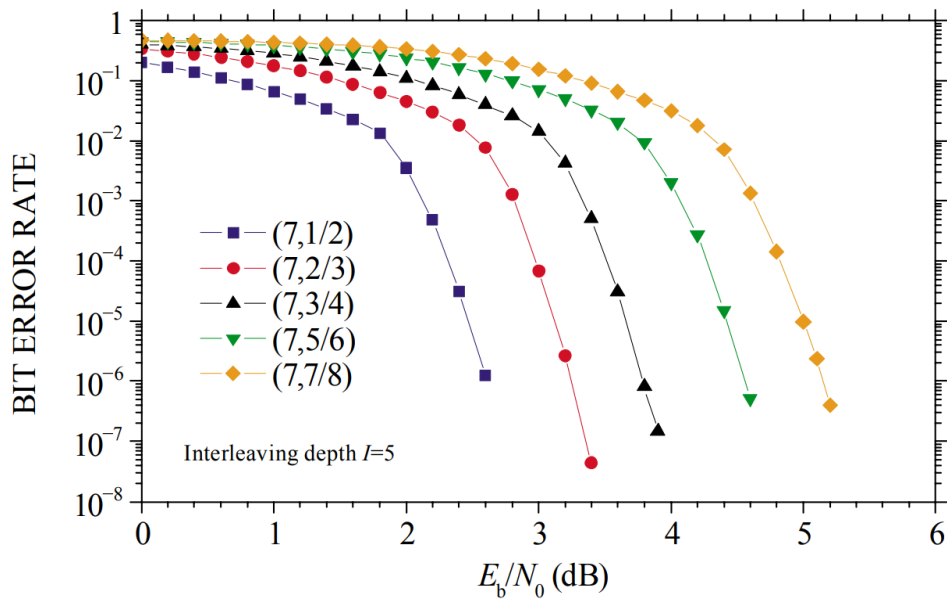Figure C.2: *BER performance of CCSDS Concatenated scheme with R-S(255,223) and Convolutional codes*

Figure C.3: *BER performance of CCSDS Concatenated scheme with R-S(255,239) and Convolutional codes*

Bibliography

[1] The Consultative Committe for Space Data System (CCSDS). *CCSDS 131.1-G-3 - Report Concerning Space Data System Standards - TM Synchronization and Channel Coding - Summary of Concept and Rationale - Green book*. NASA, 2020.

[2] The Consultative Committe for Space Data System (CCSDS). *CCSDS 230.1-G-3 - Report Concerning Space Data System Standards - TC Synchronization and Channel Coding - Summary of Concept and Rationale - Green book*. NASA, 2021.

[3] The Consultative Committe for Space Data System (CCSDS). *CCSDS 231.0-B-4 - Recommendation for Space Data System Standards - TC Synchronization and Channel Coding - Blue book*. NASA, 2021.

[4] The Consultative Committe for Space Data System (CCSDS). *CCSDS 401.0-B-32 - Recommendation for Space Data System Standards - Radio Frequency and Modulation Systems —Part 1: Earth Stations and Spacecraft - Blue book*. NASA, 2021.

[5] The Consultative Committe for Space Data System (CCSDS). *CCSDS 131.0-B-4 - Recommendation for Space Data System Standards - TM Synchronization and Channel Coding - Blue book*. NASA, 2022.

[6] S. Corpino, G. Ammirante, G. Daddi, F. Stesina, F. Corradino, A. Basler, A. Francesconi, F. Branz, and J. Van den Eynde. *Space Rider Observer Cube – SROC: a CubeSat mission for proximity operations demonstration*. International Astronautical Federation (IAF), 2022.

[7] European Cooperation for Space Standardization (ECSS). *ECSS-E-ST-50-01C - Space engineering - Space data links - Telemetry synchronization and channel coding*. ESA-ESTEC, 2008.

[8] European Cooperation for Space Standardization (ECSS). *ECSS-E-ST-50-02C - Space engineering - Ranging and Doppler tracking*. ESA-ESTEC, 2008.

[9] European Cooperation for Space Standardization (ECSS). *ECSS-E-ST-50-03C - Space engineering - Space data links - Telemetry transfer frame protocol*. ESA-ESTEC, 2008.

[10] European Cooperation for Space Standardization (ECSS). *ECSS-E-ST-50-*

04C - Space engineering - Telecommand protocols, synchronization and channel coding. ESA-ESTEC, 2008.

[11] European Cooperation for Space Standardization (ECSS). *ECSS-E-ST-50-05C - Space engineering - Radio frequency and modulation*. ESA-ESTEC, 2011.

[12] L. Ernesto. *Appunti di Elettronica per lo Spazio*. Università degli Studi di Roma Tor Vergata - Dipartimento di Ingegneria Elettronica.

[13] European Telecommunications Standards Institute (ETSI). *ETSI EN 302 307-1 V1.4.1 - Digital Video Broadcasting (DVB) - Second generation framing structure, channel coding and modulation systems for Broadcasting, Interactive Services, News Gathering and other broadband satellite applications - Part 1: DVB-S2*. EBU, 2014.

[14] R. Galuscak and P. Hazdra. *Circular Polarization and Polarization Losses*. CTU Prague - FEE - Department of Electromagnetic Field.

[15] A. Ghizzetti. *Lezioni di analisi di matematica, Vol.1*. Libreria Eredi Virgilio Veschi, 1972.

[16] A. Ghizzetti, A. Ossicini, and Marchetti L. *Lezioni di complementi di matematica*.

[17] L.J. Ippolito. *Satellite Communications Systems Engineering: Atmospheric Effects, Satellite Link Design and System Performance*. Wireless Communications and Mobile Computing. Wiley, 2008.

[18] International Telecommunication Union Radiocommunication Sector (ITU-R). *ITU-R P.838-3 - Specific attenuation model for rain for use in prediction methods*. ITU, 2005.

[19] International Telecommunication Union Radiocommunication Sector (ITU-R). *ITU-R P.676-10 - Characterization of the variability of propagation phenomena and estimation of the risk associated with propagation margin*. ITU, 2013.

[20] International Telecommunication Union Radiocommunication Sector (ITU-R). *ITU-R P.839-4 - Rain height model for prediction methods*. ITU, 2013.

[21] International Telecommunication Union Radiocommunication Sector (ITU-R). *ITU-R P.678-3 - Propagation data and prediction methods required for the design of Earth-space telecommunication systems*. ITU, 2015.

[22] International Telecommunication Union Radiocommunication Sector (ITU-R). *ITU-R P.618-13 - Propagation data and prediction methods required for the design of Earth-space telecommunication systems*. ITU, 2017.

[23] International Telecommunication Union Radiocommunication Sector (ITU-R). *ITU-R P.836-6 - Water vapour: surface densityand total columnar content*. ITU, 2017.

[24] International Telecommunication Union Radiocommunication Sector (ITU-R). *ITU-R P.837-7 - Characteristics of precipitation for propagation modelling*. ITU, 2017.

[25] International Telecommunication Union Radiocommunication Sector (ITU-R). *ITU-R P.840-8 - Attenuation due to clouds and fog*. ITU, 2019.

[26] G. C. Kronmiller and E. J. Baghdady. *The Goddard Range and Range Rate Tracking System: concept, design and performance*. NASA, 1965.

[27] D. Micheli. *Appunti di Telecomunicazioni*.

[28] A. Morello and V. Mignone. *DVB-S2 - Ready for lift off*. EBU, 2004.

[29] F. Stesina. *Appunti di Sistemi Aerospaziali – Communication system*. Politecnico di Torino - DIMEAS.

[30] F. Stesina. *Esercitazioni di Sistemi Aerospaziali – Link Budget*. Politecnico di Torino - DIMEAS.

[31] I.T. Union. *Handbook on Satellite Communications*. Wiley, 2002.